

Development of Recycle-friendly Secondary Cast Aluminium Alloy for
Cylinder Head Applications

Ghebrezghi Tesfamariam Zeru

A thesis submitted in partial fulfillment for the Degree of Master of
Science in Mechanical Engineering in the Jomo Kenyatta University of
Agriculture and Technology

2014

DECLARATION

This thesis is my original work and has not been presented for a degree in any other University.

Signature:..... Date.....

Ghebrezghi Tesfamariam Zeru

This thesis has been submitted for examination with our approval as the University Supervisors.

Signature:..... Date.....

Dr. B. R. Mose

JKUAT, Kenya

Signature:..... Date.....

Dr. T. O. Mbuya

UoN, Kenya

Signature:..... Date.....

Prof. S. M. Mutuli

UoN, Kenya

DEDICATION

To my sister Zafu

ACKNOWLEDGEMENTS

Postgraduate study is the fundamental route to more self-discovery track. This however, cannot be accomplished without proper guidance and assistance from other individuals and institutions with research facilities. During the two years of my study, I have had opportunities to interact with a number of people who are extremely devoted to research. These individuals have left an indelible mark on my professional career.

First and foremost, I would like to thank my supervisors, Dr. B. R. Mose, Dr. T. O. Mbuya and Prof. S. M. Mutuli for their unreserved support and profound intellectual and personal guidance throughout the research work. I also want to thank Dr. B. R. Mose for providing the master alloys (additive elements) used in this experimental work.

I would like to acknowledge the financial support from ADB through the National Board for Higher Education of Eritrea. I also acknowledge the University of Nairobi for providing research facilities and Mr. Matthew Piper of AMG Advanced Metallurgical Group N.V. (UK) for chemical composition analysis.

I also would like to thank a number of individuals at JKUAT and UoN who worked closely with me during lab work. In particular, I want to extend my gratitude to Mr. Mwai and his co-workers from JKUAT and Mr. Njue and his co-workers from the UoN for unreservedly sharing their knowledge in casting and their guidance in other practical aspects.

My stay in Kenya would have been incomplete without a group of close friends to help me balance work and social life. I wish them the best of luck in the fulfillment of their aspirations.

TABLE OF CONTENTS

DECLARATION	i
DEDICATION	ii
ACKNOWLEDGEMENTS	iii
TABLE OF CONTENTS	iv
LIST OF TABLES	ix
LIST OF FIGURES	xi
ABBREVIATIONS	xiv
NOTATIONxvii
ABSTRACTxviii
INTRODUCTION	1
1.1 Background	1
1.2 Problem Statement	4
1.3 Justification	5
1.4 Objective	6
1.4.1 Specific Objectives	6
1.5 Thesis Structure	7
LITERATURE REVIEW	8
2.1 Introduction	8
2.2 Cast Al-Si Alloys	8

2.2.1	Common Cast Al-Si Alloys	9
2.2.2	Al-Si Alloys for Cylinder Head Application	10
2.2.3	Required Properties of Cylinder Head	11
2.2.4	The Common Alloys Used for Cylinder Head and their Properties	12
	2.2.4.1 A356	12
	2.2.4.2 A319	13
	2.2.4.3 C355	13
2.3	Microstructure of Aluminium Cast Alloys	13
	2.3.1 Influence of Modifiers on the Microstructure of Al-Si Alloys	15
	2.3.2 Influence of Iron and Manganese	16
	2.3.3 Influence of Copper	18
	2.3.4 Influence of Magnesium	19
	2.3.5 Influence of Solidification Rate	20
2.4	Mechanical Properties of Al-Si Alloys	21
2.5	Heat Treatment of Aluminium Alloys	24
2.6	Castability of Aluminium-Silicon Alloys	27
	2.6.1 Porosity of Al-Si Cast Alloys	27
	2.6.2 Fluidity	28
	2.6.2.1 Influence of Pouring Temperature on Fluidity	28
	2.6.2.2 Influence of Alloying Elements Composition on Fluidity	29
2.7	Theory of Developing Recycle-Friendly Aluminium Alloys	30
	2.7.1 Recycle Friendly Alloy Practice	32

2.7.2	Aluminium Alloy Recycling Index	33
2.8	Predicting the Composition of an Alloy	34
2.9	Literature Survey on Alloys Used for Cylinder Head Application	35
2.9.1	Summary	36
METHODOLOGY		38
3.1	Introduction	38
3.2	Identification of the Recycle Friendly Alloy	38
3.3	Chemical Composition Analysis on Scrap Cylinder Heads	40
3.4	Experimental Work	41
3.4.1	Materials and Scrap Ingot Preparation	41
3.4.2	Preparation of Bar Casting	42
3.4.3	Preparation of test specimens	44
3.4.4	Heat Treatment	45
3.4.5	Microstructure Examination	45
3.4.5.1	Optical Microscopy	45
3.4.6	Porosity Measurement	46
3.4.7	Mechanical Properties	47
3.4.7.1	Tensile Strength	47
3.4.7.2	Impact Energy Test	48
3.4.7.3	Hardness Test	48
3.4.8	Fluidity Test of the Alloys	49
3.4.8.1	Melting and Pouring	51

RESULTS AND DISCUSSION	53
4.1 Literature Survey and Chemical Composition Analysis	53
4.1.1 Results and Discussion	53
4.1.2 Literature Survey	53
4.1.3 Chemical Composition Analysis	53
4.2 Recycle friendly Alloy Identification	54
4.2.1 Results and Discussion	54
4.3 Practical Alloy Developed	57
4.3.1 Results and Discussion	57
4.4 Microstructure	59
4.4.1 As-Cast Microstructure of the Model Alloy	59
4.4.2 Results and Discussion	59
4.4.3 Heat Treated Microstructure	64
4.4.4 Results and Discussion	64
4.5 Quantification of Si and Fe - Intermetallic particles	68
4.5.1 Results and Discussion	68
4.6 Porosity	71
4.6.1 Results and Discussion	71
4.6.2 Microstructure Observation	71
4.6.3 Porosity quantification	72
4.7 Mechanical Properties	74
4.7.1 Tensile Strength	75

4.7.1.1	Results and Discussion	75
4.7.2	0.2% Proof Stress	77
4.7.3	Percentage (%) Elongation	79
4.7.3.1	Results and Discussion	79
4.7.4	Impact Toughness	81
4.7.4.1	Results and Discussion	81
4.7.5	Artificial Ageing Study	83
4.7.5.1	Microhardness	83
4.7.5.2	Results and Discussion	83
4.8	Comparison of Mechanical Properties of the Model Secondary Alloy with Similar Primary Alloys	86
4.9	Fluidity	87
4.9.1	Results and Discussion	87
	CONCLUSIONS AND RECOMMENDATIONS	92
5.1	CONCLUSIONS	92
5.2	RECOMMENDATIONS FOR FUTURE WORK	93
	REFERENCES	94
	APPENDICES	110
	Cylinder Head Alloys	111
	Results of Mechanical Properties Tests	114

Results of Fluidity Test 117

LIST OF TABLES

Table 1.1	Common examples of 356-type alloy specifications for different countries	3
Table 2.1	Compositions of common commercial alloys	10
Table 2.2	Mechanical properties of common permanent mould cast aluminium alloys	23
Table 2.3	Values of ARI and RPI for some cast alloys	33
Table 3.1	Equivalent alloys group	40
Table 3.2	Chemical composition of the base alloy (Scrap Ingot)	42
Table 3.3	Experimental alloys developed	44
Table 4.1	Chemical composition of scrap cylinder heads	54
Table 4.2	Source alloys versus target alloys chemical composition	55
Table 4.3	The proposed target alloy chemical composition	57
Table 4.4	Quantitative measurement of eutectic - Si and Fe-intermetallic	69
Table 4.5	Comparison of the base alloy mechanical property results . . .	86
Table A.1	Cylinder head alloys produced by different manufacturers and researchers	112
Table A.2	Cylinder head alloys produced by different manufacturers and researchers continued from Table 1.1	113
Table B.1	Summary of the UTS values	114

Table B.2	Representative 0.2% proof stress	114
Table B.3	Percentage elongation of the alloys	115
Table B.4	Impact energy values of the alloys	115
Table B.5	Average micro-hardness values	116
Table C.1	Experimental results of alloys fluidity test	117

LIST OF FIGURES

Figure 2.1	Thermal loading and crack initiation area in the cylinder head	11
Figure 2.2	Typical microstructure of hypoeutectic Al-7Si-Mg (A356) alloy (Al-dendrites surrounded by Al-Si eutectic)	14
Figure 2.3	Formation of (a) α -Chinese scripts and β -Needles and (b) Al_2Cu	17
Figure 2.4	Optical micrographs of various common iron-containing inter- metallics in 319 type alloys	20
Figure 2.5	Solidification mode of aluminium and its alloys	29
Figure 3.1	Permanent metal mould	43
Figure 3.2	Sectioning of the bar casting for mechanical properties and mi- crostructure	44
Figure 3.3	Optical microscope	46
Figure 3.4	Tensile specimen prepared from the bar casting	47
Figure 3.5	Vickers Hardness Tester LV800 AT	49
Figure 3.6	Spiral mould set up and components in detailed drawing	51
Figure 4.1	Difference in composition values between the predicted and re- cycled alloy	58
Figure 4.2	Difference in composition between the proposed target and re- cycled alloy	58
Figure 4.3	Microstructure of the base alloy as-cast	60
Figure 4.4	As-cast microstructure of the 0.02% Sr modified alloy	61

Figure 4.5	Effect of Sr on the Cu - intermetallics	62
Figure 4.6	As-cast microstructure of an alloy with 0.38% Fe as-cast	62
Figure 4.7	As-cast microstructure of an alloy with 0.9% Fe and 0.45% Mn total content	63
Figure 4.8	Microstructure of the base alloy after heat treatment	65
Figure 4.9	Heat treated microstructure of the alloy modified by 0.02% Sr .	66
Figure 4.10	Microstructure of the alloy with 0.38% Fe after heat treatment	67
Figure 4.11	Microstructure of the alloy with 0.9% Fe and 0.45% Mn after heat treatment	68
Figure 4.12	Porosity level distribution in the tested samples	71
Figure 4.13	Binarized image of the alloys	73
Figure 4.14	Pore size distribution for the alloys investigated	73
Figure 4.15	Average ultimate tensile strength	75
Figure 4.16	Representative stress-strain curves	78
Figure 4.17	Average percentage elongation	79
Figure 4.18	Average impact energy in the as-cast and heat treated conditions	81
Figure 4.19	Average micro-hardness values of T4 and T6 heat treat samples	84
Figure 4.20	Variation of fluidity with alloying element	88
Figure 4.21	The outcome of the alloy's fluidity	89
Figure 4.22	Micrograph of the alloys 5 mm from the tip of the fluidity casting	90
Figure A.1	Percentage of the alloys availability based on the literature survey	111

ABBREVIATIONS

ARI	Alloy Recycling Index
AMG	Advanced Metallurgical Group
BET	Booth Extrusions Thika
DAS	Dendrite Arm Spacing
D_{eq}	Equivalent Circle Diameter
DF	Deviation Factor
F	As Fabricated
JIS	Japanese International Standard
h	Hour
HT	Heat Treated
OES	Optical Emission Spectroscope
OM	Optical Microscope
PPI	Pores Per Inch
SDAS	Secondary Dendrite Arm Spacing
SI	Scrap Ingot
SEM	Scanning Electron Microscope
RPI	Recycling Production Index
TEM	Transmission Electron Microscope
UBC	Used Beverage Cans
UK	United Kingdom
UoN	University of Nairobi

UTS	Ultimate Tensile Strength
VHN	Vickers Hardness Number
YS	Yield Strength

NOTATIONS

A	Surface Area [m ²]
E	Absorbed energy [J]
D	Distance from the center of revolving axis to gravity center [m]
n	Number of alloys used
P	Total weight of the pendulum system [kg]

ABSTRACT

Automotive components are currently manufactured from different aluminium alloys. The production of these components from primary aluminium alloys has become a huge burden in terms of economic benefits and environmental aspects. Hence, recycling aluminium alloys is adopted as a strategy in foundry industries for production of various components in the transport and other structural applications. However, the quality of secondary casting alloys is always in question in most recycling practices since alloy chemistry control is a major issue during aluminium recycling and majority of the scrap alloys have differences in chemical compositions. This in turn affects microstructure, the overall mechanical performance of the alloy and castability. It is therefore important to seek ways of maximising alloy chemistry control during aluminium recycling so as to improve the efficiency of the process as well as to utilize the scrap metals in to high quality products. The aim of this study was to identify the alloys used for cylinder head and develop an alloy that allows direct recycling of post-consumer cylinder heads for reuse in the same application and investigate its microstructure, mechanical performance and castability. An assessment was conducted in the literature and on scrap samples to investigate the chemical composition of alloys used for cylinder heads. Recycle-friendly alloy that accommodates different cylinder head scraps was identified based on the standard alloys used for cylinder head application. An alloy (base alloy (SI)) was developed from scrap cylinder heads which fall within the identified alloy chemical composition range by melting different scrap cylinder heads. Its microstructure, mechanical properties and fluidity characteristics were investigated. Further, the effect of Sr, Fe, Mn and different

heat treatment parameters were investigated on the alloy and a satisfactory mechanical properties and fluidity characteristics of the alloy was obtained. The common alloys used in cylinder heads were found to be type 319.0, 356.0, 355.0, 354.0, A380.0 and their equivalent alloys in other countries. The chemical composition analysis of the scrap samples showed that most of them were in the range of JIS AC2B alloy which is equivalent to 319.0 alloy. The microstructure of the alloy in the as-cast reveals phases such as coarse acicular eutectic silicon particles and intermetallic phases of iron and copper. Some Fe-intermetallic phases were also seen to be modified by Sr. After heat treatment, necking, fragmentation and spheroidisation of eutectic silicon particles were observed. Moreover, Al_2Cu was completely dissolved in the Al-matrix. The size and distribution of porosity was increased by the addition of 0.02% Sr as modifier and with the increase of Fe to 0.38%. The pore sizes were large with these alloys, especially with the modified one which had pore sizes above 100 μm . The addition of strontium as a eutectic modifier and iron as an impurity were observed to decrease the tensile strength (UTS) and ductility due to associated porosity and intermetallic phases. The average UTS in the as-cast alloy was 209.5 MPa, 203.6 MPa, 195.4 MPa and 201.5 MPa in the base, Sr, Fe and Mn added alloys respectively. After T6 heat treatment; the UTS, impact toughness and hardness increased while ductility decreased. The highest micro-hardness value was registered by the alloy containing 0.38% Fe after 2 h aging time and at 170°C aging temperature. The suitable aging time of the alloy for obtaining high values of hardness was found to be between 2 and 6 hours at 170°C and T4 treatment was also found convenient than aging for long hours. The fluidity of the base alloy was found to

possess the highest flow length in a curved channel while addition of 0.02% Sr to the base alloy was observed to reduce the fluidity by 5.2%. The increase of Fe content of the base alloy to 0.38% reduced the fluidity by 21.9%. However, the combined addition of 0.9% Fe and 0.45% Mn was observed to reduce the fluidity by 12.1%.

CHAPTER 1

INTRODUCTION

1.1 Background

The demand for aluminium alloys in the manufacturing industries such as the automobile and aerospace sectors is increasing due to the cumulative advantages they have over ferrous alloys [1]. For example, they are used in many automobile components such as pistons, wheels, cylinder heads, engine blocks, manifolds and valve filters [2]. Their relatively high strength to weight ratio is of particular importance due to the increased demand for light-weighting in the transportation industry for fuel efficiency and reduced emissions. The excellent light weighting has attracted use of Al- alloys in many other specific and general applications [1, 3].

It is reported that an increase in the amount of aluminium in a car by 1 kg reduces CO₂ emissions by 19 kg during its whole life-cycle [4]. In addition, 5%–7% fuel savings can be realized for every 10% weight reduction by substituting heavier steel with aluminium through appropriate design. North American light vehicles have the highest total aluminium content with an average of 148 kg per vehicle, followed by European vehicles at 124 kg per vehicle and Japanese vehicles at 118 kg per vehicle [5]. The application of aluminium in passenger vehicles and light trucks manufactured in 2006 is reported to contribute to potential savings of approximately 140 million tonnes of CO₂ emissions and to energy savings of equivalent to 55 billion liters of crude oil over the life cycle of

these vehicles [5]. Hence, most automotive manufacturers have adopted reducing weight as a prime solution for improving fuel consumption, performance, safety and comfort features [1, 6].

It is estimated that aluminium recycling reduces the energy use by about 95% from that required to produce primary aluminium [7, 8]. Cast aluminium alloy products are widely used and the transportation area creates the major end-use market for aluminium-containing products and this is expected to increase. Therefore, the increasing demand for aluminium-based products and the globalization of the aluminium industry have contributed significantly to the higher increased reuse of aluminium scrap for re-production of aluminium alloys. Today, a large amount of new aluminium products are made by recycled alloys [9]. Furthermore, up to 75% aluminium recycled in Europe is used in transportation [10]. It is also predicted [11] that there will be an over-flow of about 6.1 metric tonnes of cast alloy scrap in the year 2030 due to the high concentration of alloying element, effectiveness of scrap sorting and the introduction of electric vehicles.

After the service life of the components is over, many foundry industries recycle the scrap into secondary alloys for reuse in casting various other components. However, the castability, microstructure and mechanical performance of these recycled alloys are more susceptible to detrimental effects compared to the primary aluminium alloys. This is mainly due to the inherently high levels of impurity elements as well as varying degrees of minor elements. Moreover, they are highly dependent on the alloy chemistry, casting process conditions as well as mould and casting design [3, 12–14]. For example, a variety

of cast aluminium alloys are used in producing automobile wheels depending on the manufacturer. Table 1.1 shows that although there is significant similarity in the major alloying element compositions, there is indeed significant variation in the composition of minor elements.

Table 1.1: Common examples of 356-type alloy specifications for different countries.

Country	Alloy	Cu	Mg	Si	Fe	Mn	Ni	Zn	Pb	Sn	Ti	other
USA	356	0.25	0.20/0.45	6.5/7.5	0.60	0.35		0.35			0.25	
	A356	0.20	0.20/0.45	6.5/7.5	0.20	0.10		0.10			0.04/ 0.2	
	A357	0.20	0.40/0.70	6.5/7.5	0.20	0.10		0.10			0.20	Be 0.04/0. 07
U.K	BS 1490 LM25	0.20	0.20/0.60	6.5/7.5	0.50	0.30	0.10	0.10	0.01	0.05	0.20	
Japan	AC4C (AC4C.1)	0.25	0.25/0.40	6.5/7.5	0.40	0.60	0.05	0.30	0.05	0.05	0.20	Cr 0.1
	AC4CH (AC4CH.1)	0.10	0.30/0.45	6.5/7.5	0.17	0.10	0.05	0.10	0.05	0.05	0.20	Cr 0.1
Australia	AA601	0.05	0.30/0.40	6.5/7.5	0.20	0.05	-	0.05	-	-	0.20	0.05
	AA603	0.05	0.45/0.7	6.5/7.5	0.15	0.03	-	0.05	-	-	0.20	0.05

It is thus evident that recycling aluminium wheels without regard to their original alloy specification can result in secondary alloys with varying degrees of minor and impurity elements such as Pb, Sn, Zn, Ni, Fe and Mn. The situation is more complicated for products such as automotive engine cylinder heads which are routinely produced from a wide variety of cast aluminium alloys. The question therefore is how can efficiently recycle these alloys in a manner that allows to control the alloy chemistry as well as the mechanical performance of the resulting alloys.

To make use of automotive component aluminium scrap in high quality products it is important to identify alternative recycling approaches that are better suited to address the

growing compositional diversity of aluminium products. Therefore, the current research will concentrate on recycling of scrap cylinder heads for use in the same application. Component to component recycling is not common so far except in some products like used beverage can (UBC) which is fully reused for the same application. Companies like Nissan Motor Corporation are taking measures to utilize automotive component for high quality products such as bumper to bumper and small vehicle wheels into suspension parts [15]. Furthermore, wheels have the largest potential for component-to-component recycling. They are the largest component group, easy to dismantle, and manufactured from homogenous alloys [16].

1.2 Problem Statement

One of the challenges recognized as a key pillar in maximising aluminium recycling efficiency is the number of available alloys whose specifications will readily accept recycled metal and yet perform well in high quality, value added products. This aspect has generally received little attention in aluminium recycling and yet the potential economic and environmental benefits, especially as pertains to the Kenyan industry, warrant its consideration. For example, cast aluminium alloys for automotive applications which are recycle-friendly have largely been limited to the 380 type alloys. Although these alloys are widely used in automotive applications, there are a number of automotive components, such as pistons, for which they cannot be applied. Alternative recycle friendly alloys therefore need to be developed that can be used in some of these high value automotive applications. It is this aspect that this project aims to address.

1.3 Justification

The use of aluminium in the automotive industry is likely to increase because of its excellent light weighting potential. Increased efficiency of aluminium recycling is therefore necessary because of its obvious economic and ecological benefits as well as to ensure its continued availability at reasonable cost. Some of the benefits of using recycled aluminium as opposed to primary aluminium include the following:

1. Massive energy savings - It is estimated that aluminium recycling reduces the energy use by about 95% from that required to produce primary aluminum (i.e. from about 45 kWh/kg of primary aluminium to about 2.8 kWh/kg of secondary aluminium) [7].
2. Reduced waste disposal - Primary aluminium production generates lots of solid waste such as mine wastes and the red mud residue created during alumina purification. Solid and hazardous wastes from aluminium recycling (primarily dross and salt slag created during remelting) are reduced by about 90% [7].
3. Reduced emissions - Primary aluminium production generates both hazardous (fluorides, sulfur dioxide) and nonhazardous (carbon dioxide) emissions. Aluminium production via recycling reduces emissions by over 90% per tonne.
4. Reduced capital cost - a mining operation and an aluminium extraction plant are not required.

5. Moreover, for some countries like Kenya, aluminium scrap is the most readily available source of aluminium for use by local industries and therefore significantly economical.

Based on these benefits, it has been suggested that the aluminium industry needs to look at opportunities for maximising the advantages of aluminium recycling.

1.4 Objective

The overall aim of this research program was to identify and develop high performance recycle-friendly secondary alloy for cylinder head application by recycling the available aluminium-silicon alloy scraps and to investigate their microstructure and mechanical properties. Hence the specific objectives were.

1.4.1 Specific Objectives

- To develop a recycled alloy that can be used for cylinder heads through assessments of the chemical composition range of standard alloys used for the same application.
- To investigate the microstructure and defect analysis using optical microscopy.
- To evaluate the mechanical properties as well as the fluidity characteristics of the developed secondary alloy.

1.5 Thesis Structure

This thesis is divided into five chapters. Chapter 1 highlights the background of the research, the problem statement and objectives. Chapter 2 presents the literature review on the fundamentals of aluminium silicon alloys, parameters that affect castability, microstructure and mechanical properties of the alloys. The chapter also presents the theory of alloy development from post consumer products. Chapter 3 presents the methodology used in carrying out this research. Chapter 4 reports the experimental results obtained and a detailed discussion of these results. Finally, chapter 5 gives a summary of all findings and conclusions drawn from this work.

CHAPTER 2

LITERATURE REVIEW

2.1 Introduction

Recycling of aluminium alloys from scrap is becoming increasingly important with increasing public awareness of environmental issues, energy consumption and depleting natural resources [17, 18]. However, the use of recycled aluminium casting alloys is affected by a number of factors such as the chemical composition of the alloy and the impurity or cleanliness of the melt during casting [19, 20]. These parameters have an impact on the microstructure and mechanical properties of the alloys due to their profound influence on the microstructure and soundness of the resultant castings. Numerous works have been carried out to provide a better understanding of the operating process-microstructure-property relationships [3, 14, 17, 19]. However, due to the wide range of possible process-microstructure-property relationships, more systematic work is still needed to fully characterize these alloys.

2.2 Cast Al-Si Alloys

Al-Si casting alloys are among the most widely used alloys in the foundry industry because of the best combination of properties imparted by the high silicon content [21]. For example, silicon reduces the thermal expansion coefficient, increases corrosion and wear resistance, and improves castability characteristics of the alloy (especially fluidity

and porosity formation) [22]. These alloys can also be designed to acquire the required combination of strength and ductility after heat treatment [23]. The most common of these alloys belong to the hypoeutectic group in which the silicon content is below the eutectic composition of around 11.7% wt Si [24].

2.2.1 Common Cast Al-Si Alloys

Al-Si casting alloys are widely used alloys in the automotive and aerospace industries on account of their high strength to weight ratio and the ability to cast into desired shapes. Common alloys include the 319-type cast Al-Si alloy, which is typically a secondary alloy that contains Cu and Mg amongst other elements [3]. The 380 alloy type is one of the most widely used aluminium die casting alloy in the automotive industry and belongs to the Al-Si-Cu family [25]. Moreover, A413 type Al-Si casting alloys are characterized by their superior casting characteristics and low shrinkage resulting from their high silicon content (11-13 % wt) and are used for several engineering applications. The Al-7%Si-Mg family of alloys (e.g., A356 and A357) are used extensively in the production of commercial castings due to their excellent castability and good mechanical properties [26].

Some of the common aluminium alloys are listed in Table 2.1, which include the popular 356 and 357; both of which contain 7% Si but different Mg levels of approximately 0.3 and 0.6% Mg respectively. These alloys are widely used in automotive components such as wheels and cylinder heads and are often used in the T6 heat treatment condition [27].

Table 2.1: Compositions of common commercial alloys [28–30]

Alloy	Si	Cu	Mg	Fe	Mn	Ni	Zn	Ti
319.0	5.5-6.5	3.0-4.0	0.1	1.0	0.5	0.35	1.0	0.25
A356.0	6.5-7.5	0.2	0.25-0.45	0.2	0.1	-	0.1	0.2
A357.0	6.4-7.5	0.2	0.45-0.7	0.2	0.1	-	0.1	0.2
A360	9-10	0.6	0.4-0.6	1.3	0.35	0.5	0.5	-
A380	7.5-9.5	3.0-4.0	0.1	1.3	0.5	0.5	3.0	-
B390	16-18	4-5	0.45-0.65	1.3	0.5	0.1	1.5	0.2
A413.0	11-13	1.0	0.1	1.3	0.35	0.5	0.5	-

Compositions are in wt.% and single values are maximum limits. The balance is aluminium and other trace elements such as Cr, Pb and Sn.

2.2.2 Al-Si Alloys for Cylinder Head Application

Cylinder heads are cast from a variety of Al-Si alloys with varying chemistries including 354 (AlSi9Cu1.6Mg), A356 (AlSi7Mg), 319 (Al-Si-Cu) as shown in the compiled data in Appendix A Table A1 [31, 32]. It is thus less likely to expect repeatable equivalent composition in alloys recycled from them. Among the commercial Al-Si casting alloys, the 319 type alloys are the most commonly used for the application of cylinder heads and engine blocks due to the balance of properties that can be achieved using suitable heat treatments. [33].

2.2.3 Required Properties of Cylinder Head

Cylinder heads are subjected to high thermal fatigue in the combustion chamber and mechanical fatigue in the medium-high zone of the heads and more specifically near the water ducts [34, 35]. The thermal fatigue arising from thermal cycling between ambient and about 300°C causes repeated constrained thermal expansion and contraction while mechanical fatigue is a high cycle mode dependant on the rotation of the engine system (crankshaft). The mechanical fatigue may cause cracks in the moderately warm areas between 120 and 170°C [34]. Figure 2.1 shows the thermal loading due to high temperature in (a) and mechanical crack initiation sites in the thin section on the valve bridge adjacent to the water ducts in (b).

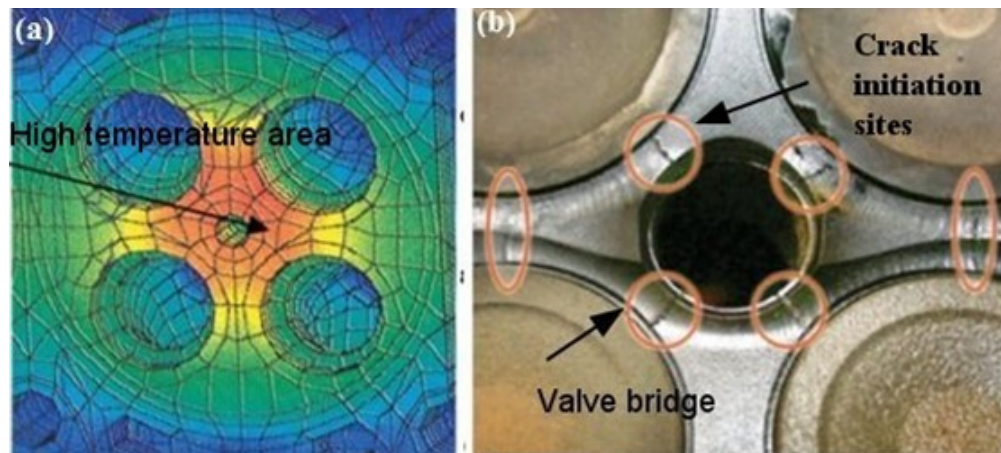


Figure 2.1: Thermal loading and crack initiation area in the cylinder head [36]

The properties required for both diesel and gasoline engines are generally similar. The main difference is that the diesel engines are more prone to high stress amplitudes and fatigue complications associated to the gas pressure resulting from the combustion [36]. The material suitable for this application must therefore have a low thermal expansion

coefficient, high tensile and compression strength, high ductility and a high creep resistance at all service temperatures. Furthermore, the alloy should have a high thermal conductivity, high castability and machinability. This is a challenging combination of properties to achieve as some of the requirements are in conflict and an optimum balance is required [32].

2.2.4 The Common Alloys Used for Cylinder Head and their Properties

2.2.4.1 A356

The AlSi7Mg-T6 (A356) alloy is the most commonly used cast aluminium for automotive components specially wheels and diesel engine cylinder heads [35]. However, AlSiCu alloys could withstand the thermal-mechanical loading almost twice as long compared to AlSi7Mg-T6 due to the higher tensile strength. The alloy has been reported [34] to possess sufficient mechanical characteristics up to 250°C but reduces at higher temperature around 300°C. The new A356+0.5Cu alloy is said to have good strength in the 200-250°C temperature range while the ductility is the same as A356 [34,37]. AlSi7Mg0.3, with the addition of 0.50% Cu and T7 heat treated, is widely used in industry today for cylinder head application, since it provides noticeable gain of yield strength at 250°C, without loss of elongation. However, the gain in mechanical properties due to Cu addition is reported to disappear completely at 300°C [34].

2.2.4.2 A319

Alloys such as Al-Si-Cu-Mg are widely used in cylinder head application [32, 34, 35, 38]. They have better strength at elevated temperature but low ductility which makes them susceptible to cracking by thermal fatigue. However, the performance of these alloys depends on their iron content. Alloys with Fe content below 0.20% are known as primary alloys, and have good ductility at elevated temperature but remain brittle at ambient temperature. A family of alloys known as secondary alloys possess higher iron content from 0.40-0.80% and sometimes 1%, and have low ductility at elevated and ambient temperature [38]. Alloys such as A319 are brittle at low temperature but can be improved by heat treatment or alloying with elements like strontium.

2.2.4.3 C355

Aluminum alloys like C355.0 are important for industrial application. They are widely used especially in automotive engine cylinder heads due to their high strength at room and elevated temperature. These alloys possess high strength and hardness even in the as-cast state by forming intermetallic phases such as Al_5FeSi , Al_2Cu , $\text{Al}_5\text{Cu}_2\text{Mg}_8\text{Si}_6$ [39]. The strength of the alloy was also reported to increase with T6 heat treatment.

2.3 Microstructure of Aluminium Cast Alloys

The Al-Si system is a simple binary eutectic in which Si has limited solubility in Aluminium. The solubility of Si in Al reaches a maximum of 1.65 wt.% Si at the eutectic

temperature of 577°C [28,40]. As the Al-Si alloy solidifies, the primary aluminium forms and grows into dendrites or in the case of hypereutectic Si compositions, the silicon phase forms and grows into angular primary particles. At room temperature, hypoeutectic alloys comprise a soft and ductile primary aluminium phase and a hard and brittle silicon phase. Figure 2.2 shows a typical microstructure of hypoeutectic Al-Si foundry alloy. Hypereutectic cast Al-Si alloys usually contain coarse, angular primary silicon particles as well as an Al-Si eutectic containing eutectic silicon and eutectic Al phases.

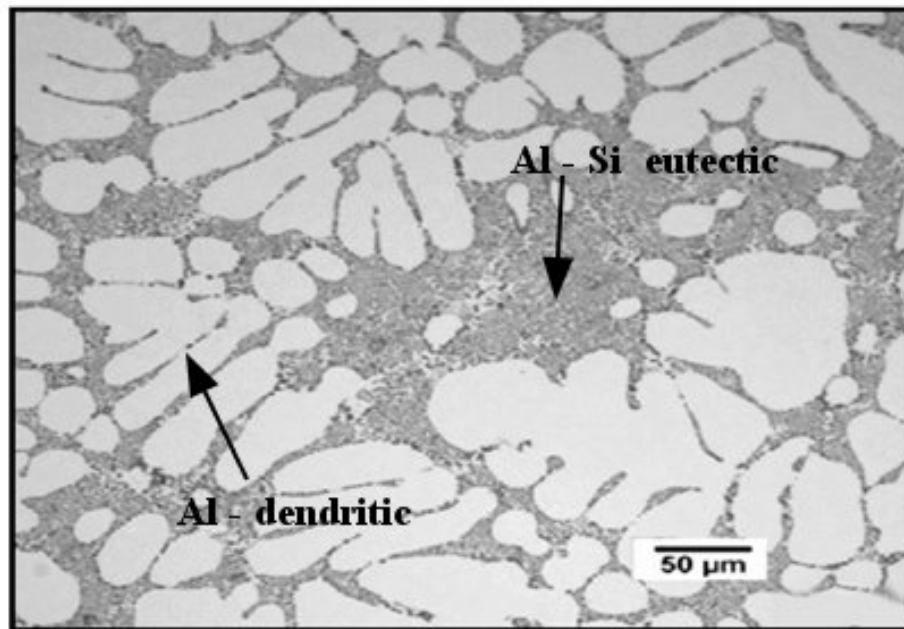


Figure 2.2: Typical microstructure of hypoeutectic Al-7Si-Mg (A356) alloy (Al-dendrites surrounded by Al-Si eutectic) [41]

Commercial aluminium alloys have different levels of other alloying elements which are added to enhance their microstructure for the recommended applications. Properties of cast Al-Si-Mg alloys are predominantly governed by the microstructural characteristics such as morphology of silicon particles and presence of intermetallic compounds

depending upon the presence of alloying elements [28, 29]. The intermetallic compounds and morphology of silicon particles are largely affected by the alloy chemistry, solidification rate and heat treatment conditions [42]. At high solidification rates, a uniform microstructure with the potential for closely distributed and fine particles are commonly expected [43, 44].

The microstructure of Al-Si-Cu-Mg casting alloys is essentially made up of three components, the proportions of which are governed by the alloy composition and solidification conditions. The two main components are the primary α -Al solid solution phase and Al-Si eutectic. The third component of the microstructure can be broadly termed intermetallic compounds and these arise from excess amounts of Mg, Cu, Fe and Mn that cannot be contained in α -Al solid solution phase [43]. The intermetallics adopt various morphologies and form at various stages, prior to, during or after the Al-Si eutectic formation period, and can significantly affect the mechanical properties of the alloys.

2.3.1 Influence of Modifiers on the Microstructure of Al-Si Alloys

It is well established that modification of eutectic silicon can be achieved by several methods such as faster solidification, mould vibration, melt agitation in mushy state and melt inoculation using some elements, e.g., Na, Sr, Sb and certain rare earth metals. Among the modifiers used, Sr and Sb are known to result in good modification in hypoeutectic Al-Si alloys [45–47]. Metallographic studies [46] on A356 alloy reveal that the structure changes from plate like eutectic silicon to fine particles on addition of 0.2 wt.% of Al-

10% Sr modifier. Excess amount of Sr leads to porosity, which among others has been attributed to reduced surface tension of the melt and increased volumetric shrinkage [3].

As an additive, strontium improves mechanical properties and disperses porosity as it modifies the eutectic structure and suppresses the formation of primary silicon in hypereutectic Al-Si alloys. This generally improves the ductility and toughness of the alloys.

Mose *et al.* [47] observed that addition of Sr at levels of 0.02% and 0.05% to LM13-type recycled alloys modifies the acicular Si particles to a fine fibrous form but increases porosity. However, the ultimate tensile strength and ductility of the alloys were observed to increase.

2.3.2 Influence of Iron and Manganese

Dinnis *et al.* [48] observed that iron addition to Al-Si alloys reduces the number of nucleation events of the Al-Si eutectic whereas Mn addition increases the number of nucleation events in Fe-containing alloys. Iron is a well known impurity element in aluminium alloys while Mn is usually added to neutralise the effect of Fe. The solubility of iron is very low in aluminium alloys and tends to form intermetallic phases such as β -Al₅FeSi platelets, α -Al₁₅Fe₃Si₂ phase with a Chinese script morphology and the π -Al₈Mg₃FeSi₆ phase which also has a Chinese script morphology but depends on the level of Mg present in the alloy [49]. The β -Al₅FeSi phase is considered detrimental to ductility of the alloys due to its stress raising potential and poor binding strength with the Al- matrix [14]. It has been reported that increasing the Fe content in Al-7Si-0.3Mg alloys results in

the precipitation of long platelets of the β -phase, whose amount and size increase with increasing Fe content [50,51].

When Mn is present with iron, there is an increased tendency for the α - $\text{Al}_{15}(\text{Fe Mn})_3\text{Si}_2$ Chinese script phase to form as shown in Figure 2.3a. The presence of α -phase particles instead of than β -platelets improves mechanical properties, particularly ductility [23,52]. In general, a Mn/Fe ratio of 0.5 is considered sufficient to promote complete substitution of β with α during typical commercial casting conditions. However, the overall volume fractions of intermetallic phases will increase in this event.

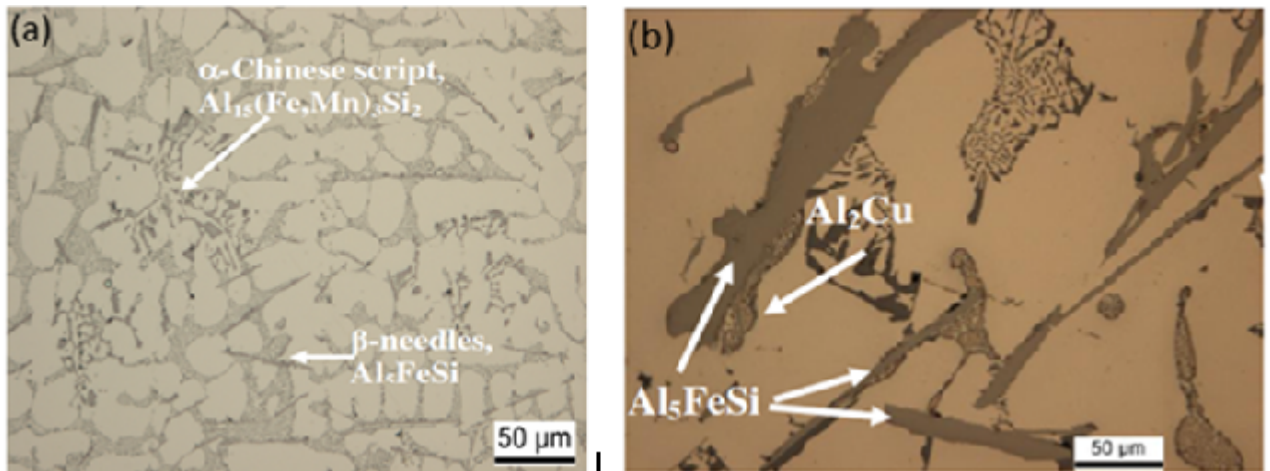


Figure 2.3: Formation of (a) α -Chinese scripts and β -Needles and (b) Al_2Cu [53]

In a report by Hwang *et al.* [33] for an alloy containing 0.5% Fe, it was noted that 0.6% Mn could completely convert the β -phase into α -phase. Higher Mn additions were however reported to create porosity in the alloy. Moreover, Khalifa *et al.* [54] reported that addition of 0.4% Mn to 356 and 319 alloys containing 0.8-1.0% Fe favours the formation and domination of the Chinese script phase (i.e. α - AlFeSi phases) and no images of β - AlFeSi phases were observed in the 356 alloy. However, β - AlFeSi phases

were seen in the 319 alloy having 3.25 wt.% Cu and 0.1 wt.% Mg. This implies that the effectiveness of Mn in modifying the Fe-intermetallics decreases in alloy containing Cu and Mg. Beryllium is also used to change the platelet morphology of the iron phase to Chinese script form [17], but it is toxic which can result harm during adding to the melt.

2.3.3 Influence of Copper

Copper is partially soluble in α -Al solid solution with a maximum equilibrium solubility of 5.65 wt% [43, 55] although the dissolution of Cu levels in as-cast Al-Si-Cu alloys is around 1%. Therefore, for alloys with 1 to 4 wt. % copper, Cu-rich intermetallic (Al_2Cu) phases typically form in the microstructure as seen in Figure 2.3b. In the presence of Mg, the $\text{Al}_5\text{Cu}_2\text{Mg}_8\text{Si}_6$ phase forms [56]. The two phases of Cu form after the main Al-Si eutectic reaction, hence their solidification temperature is low. A high content of Cu in aluminium alloys leads to an increase in porosity [57]. A blocky intermetallic phase was reported with 4.09% Cu in a 380 alloy that nucleated at the interface of other microstructural constituents such as silicon, α -Fe, β -Fe phases since it solidifies last [58]

In alloys containing copper, such as 319 and 332, the presence of copper significantly lowers the impact properties as the fracture behavior is influenced more significantly by the CuAl_2 phases than by the Si particles [59]. In another observation, the copper content has been reported to play a greater role than silicon in reducing DAS [31]. The DAS of 319 alloy could be smaller than that of 354 because of the effects of both silicon and copper. However, the most important aspect in mechanical property is the size of

the secondary dendrite arm spacing (SDAS). The best properties are always associated with smallest SDAS. Dendrite arm spacing (DAS) is the distance between the developed secondary arms.

2.3.4 Influence of Magnesium

Magnesium is soluble in aluminium up to a maximum of 17.4wt% at 450°C [58]. However, even at the low amounts typically added to Al-Si based foundry alloys (between 0.3 to 0.7 wt%), some Mg will precipitate as Mg₂Si as a constituent of the Al-Si-Mg₂Si ternary eutectic. The Mg₂Si phase forms with a Chinese script morphology but readily dissolves upon solution treatment and enters the solid solution [60].

Samuel and Samuel [58] have reported that magnesium containing phases (Mg₂Si or Al₅Mg₈Si₆Cu₂) are not detectable up to the 0.5wt.% Mg level. When the Mg content is high and iron is present, the π -phase (Al₉FeMg₃Si₅) particles with Chinese script morphology will be formed in Al-Si-Mg alloy [61,62]. High levels of Mg counteracts the effect of Mn in stabilizing the α -AlFeSi phases [54]. In another report [63], Mg is observed to refine eutectic Si slightly in unmodified 319 alloys containing mainly β -Fe intermetallics and has also a negative effect on α -Fe intermetallics. Figure 2.4 shows the various intermetallic phases reported for this alloy. These phases are β -Fe, α -Fe, Al₂Cu-phases and eutectic Si particles in alloys (a) Al-5.61%Si-3.2%Cu-0.27%Mg-1.05%Fe, (b) Al-5.89%Si-3.22%Cu-0.273%Mg-1.11%Fe-0.0185%Sr, (c) Al-5.42%Si-3.065%Cu-0.289%Mg-1.042%Fe, (d) Al-5.66%Si-3.09%Cu-0.268%Mg-1.06%Fe-0.02%Sr.

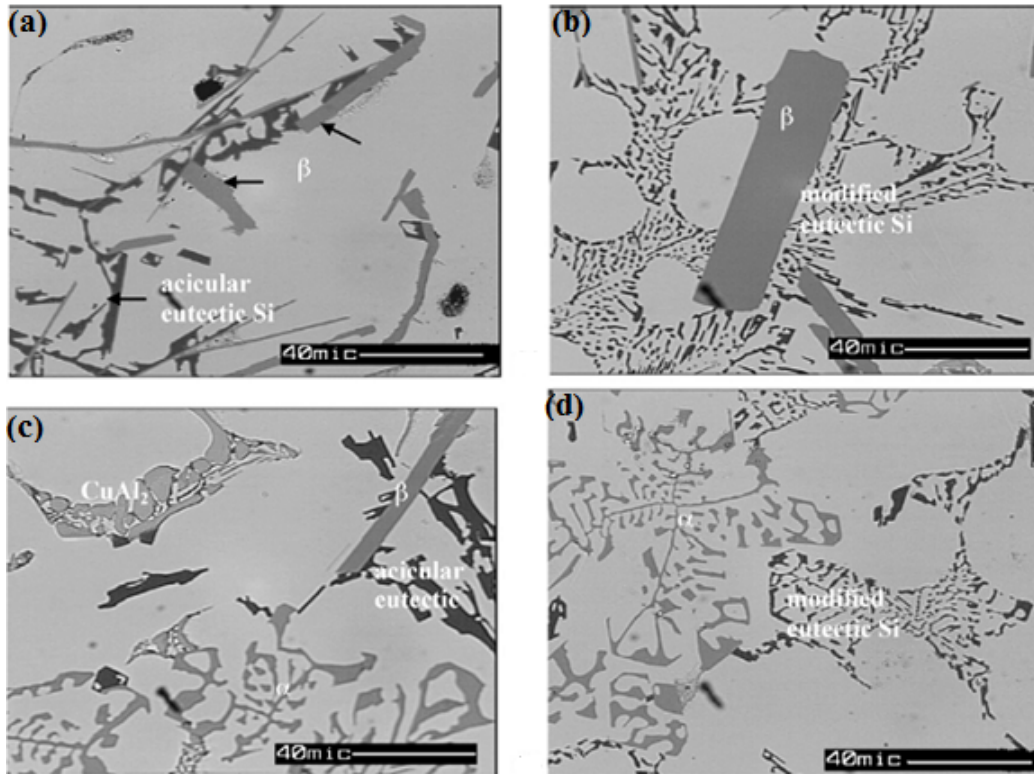


Figure 2.4: Optical micrographs of various common iron-containing intermetallics in 319 type alloys [63]

2.3.5 Influence of Solidification Rate

The solidification of cast aluminium starts with separation of the primary alpha phase from the liquid. After nucleation, when the temperature lowers, the primary phase grows as solid crystals having dendritic shape [31] and at the eutectic temperature Al-Si eutectic solid phase also solidifies in the space left between dendritic arms.

Higher solidification rates retain Fe in solid solution or provides finely distributed hexagonal $\alpha\text{-Al}_8\text{Fe}_2\text{Si}$ with skeleton-like morphology [58]. The silicon particles that appear

coarse, acicular and needles in the microstructure under normal cooling conditions act as crack initiation sites and lower the mechanical properties of Al-Si alloys [63]. Cooling rate profoundly changes the mechanical properties of secondary cast Al-Si alloys by changing the secondary dendrite arm spacing (SDAS), grain size and refinement of secondary phase constituents.

With a higher cooling rate, grain density increases, secondary dendrite arm spacing (SDAS) decreases and the average pore size decreases. However, with low cooling rate, more gas can precipitate and thus higher porosity could be produced. Slowly solidified microstructure possesses large and elongated particles. The increase in the proportion of large and elongated particles with slower solidification is simply due to the increase in diffusion [64].

2.4 Mechanical Properties of Al-Si Alloys

Mechanical properties of Al-Si cast alloys depend not only on the chemical composition but, more importantly, on microstructural features such as the morphology of dendritic α -Al, and other intermetallics which are present in the microstructure. The morphology and size of eutectic Si as well as the precipitation hardening phases during heat treatment also exert an important influence on the mechanical properties. The combined effects of such microstructures are somewhat complicated [3, 23, 42]. An increase in the silicon content from 4 to 20% influences the tensile strength, ductility and hardness of Al-Si-Mg alloys. The ductility of the alloy reduces monotonically while hardness increases over the

range of Si increase. Furthermore, tensile strength increases up to 16% Si, but reduces at higher silicon contents [42].

Higher mechanical properties can be achieved by optimizing the amounts of constituent elements such as Si and Mg as well as by controlling the amounts of impurities such as Fe and Mn [65]. Iron is the most common and harmful impurity in cast aluminium alloys forming the platelet β -Fe intermetallic phase, which is detrimental to mechanical properties. It is common practice to neutralize the detrimental effects of iron by adding certain minor elements such as Mn as previously discussed. According to Hwang *et al.* [33] increasing the Mn content up to 0.65% (ratio of Mn/Fe = 1.2) in 319 alloys, the UTS and elongation were increased. Recently, it was found that as the manganese content increases over 0.5% in aluminium alloys, both yield and ultimate tensile strength increased significantly without decreasing ductility [66]. Adding manganese to aluminium alloys enhances the tensile strength as well as significantly improving low-cycle fatigue resistance.

For a given Mg content, the mechanical behaviour of the alloys is a function of the dendritic structure, the size and shape of Si and intermetallic particles, solution treatment and ageing condition. An increase in the Mg content lowers the ductility of both unmodified and Sr-modified alloys [67]. Ductility and impact energy are the most significant properties reduced by increasing porosity content, which can effectively alter thermal fatigue life [68].

Typical mechanical properties of permanent mould cast aluminium-silicon alloys are

given in Table 2.2. The typical values represent the average of the range for all compositions of the respective alloy and temper [2]. Hence minimum values for design could be expected below the typical properties.

Table 2.2: Mechanical properties of common permanent mould cast aluminium alloys [2]

Alloys	HT	UTS (MPa)	YS (MPa)	%El	BH
319.0	F	235	130	3	85
	T6	275	185	3	95
354.0	T6 ₂	380	310	3	
355.0	F	185	105	4	
	T6	290	185	4	90
C355.0	T6	330	195	8	90
	T6 ₂	330	255	5	100
356.0	F	180	125	5	
	T6	260	185	5	
A356.0	F	185	90	8	
	T6	285	205	12	80
380.0	F	315	160	4	80
A380.0	F	325	150	4	80

T6₂ = Solution heat treated and then artificially aged by the user.

Li *et al.* [3] on their study on parameters controlling the performance of AA319-type alloys observed a reduction in tensile strength, yield strength, impact energy and % elongation with decrease in cooling rate (i.e., increase in SDAS) regardless of the alloy composition in both T5 and T6 heat treatment conditions. Hardness and strength of Mg containing alloys decrease with addition of Sr due to the sluggish dissolution of the $\text{Al}_5\text{Cu}_2\text{Mg}_8\text{Si}_6$ phase during solution treatment and a delay in the precipitation of Mg_2Si or Al_2Cu phase during artificial aging. Ni addition up to 1.41% is observed to decrease the mechanical properties in T6 condition [12]. Nickel is commonly used with copper to

improve the mechanical properties of alloys at elevated temperatures. Addition of copper to Al-Si alloys increases their strength and fatigue properties without loss of castability [69]. Mohamed *et al.* [23] have reported that the impact energy is relatively low with increase in the Cu and/or Mg content, but the combined addition of modifier and grain refiner to a near-eutectic Al-10.8Si alloy produces a significant improvement in impact toughness.

Kumar *et al.* [17] reported that addition of Be, Ca and Sr to an Al-7Si-0.3Mg-0.8Fe alloy significantly improves the impact strength by modifying the eutectic Si from acicular to fibrous form and refinement of the platelet β -phases. The best combination of both tensile and impact properties were observed in the combined addition of Be+Mn, Ca+Mn and Sr+Mn to the Al-7Si-0.3Mg-0.8Fe alloy.

2.5 Heat Treatment of Aluminium Alloys

Heat treating is often used in the aluminium industry to achieve maximum strength or hardness in a suitable alloy. Moreover, heat treatment plays a major role in microstructural homogenization, residual stress relief, to improve dimensional stability, machinability and corrosion resistance [70, 71]. The T6 heat treatment temper is commonly used due to the capability of yielding the best properties. In T6 treatment, three basic operations are carried out when heat treating a product fabricated from aluminium castings: solution heat treating, quenching and aging [71]. Addition of Mg, Cu, and Zn to Al-Si alloys makes them heat treatable, thus providing the means to enhance the properties

using appropriate heat treatment procedures and practices [12].

Solution treatments dissolve the solutes present in the alloy which are responsible for the hardening response, homogenize the casting and spheroidize the eutectic silicon. The main purpose of the solution heat treatment is to obtain a supersaturated solid solution but in order to maintain this desired condition at low temperatures, quenching is needed [72]. The solution treatment also improves the distribution of eutectic silicon particles besides their spheroidisation. It was also reported that the morphology of primary silicon particles is not affected by heat treatment [42]. Standard T6 treatment specifies that the solution heat treatment of 319 alloys should be carried out at approximately 505°C and maintained for 4 - 12 hours depending on the casting method. Shorter periods of time are recommended for permanent mould castings and longer times for sand castings [73].

Industrial solution heat treatments are performed well below eutectic solidus temperatures. It is also good to hold a material at relatively high temperature long enough to allow constituents to dissolve into a solid solution during homogenization and solution heat treatments [74]. However the temperature should be restricted to a range below the solidification point so as to avoid incipient melting while at the same time taking into consideration the fact that if the solution temperature is too low, a reduction of mechanical properties will result.

Tash [63] found out that for 356 and Mg containing 319 alloys having both α -Fe and β -Fe intermetallics, peak hardness is obtained at 180°C for 4h during aging. Moreover,

for the same concentration of Mg in both alloys, the 319 displayed high hardness due to cooperative precipitation of Al_2Cu and Mg_2Si phase particles. Magnesium and Sr modification lead to segregation of the Al_2Cu phase in areas free of eutectic Si particles, explaining the fairly sluggish dissolution rate of the copper phase upon solutionizing at 505°C [44, 63].

Artificial aging of Al-Si-Mg alloys in the temperature range of $170\text{-}210^\circ\text{C}$ gives peak yield strength while Cu containing alloys show a decrease in peak yield strength with increasing ageing temperature [75]. Solution treatment at 505°C for 6 h, water quenched and artificial aging at 170°C for 8 h of AlSi_6Cu_4 alloy has been reported to improve the mechanical properties. The YS was elevated from 137 MPa as-cast to 384 MPa after T6 and the UTS from 194 to 408 MPa [76]. Artificial aging treatment for 8 h at 170°C with small additions of 0.4 wt% Mg has been reported to produce higher values of properties such as tensile strength and microhardness at the expense of reduced elongation and impact toughness in the 319 base alloy [72].

In another research by Jung *et al.* [77] on Al-6.2Si-2.9Cu AC2B alloy, the phases in as-cast condition such as Al- Al_2Cu eutectic, Al_2Cu and $\text{Al}_5\text{Cu}_2\text{Mg}_8\text{Si}_6$ were observed to reduce gradually with the increase in solution treatment time at 500°C and finally disappeared after 5 h soaking time. However the mechanical properties, such as hardness, tensile strength, and elongation, were improved after 5 h soaking time due to the dissolution of the Al_2Cu particles. Accordingly, the optimal solution heat treatment condition of the Al-Si-Cu (AC2B) alloy is considered to be 5 h at 500°C .

2.6 Castability of Aluminium-Silicon Alloys

Castability is the ability of a metal or an alloy to be effectively cast to a given shape/pattern without formation of casting defects such as cracks, segregation, hot tearing or pores [78].

Castability is mostly measured by the porosity generated in the castings and the fluidity characteristics of the molten metal [79].

2.6.1 Porosity of Al-Si Cast Alloys

Casting defects like porosity, in cast aluminium components greatly affect their mechanical properties especially fatigue [80]. Porosity is expressed as voids or cavities that are formed within a casting during solidification and it is the major cause of rejection in material production of castings. The causes of porosity are shrinkage resulting from the volume contraction associated with solidification as well as, inadequate flow of molten metal and hydrogen gas evolution.

Modifiers of Al-Si alloys refine the eutectic silicon particles and improve the mechanical properties of casting, but usually increase the porosity and decrease hydrogen solubility in solid metal by depressing the solidification temperature [22]. And the decrease in hydrogen solubility result in increased porosity level in an alloy. Porosity acts as the main crack initiation site leading to a reduction in fatigue life especially as the size of the surface pore increases [80, 81].

Fe - intermetallics such as β -Al₅FeSi phases are reported to generate porosity [33]. This is because β - phases have higher potential in blocking the channels that feed solidification

shrinkage. Hence, with the increase of iron level in an alloy, porosity will increase due to the formation of β - phases.

2.6.2 Fluidity

Fluidity of Al-Si alloys has been investigated by many researchers and is known to be affected by many factors such as channel thickness, melt head, mold temperature, superheat, solidification range, viscosity, mould surface, grain refining, inclusion and intermetallic phases [76, 82, 83].

2.6.2.1 Influence of Pouring Temperature on Fluidity

Increasing the casting superheat has a direct influence on the fluidity of Al-Si alloys. According to Disaba [84] the fluidity length of an alloy increases by approximately 1% with an increase of superheat of 1°C in the temperature range of 700-730°C. Increasing the pouring temperature delays the nucleation and growth of fine grains at the tip of the flowing metal in the test channel, hence the fluidity length increases. Hypereutectic Al-Si has good fluidity since pure silicon has a latent heat of fusion about 3.4 times greater than that of aluminium [85]. For pure metals and alloys with eutectic composition, flow stops when the columnar grains from both sides of the wall meet as shown in Figure 2.5 (a). However the flow of long freezing range alloys stops at the leading tip of the flowing stream [83] as shown in Figure 2.5 (b). The dendrites stop the flow when they reach a critical fraction solid [86].

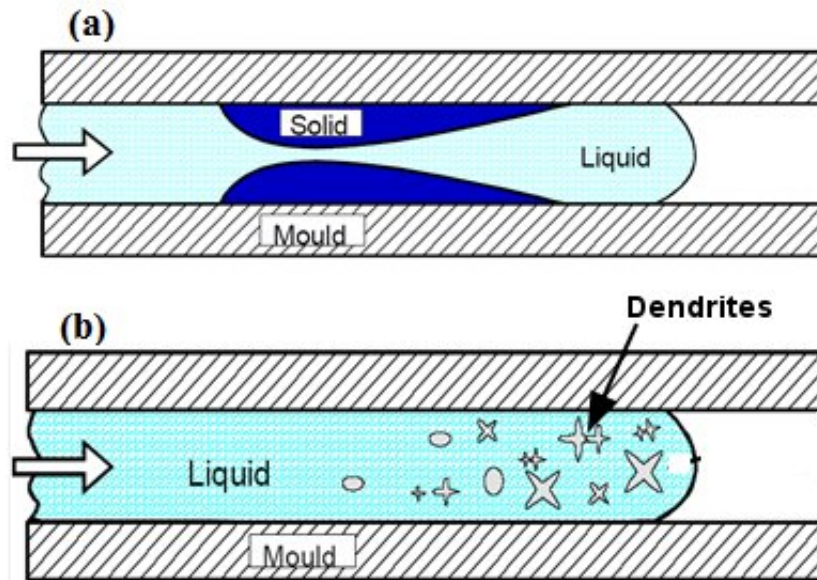


Figure 2.5: Solidification pattern (a) in pure metals by complete solidification; and (b) in long-freezing-range alloys by partial solidification [85]

2.6.2.2 Influence of Alloying Elements Composition on Fluidity

Alloy chemistry is one of the main factors influencing fluidity [87,88]. Alloys with eutectic or near eutectic composition possess the best fluidity at conventional pouring temperature [2]. Hypereutectic alloys possess high fluidity due to less friction in the liquid because of the formation of primary Si as well as lack of dendritic interlocking which does not take place in these alloys. Therefore increasing the silicon content of the alloy increase fluidity with a maximum at around 17-18 wt.% Si [89]. The latent heat of fusion of Si is also among the highest elements. Generally, Al-Si alloys increase their fluidity with increasing silicon content as a result of the powerful effects of Si [90]. The effects of titanium and strontium on the fluidity of A319 and A356 alloys were investigated by Sanchez *et al.* [91]. It was found that an increase in titanium enhances the fluidity of the

A319 alloy due to its high potential to refine the grain size. Further, the fluidity index of the A356 alloy was found to increase with the increase of Sr.

Strontium addition to levels of 0.015 wt.% and 0.02 wt.% increases fluidity while a combined addition of 0.02 wt.%Sr and 0.28% Al-5Ti-1B decreases the fluidity of LM25 and LM27 alloys [88]. Addition of grain refiner to AlSi7Mg and AlSi11Mg alloys was reported to affect fluidity. The fluidity was observed to decrease when the level of Ti is below 0.12 wt.% and increases above this level in both alloys [86]. Addition of 0.1 wt.% Cr to LM6 was reported to decrease the fluidity due to the formation of sludge [92].

According to Mose *et al.* [88] no change in fluidity was observed during addition of Fe from 0.14% to 0.4 wt.% on LM25. However, 21% increase was noted by increasing Fe level to 0.48 wt.%. A study made by Gowri and Samuel [93] on 380 alloy, Fe levels of 1.5 and 1.7 wt.% were reported to decrease the fluidity by 4% and 6% respectively. This decrease in fluidity is associated with the formation of β - Fe phases which have the potential to block the feeding channels.

2.7 Theory of Developing Recycle-Friendly Aluminium Alloys

A recycle-friendly alloy allows utilization of post consumer products into standard or non-standard composition alloys that possess acceptable properties for application [7,94]. The objective of identifying new recycle-friendly aluminium alloy compositions is to increase opportunities of direct reuse of recycled aluminium products . Such an approach requires compositions with relatively broad specification limits on major alloying elements such

as Si, Cu and Mg, plus more tolerant limits on Fe and other impurities. According to Das [7], fully developing this approach requires several important steps which include the following;

1. Precise identification of the sources of scrap materials and expected ranges of chemical compositions. Hence, it clearly requires sorting and chemical composition analysis of the incoming scraps.
2. With the type of alloys and mass of each alloy in hand, identify candidate alloy composition limits that would most effectively directly utilize the anticipated recycled metal and seem likely to provide acceptable/desirable performance characteristics for a wide variety of applications.
3. The recycle-friendly alloys should also be produced experimentally and evaluated their microstructure, mechanical properties performance and castability in order to assess their suitability for representative applications as compared to existing alloys.

Mixing various fractions of scrap with different alloying chemistries is practically challenging to get the standard ones and it should be expected that there will be negative effects of higher impurity levels due to the intricate mixture of alloys found in post consumer scrap. The mixture that could be obtained by combining such different fractions of scrap may result in the element percentage composition higher, lower or within the standard alloys. Hence, sorting out of components and close control of chemical composition is necessary.

2.7.1 Recycle Friendly Alloy Practice

The primary challenge of evaluating the recycle-friendly alloy is the amount of scrap an alloy can accommodate, the types of scrap metal available to producers, the compositional characteristics of these scrap metal, and the metallic yield (the percentage of raw material that ends up as usable product) [95]. In practice, different scrap alloys can be utilized for developing an alloy with pre-melt sorting, mixing appropriate quantities of scrap, diluting with primary aluminium and adding alloying elements [96]. However, this practice is not fully applied for high quality value added products except in some scrap such as bumper and used beverage can (UBC) which are used for the same application [15,97].

Study by Dimos *et al.* [97], on the production of 380.0 and AA3104 alloys by blending post consumer scrap alloys with pure metals indicated that, the 380.0 alloy can accommodate 99.7% scrap of aluminium engines and transmissions and needs only about 0.3% pure metal addition for the adjustment of its chemical composition. Whereas AA3104 alloy can be produced from 100% scrap of used beverage cans (UBC) and it can also accommodate 7.8% of scrap aluminium engines and transmissions but needs 92.2 % of pure metals addition. Hence, production of 380.0 from scrap is effective due to its broad compositional range while AA3104 has tight composition range for alloying elements such as Cu and Si.

2.7.2 Aluminium Alloy Recycling Index

The aluminium recycling index (ARI) is proposed as an industry aid for identifying the potential for recyclability of aluminium alloys [98]. The ARI is expressed as, $ARI (\%) = (100 - \text{Total solute content of the alloy})$. Table 2.3 shows the ARI and Recycling Production Index (RPI) values of some cast aluminium alloys.

Table 2.3: Values of ARI and RPI for some cast alloys [98]

Alloy	Nominal alloying content (%)	Nominal impurity content (%)	Sum element content (%)	Nominal aluminium content ARI (%)	Potential for recycling (RPI)
356.0	7.3	1.0	8.3	91.7	Medium
A356.0	7.4	0.5	7.9	92.2	Unlikely
319.0	9.5	1.9	11.4	88.6	High
380.0	12.0	3.5	15.5	84.5	High
354.0	11.1	0.4	11.5	88.6	Medium
355.0	6.7	1.0	7.8	92.3	Medium

The ARI can play a role in identifying which existing alloys can be most readily recycled for direct reuse or most difficult for recycling because of the presence of undesirable elements such as Ag, Be, Pb, or Li and because of the presence of very high levels of elements such as Cu, or Zn [98]. However, the recycling index, groups alloying elements into one entity, irrespective of their effect, hence, requires further compositional analysis of each elements [99].

RPI is another measure of guidance for producing an alloy directly from recycling of scrap. RPI measures capability of producing alloys directly or with minimum processing

from scrap and utilized in the production of the same product or another high value product [98].

Cast alloys have generally higher tolerance limits for all constituent elements compared to wrought alloys. The common restraint of the existing wrought alloys is that their alloying element compositional limit is not tolerant enough to be produced by direct mixing and melting of scrap batches without sorting of the mixed scraps to the desired level.

2.8 Predicting the Composition of an Alloy

The composition of an alloy can be predicted using Rao's [99] approach expressed by equations 2.1. This method relates the chemical composition of a recycled alloy, the suggested recycled alloy and the standard alloy. The formula is used for computing the compositions of individual elements in the suggested alloy.

$$C_{rp} = \sum_{i=1}^n \frac{C_i}{n} \quad (2.1)$$

$$DF_i = C_{si} - C_{ra}$$

Where

C_{rp} is the wt% of a given alloying element present in the predicted recycled alloy.

C_i is the wt% of a given alloying element present in an individual scrap alloy.

n is the Number of scrap alloys used.

DF is the Deviation Factor.

C_{si} is the wt% of a given alloying element present in the most equivalent standard alloy.

Cra is the wt% of a given alloying element present in the synthesized actual recycled alloy.

2.9 Literature Survey on Alloys Used for Cylinder Head Application

Automotive components are fabricated from a variety of alloys. These include wrought alloys like auto bumper (7029) and auto body (AA6022) and cast alloys such as automotive wheels (A356), engine blocks and cylinder heads (319) [34,100]. Cylinder heads are especially manufactured from a number of different aluminium cast alloys. Based on the literature survey carried out in this research, a compiled data is presented in (Table A.1) Appendix A . The list of alloys shown in Appendix A includes the standard alloys which are used for cylinder heads and their modified versions developed by researchers for improved performance. The focus on this data was toward the chemical composition of the alloys as it was anticipated to give more input on the secondary alloy development.

Developing an alloy based on the literature survey may not provide full guidance on recycle friendly alloys. However, it provides useful information on the chemical composition specifications of the alloys in the market. Chemical composition analysis, sorting scrap component by component and considering some compositional adjustment will provide a suitable route for developing recycle friendly candidate model alloys further evaluated for use in automotive and other engineering applications.

2.9.1 Summary

The literature indicates that Al-Si based alloys are highly affected by chemical composition, moulding parameters, solidification rates and heat treatment [23,29,33]. The above considerations profoundly change the mechanical properties of the alloys by changing the microstructure (e.g., dendrite arm spacing, the intermetallic phases, and the eutectic Si particles).

Addition of alloying elements and heat treatment are the most widely practiced methods of improvement of mechanical properties in the foundry industry. Elements such as iron, magnesium and copper contribute to the strength and hardness of the alloy. However, if these elements are in excess, they form hard intermetallic phases whose contribution is deleterious [54]. Higher mechanical properties can be achieved by optimizing the amount of major elements such as Si, Cu and Mg as well as by controlling the amounts of minor elements and impurities such as Fe and Mn [65].

Moreover, the alloys used for cylinder heads have high amount of variations in their chemical composition in all major and minor alloying elements. Hence, recycling different post-consumer cylinder heads without giving attention to their chemical composition can result in an alloy with poor performance.

Recycling aluminium scrap for high quality application is not common in most of the foundry industries except for some scrap metals such as used beverage cans (UBC) which are fully utilized for the same application. This is due to the concentration of alloying

element and effectiveness of scrap sorting [11].

The aim of this study is to identify and develop a recycle-friendly aluminium alloy that allow direct reuse of cylinder head scrap and to investigate its microstructure, mechanical properties and castability. It is anticipated that this will help in improving recycling efficiency and encourage the use of recycled alloys for the production of premium castings.

CHAPTER 3

METHODOLOGY

3.1 Introduction

This research project aims to utilize the available scrap aluminium alloys for the application of high quality product castings. The preparation of the scrap ingots and fabrication of fluidity moulds were carried out at Jomo Kenyatta University of Agriculture and Technology. The chemical analysis of the base alloy and scrap cylinder heads were carried out by AMG in the UK and some chemical composition analysis were carried out by Booth Extrusions in Thika. Alloy preparation, fluidity testing, tensile testing, micro-hardness measurements and metallography images were carried out at the University of Nairobi while the impact energy testing was carried out in Jomo Kenyatta University of Agriculture and Technology.

3.2 Identification of the Recycle Friendly Alloy

The composition of the recycle friendly alloy was identified based on the standard alloys used for cylinder head application. It is these standard alloys that will be supplied as scrap alloys at their end of life. The standard alloys obtained from the literature survey were grouped into five categories with the aid of their chemical composition. The groups were arranged further as source and target alloys. This was to identify alloys that could potentially serve as alternative targets (recycle friendly) and to identify which alloys are

most suitable as source alloys.

The industrial commercial Al-Si alloys shown in Table 3.1 were used in developing a model recycle-friendly alloy. The alloys have been categorized such that each group has alloys with minor difference in some alloying elements.

Group A alloys have differences only in the Fe content. In A356, EN AC-4200 and ZL101A alloys, the Fe content is 0.2 wt% while it is 0.5 wt.% in JIS AC4C and LM 25 alloys. Manganese is also high in these latter alloys but this is expected since it is usually added to neutralize the effect of iron, hence, it goes parallel with the level of iron. Similarly, in group B there are minor differences in Si and Zn. Group C alloys comprises of secondary alloys whose chemical composition is expected to vary depending on the manufacturer. Moreover, the elemental deviation in group D alloys as well as group E alloys is minimal. Hence, the difference in chemical composition among the equivalent alloys is low.

The calculation was based on the maximum compositional limits of each alloy's element present in the group of the standard alloys. The scrap (source) which has elemental composition more than the target alloy could not be suitable as a source because this will require significant dilution. The target alloy which accommodates more types of scrap (source) alloys is the one which serves as the recycle-friendly alloy.

Table 3.1: Equivalent alloys group [31, 33, 101–104]

Group	Standard alloys	Si	Cu	Mg	Fe	Mn	Ti	Zn	Ni	Others (Sn, Pb, Zr...)
A	A356	6.5/7.5	0.2	0.2/0.45	0.2	0.1	0.2	0.1		
	JIS AC4C	6.5/7.5	<0.2	0.2/0.4	<0.5	<0.3	<0.2	<0.3		
	LM25	6.5/7.5	0.2	0.2/0.6	0.5	0.3	0.2	0.1	0.1	0.05
	EN AC-42100	6.5/7.5	0.05	0.25/0.45	0.19	0.1	0.08/0.25	0.07		0.1
	ZL101A	6.5/7.5	0.1	0.25/0.45	0.2	0.1	0.08/0.25	0.1		0.25
B	319.0	5.5/6.5	3.0/4.0	0.1	1.0	0.5	0.25	1.0	0.35	0.5
	JIS-AC2B	5.0/7.0	2.0/4.0	<0.5	<1.0	<0.5	<0.2	<1.0	<0.3	
	LM 4	4.0/6.0	2.0/4.0	0.2	0.8	0.2/0.6	0.2	0.5	0.3	0.2
	EN AC - 45100	4.5/6.0	2.6/3.6	0.15/0.45	0.60	0.55	0.25	0.2	0.1	0.3
	EN AC - 45200	4.5/6.0	2.5/4.0	0.4	0.80	0.2/0.4	0.20	0.55	0.30	0.55
C	A380.0	7.5/9.5	3.0/4.0	0.1	1.3	0.5		3.0	0.5	0.5
	JIS AC4B	7.0/10.0	2.0/4.0	<0.5	<1.0	<0.5	<0.2	<1.0	<0.3	
	LM27	6.0/8.0	1.5/2.5	0.30	0.8	0.2/0.6	0.20	1.0	0.35	0.3
	EN AC-46200	7.5/9.5	2.0/3.5	0.05/0.55	0.8	0.15/0.65	0.25	1.2	0.55	0.6
	EN AC-46600	6.0/8.0	1.5/2.5	0.35	0.8	0.15/0.65	0.25	1.0	0.35	0.5
D	354.0	8.6/9.4	1.6/2.0	0.45/0.6	0.2	0.1	0.2	0.1		0.15
	ZL111	8.0/10.0	1.3/1.8	0.4/0.6	0.4	0.1/0.35	0.1/0.35	0.1		0.06
E	355.0	4.5/5.5	1.0/1.5	0.4/0.6	0.06/0.6	0.03/0.5	0.04/0.25	0.03/0.35		0.15
	LM 16	4.5/5.5	1.0/1.5	0.4/0.6	0.6	0.5	0.2	0.11	0.25	0.15
	EN AC - 45300	4.5/5.5	1.0/1.5	0.35/0.65	0.65	0.55	0.05/0.25	0.15	0.25	0.2
	ZL105	4.5/5.5	1.0/1.5	0.4/0.6	1.0	0.50		0.30		0.06

3.3 Chemical Composition Analysis on Scrap Cylinder Heads

Chemical composition analysis was carried out for randomly selected scrap automotive engine cylinder head used for small vehicles. The scrap cylinder heads were obtained from different vendors in Nairobi and their chemical composition analysis was carried out using an optical emission spectroscope (OES) spark machine by AMG in UK and by Booth Extrusions in Thika.

3.4 Experimental Work

3.4.1 Materials and Scrap Ingot Preparation

The main sources of material for the research were the cylinder heads obtained from different vendors. About 85 kg of post-consumer cylinder heads were randomly sourced from scrap vendors in Nairobi. After removing all external parts and cleaning, the materials were set ready for melting. The melting of the cylinder heads was carried out at Jomo Kenyatta University of Agriculture and Technology in an oil fired graphite crucible furnace with melting capacity of 70 kg. Seven cylinder heads were melted under cover flux to a temperature of 720°C. An amount of 0.35 percent of the total weight of metal melt powder coverall flux was introduced at two stages, during the initial stage of melting and when the metal reached the pouring temperature. The melt was skimmed off before pouring.

Silica sand bonded by sodium silicate/ CO_2 was used to fabricate a conical 4 kg capacity ingot moulds. The ingot moulds were heated by oxyacetylene flame till all the moisture was removed and the molten metal was poured using preheated ladle. Samples for chemical analysis were rapidly solidified in specially fabricated copper ingot moulds by immediately immersing in cold water. The chemical composition of the base alloy (scrap ingot) is shown in Table 3.2.

Table 3.2: Chemical composition of base alloy (Scrap Ingot)

Alloy	Si	Cu	Mg	Fe	Mn	Cr	Zn	Ni	Ti	Pb	Sn
Base alloy (SI)	6.01	2.62	0.24	0.28	0.21	0.02	0.12	0.02	0.02	0.01	0.01

3.4.2 Preparation of Bar Casting

Melting of the cylinder head ingots for obtaining the test bar castings was carried out in a 4 kg capacity SiC crucible, using an electric muffle furnace at University of Nairobi. Nitrogen gas was used for degassing the melt by immersing a ceramic tube deep into the molten metal to allow removal of hydrogen. The melt temperature was kept at 740°C during pouring. K-type thermocouple was employed to measure the temperature of the molten metal.

Master alloys of Al-10% Sr in the form of metallic rod and Al-75% Fe and Al-75% Mn in the form of briquettes were used to achieve Si eutectic modification and to investigate the model alloy's tolerance to impurity levels respectively. After completely stirring to dissolution and homogenization of the alloy chemistry, the molten metal was skimmed to remove dross and surface oxides prior to pouring. The degassed melt was then poured into a permanent metal mould. The permanent metal mould was preheated to a temperature of 450°C. Figure 3.1 (a) shows the permanent metal mould used for successive casting and (b) the bar casting produced using the mould. The mould has a wedged-shaped geometry which provides efficient feeding and variable cooling rate.

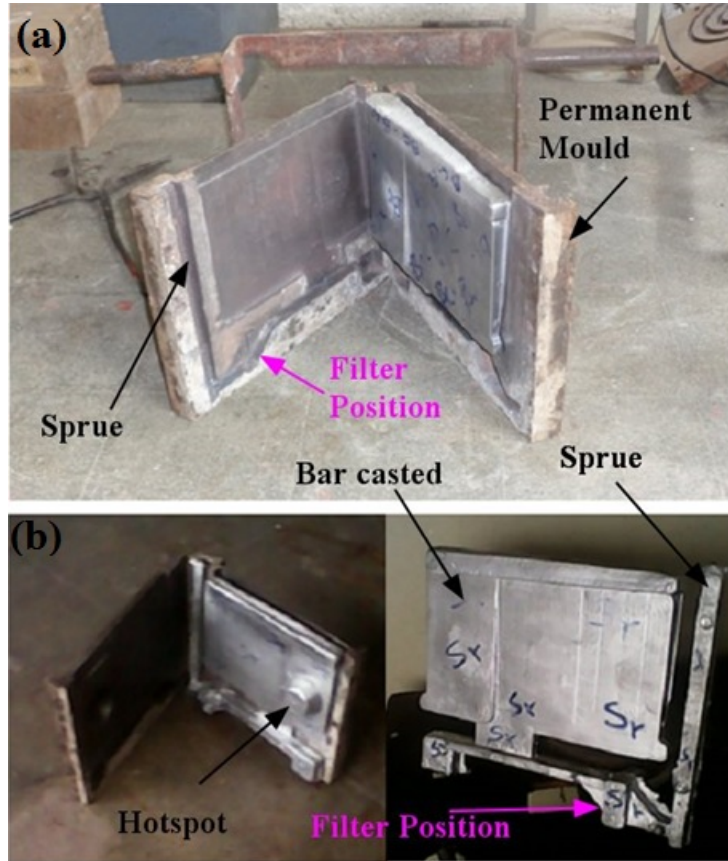


Figure 3.1: (a) Permanent cast iron mould and (b) Sample bar casting

A ceramic foam filter with a dimension of 50x50x20 mm and 30 pores per inch (PPI) was used for each casting to minimize turbulence during pouring and for trapping of inclusions. After solidification, sample bars were sectioned from different positions in order to obtain specimens for tensile, impact toughness, hardness and microstructure analysis.

The composition of the alloys developed for investigation is shown in Table 3.3. The weight percentage of the added elements that are shown in the table reflects the final composition of the element in the alloy.

Table 3.3: Experimental alloys developed

Sr.No.	Experimental alloys with total composition of each additive element in the alloy
1	Base alloy (SI)
2	SI + 0.02% Sr
3	SI + 0.38% Fe
4	SI + 0.9% Fe + 0.45% Mn

3.4.3 Preparation of test specimens

The specimens for mechanical properties and microstructure investigation were generated from the bar casting. Sample bars were sectioned as indicated in Figure 3.2.

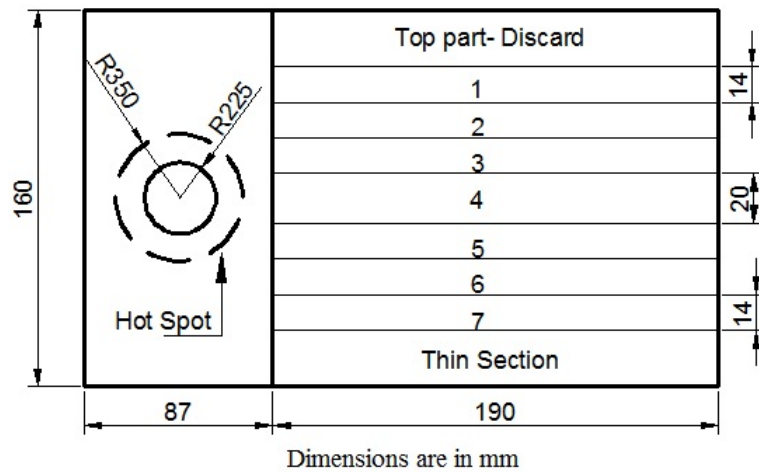


Figure 3.2: Sectioning of the bar casting. section 1, 2 and 3-tensile specimens; section 4-microstructure and micro-hardness and; section 5, 6 and 7-impact energy

Sections 1 to 3 were used for tensile testing while section 4 was utilized for microstructure and micro-hardness analysis. Finally section 5, 6 and 7 were used for impact energy testing analysis.

3.4.4 Heat Treatment

The test samples were solution heat treated for 6 hours at 495°C, and quenched in 65°C water. After solution treatment and quenching, the samples were left at room temperature for natural aging for 24 hours. The samples for tensile and impact energy testing were then artificially aged for 8 hours at 170°C.

The samples for micro-hardness were heat treated in the T4 and T6 temper. In the T4, the samples were solution heat treated for 6 hours at 495°C, quenched in 65°C water and then left at room temperature for 24 hours for natural aging while in the T6, the samples were solution treated for 6 hours at 495°C, quenched in 65°C water and finally artificially aged at time intervals of 2, 4, 6, 8, 10, 12, 16, 18 and 24 hours at 170°C in an air circulated furnace.

3.4.5 Microstructure Examination

3.4.5.1 Optical Microscopy

The samples were sectioned and organized for metallographic examination using Optika - optical microscope B - 353 MET shown in Figure 3.3. Each sample was ground by successively rubbing on different grades of 240, 320, 400 and 600 SiC paper under a flow of water. The specimen was washed between each paper finish to remove any grit and rotated through 90° before the next paper. After the last paper, the specimen was washed well in water and then methanol and dried.

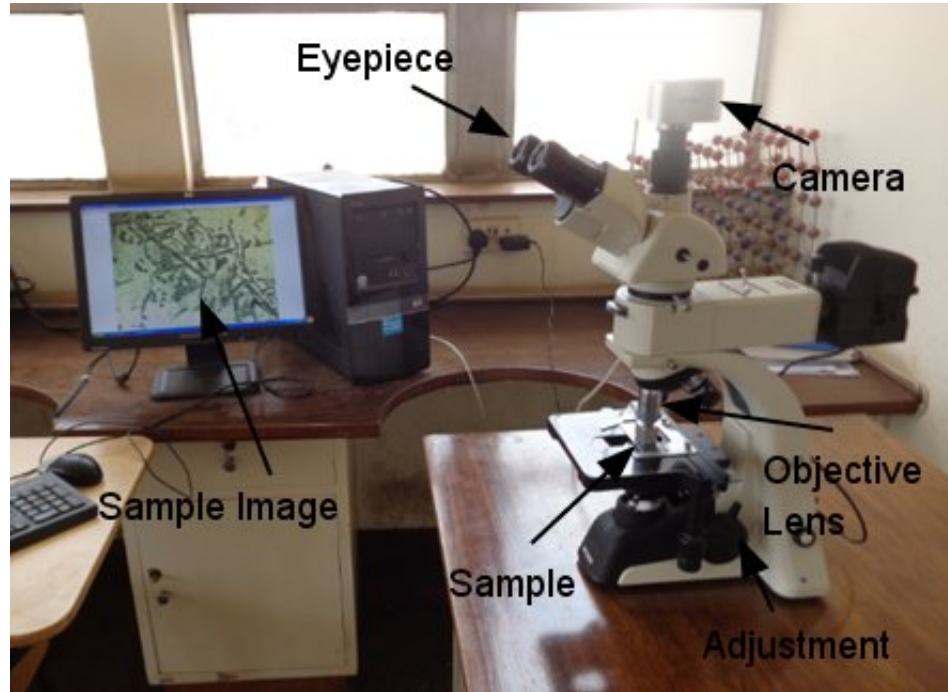


Figure 3.3: Optical microscope connected to the computer at the University of Nairobi.

The samples were then successively polished on a rotating wheel covered with a suitable cloth impregnated with a polishing diamond compound of $6\mu\text{m}$, $1\mu\text{m}$ and $\frac{1}{4}\mu\text{m}$. They were then washed with water and methanol and hot-air dried. Both as-cast and heat treated samples were carefully polished for metallographic examination, after which their images were taken for microstructural analysis. No metallographic etchants were used in this process.

3.4.6 Porosity Measurement

Porosity observation on the T6 heat treated samples used for mechanical properties tests were investigated using optical microscope on their polished surface. Magnification of 80x was used to investigate the pores size and distribution on the castings.

The pores size of cast aluminium alloys is mostly expressed in terms of equivalent pore diameter ($D_{eq} = \sqrt{4A/\pi}$) or maximum feret diameter [105]. Equivalent pore diameter approach was used for this work for comparison of the pores among the alloys and for assessing the effect of porosity on the mechanical properties. The surface area (A) of the pores on the sample were obtained from the micrographs using imageJ and then after the equivalent pore diameter was calculated.

3.4.7 Mechanical Properties

3.4.7.1 Tensile Strength

The tensile specimens were machined according the ASTM B557M standard with the dimensions shown in Figure 3.4 (a). Figure 3.4 (b) shows actual machined tensile test specimens.

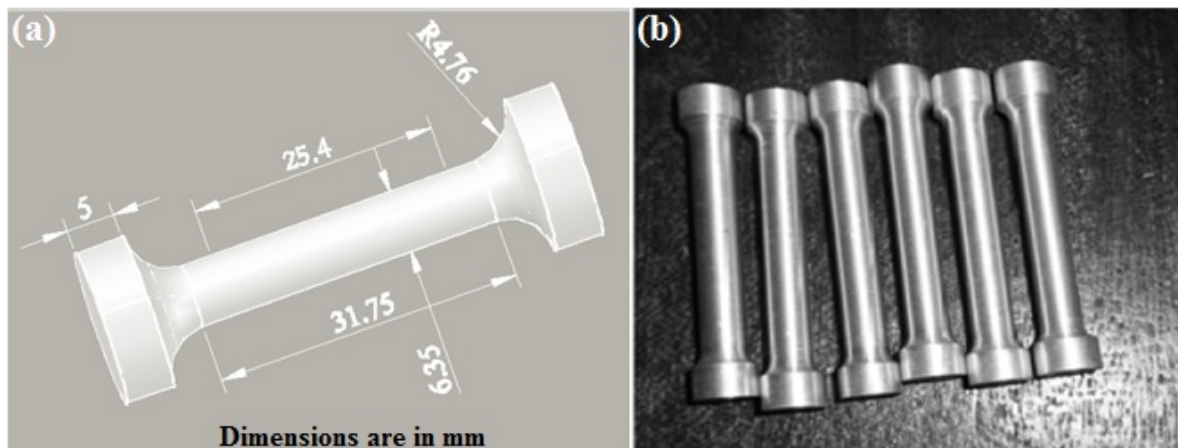


Figure 3.4: Tensile specimen prepared from the bar casting.

The tensile tests were performed at room temperature using the Hounsfield Tensometer located at University of Nairobi. Six as-cast and heat treated specimens for each alloy

were subjected to a uniaxial force . The yield stress was based on the standard 0.002 plastic offset strain. The tensile specimens were re-assembled after fracturing to get the change in elongation from which percentage elongation was calculated.

3.4.7.2 Impact Energy Test

Impact toughness test samples were also machined and prepared from the bar castings according to the ASTM E23 standard. The surfaces of the specimens were polished with 220 grit SiC paper to eliminate any surface irregularities that might affect the result. The specimen dimensions were 10 mm x 10 mm x 55 mm. For each alloy, seven un-notched specimens were used. The impact energy of the specimen was measured using Charpy impact tester Model CI-30 with total weight of the pendulum 25.71 kg, distance between impact center to pendulum revolving center 0.65 m and a maximum lift angle of the machine is 142.5 degrees. The impact energy data was taken by recording the lift and swing angles of the striking hammer during testing.

3.4.7.3 Hardness Test

Hardness measurements were taken for each alloy's specimen using the Vickers Hardness Tester LV-800 AT located at University of Nairobi and shown in Figure 3.5. The available loads of the testing machine range from 2.942 N to 294.2 N. However, the load used for this experiment was 29.42 N for a dwell time of 10 seconds. The testing machine had a diamond indenter of a square shaped base and an angle of 136° between faces.

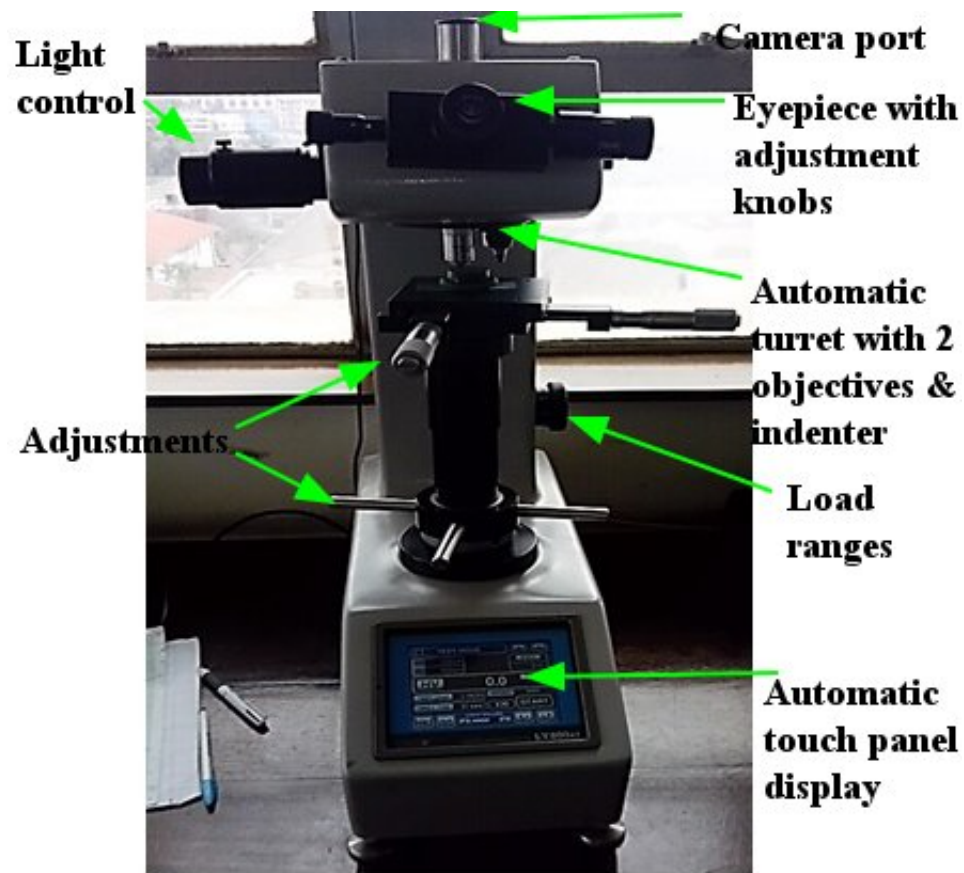


Figure 3.5: Vickers Hardness Tester LV800 AT

The samples for micro-hardness were prepared in a similar way as the metallographic samples. Twenty readings were taken for each sample to get the representative (accurate) hardness of the material since taking few reading may falsify the result by all the data points falling on the hard intermetallic phases or on the soft aluminium matrix.

3.4.8 Fluidity Test of the Alloys

The mould used for testing the fluidity of the alloys was fabricated from silica sand bonded by sodium silicate/CO₂. The mould consisted of a pouring basin incorporated with the cope, a rectangular tapered sprue with small circular section that extended to

the drag, and spiral cavity completely in the drag and the wide opening of the cavity was also pointing upward. The dimensions of the mould were 290 mm x 275 mm x 40 mm and with pressure head height of 99 mm. The moulds were fully vented during fabrication to remove the moisture. An aluminium spiral pattern was cast in already existing permanent spiral mould that had been designed and machined from cast iron during previous study [47]. The spiral pattern was then subsequently used in the preparation of the spiral sand moulds. Moreover, the spiral pattern, the complete set-up and sectional view of the fluidity mould used for successive casting are indicated in Figure 3.6.

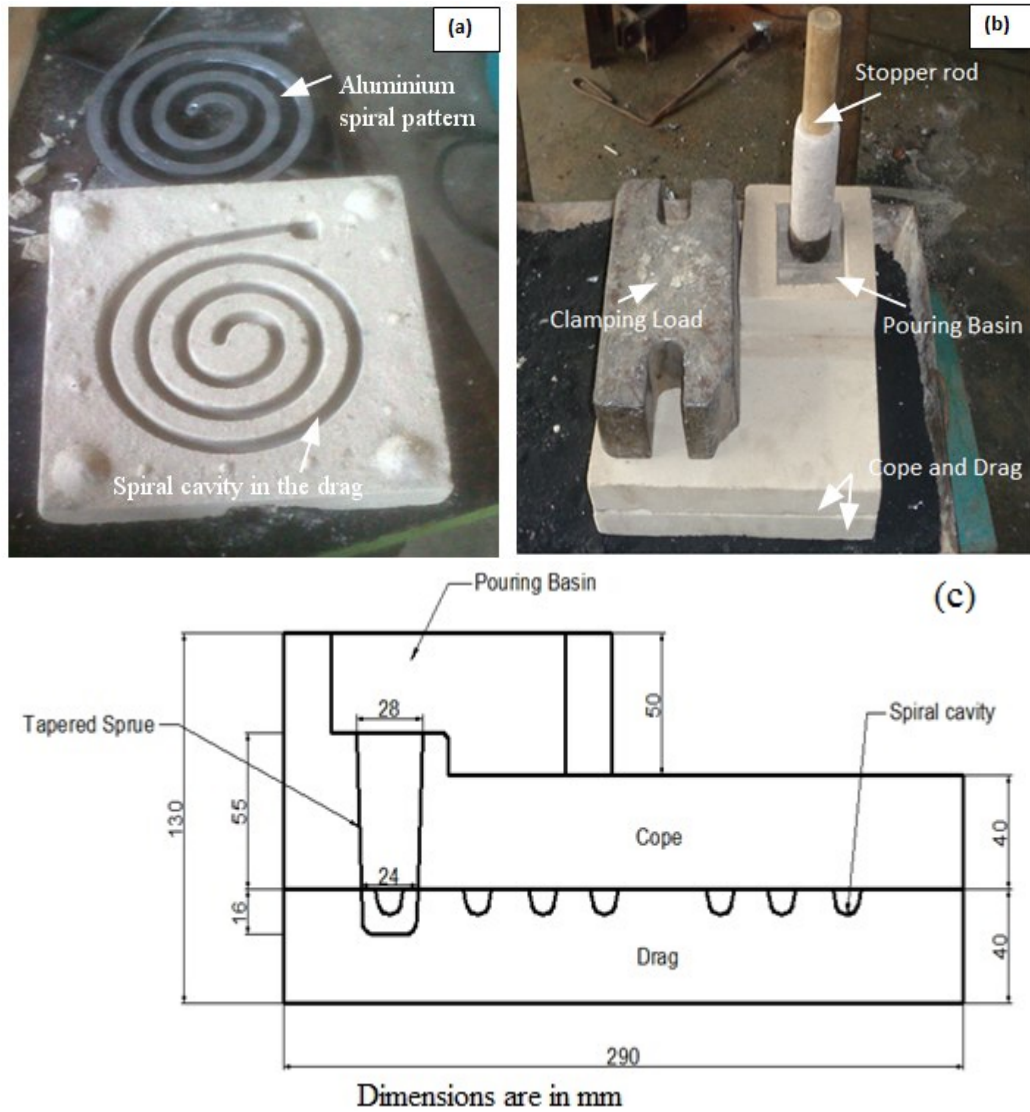


Figure 3.6: (a) The spiral pattern and drag with spiral cavity, (b) The complete mould of the fluidity test and (c) The dimensional detail of complete system of fluidity testing mould.

3.4.8.1 Melting and Pouring

The ingots of the alloy developed were heated to a temperature of 760°C in an electric muffle furnace located at University of Nairobi. The effect of Fe, Mn and eutectic Si

modification by Sr on the fluidity of model secondary alloy was investigated. The Sr modifier was available in the form of Al-10% Sr master alloy metallic rods while Fe and Mn were available as Al-75% Fe and Al-75% Mn briquettes. The effect of Sr was investigated through addition of 0.02 wt.% Sr while that of Fe was investigated by increasing the Fe content in model alloy to 0.38 wt.% and 0.9 wt.%. However, the 0.9 wt.% Fe alloy also included a Mn addition of 0.45 wt.%

The alloying process was done when the temperature of the molten metal reached between 730°C and 750°C. The pouring temperature of the metal was maintained within $720 \pm 3^\circ\text{C}$ for all successive tests. K-type thermocouple was employed to measure the temperature of the molten metal while it was in the 4 kg capacity SiC crucible. Pouring time range; that is; the time between filling the basin and removal of the stopper rod was kept the same for each experiment. The pouring basin was filled completely as fast as possible before and after the removal of the stopper rod to give the same head pressure for all successive tests. Three tests were taken for each of the alloy developed to incorporate the possible errors that could emerge due to personnel, mould and test variables.

CHAPTER 4

RESULTS AND DISCUSSION

4.1 Literature Survey and Chemical Composition Analysis

4.1.1 Results and Discussion

4.1.2 Literature Survey

The result of the literature survey on alloys used for cylinder heads application is compiled in (Table A.1) Appendix A. The survey on the literature indicates that the most common alloys used for engine cylinder head application are 319, 356, 355, 354 and 380 type alloys and their equivalents from other countries. The 319 and 356 alloys have wide distribution according to researchers and are followed by 355 and 380 type alloys. The broad specification range for alloying elements and excellent mechanical properties at elevated service temperatures, the 319 alloy made influential in the application of automotive engine components especially cylinder head. Several automakers also favor very ductile 356 family alloys, although their strength rapidly reduces at elevated temperature [34].

4.1.3 Chemical Composition Analysis

Table 4.1 shows the results of the chemical composition analysis obtained for the scrap cylinder heads named CH1 to CH7. From the composition results in Table 4.1 it can be

inferred that aluminium alloys used in cylinder heads fitted into small vehicles imported to Kenya possess the chemical composition of alloy manufactured in Japan with designation of JIS AC2B which is equivalent to 319 alloy. The composition specification of this alloy is indicated in Table 3.1.

Table 4.1: Chemical composition of scrap cylinder heads in wt%.

Scrap code	Cr	Cu	Fe	Mg	Mn	Ni	Pb	Si	Sn	Ti	Zn	Place
CH1	0.02	2.45	0.36	0.31	0.24	0.04	0.02	6.4	0.01	0.03	0.19	UK
CH2	0.02	2.33	0.34	0.27	0.21	0.08	0.01	6.46	0.01	0.03	0.13	UK
CH3	0.03	2.96	0.40	0.23	0.25	0.03	0.03	6.31	0.02	0.03	0.29	UK
CH4	0.05	2.868	0.215	0.213	0.136	0.039	0.00	6.433	0.022	0.012	0.026	BET
CH5	0.08	2.678	0.345	0.265	0.251	0.042	0.008	6.289	0.027	0.019	0.127	BET
CH6	0.037	2.998	0.302	0.311	0.280	0.034	0.01	6.805	0.016	0.015	0.083	BET
CH7	0.043	2.273	0.401	0.373	0.259	0.038	0.009	6.570	0.024	0.016	0.084	BET

4.2 Recycle friendly Alloy Identification

4.2.1 Results and Discussion


The source alloys versus target alloys Table 4.2 shows the possibility of an alloy to be recycled from its group or from the other groups. The source alloy A and the target alloy A have the same chemical composition. This chemical composition is governed by the maximum composition of each element present in the group. For instance, the maximum composition specification of each element for target alloy A is the largest value of each element in group A in Table 3.1 i.e. Si (7.5 wt.%), Cu (0.2 wt.%), Mg (0.6 wt.%), Fe (0.5


wt.%), Mn (0.3 wt.%) and Zn (0.3 wt.%). For target B also Si (7 wt.%), Cu (4 wt.%), Mg (0.5 wt.%), Fe (1 wt.%), Mn (0.6 wt.%), Zn (1 wt.%) and Ni (0.35 wt.%). Similarly, it applies for the other groups.


The colours and numbers in Table 4.2 demonstrate that, the tan-colour indicates recycling within the group, the red-colour illustrates the source alloy chemical composition is within the range of the target alloy and the gray-colour reflects excess of the element composition in percentage of the source maximum value minus the target maximum value (Percentage excess = Source maximum - Target maximum) for each element.

Table 4.2: Source alloys versus target alloys chemical composition

Source	Target alloys				
	A	B	C	D	E
A		Si +0.5			Si+2
B	Cu+3.8			Cu+2	Si+1.5
	Fe+0.5			Fe+0.6	Cu+2.5
	Mn+0.3			Mn+0.3	Fe+0.4
	Zn+0.7			Zn+0.9	Zn+0.65
	Ni+0.2				
C	Si+2	Si+3		Cu+2	Si+4.5
	Cu+3.8	Fe+0.3		Fe+0.9	Cu+2.5
	Fe+0.8	Zn+2		Mn+0.3	Fe+0.3
	Mn+0.3			Zn+2.9	Zn+2.7
	Zn+2.7			Ni+0.5	
	Ni+0.4				
D	Si+2.5	Si+3			Si+4.5
	Cu+1.8				Cu+0.5
E	Cu+1.3			Fe+0.4	
	Fe+0.1			Mn+0.2	
	Mn+0.25				

 Source is within the target

 Source and target the same

 Elements in excess of target

Therefore the table describes which scrap cylinder head groups can be utilized as source material to the target alloy with broad composition specification range.

From Table 4.2, it can be observed that developing an alloy from group A targeting A is very much possible, however, from B targeting A is not easily achievable, since there are elements such as Cu, Fe, Mn, Zn and Ni whose composition is in excess of the specification for target alloy A . Hence, it will require diluting them with pure aluminium. Target alloys B and C have broad range for the alloying elements as can be seen in the table. The excess elements are only Si, Fe and Zn in B while in C no excess element is reflected. Target alloy D cannot be recycled directly from A, B and C without diluting them with pure aluminium but can be produced from A with addition of alloying elements Si and Cu. The target alloy E has a narrow Si composition range, hence, producing from other scrap cylinder head groups will require primary aluminium addition.

Therefore, to recycle scrap cylinder heads, in a country where all the group alloys are available, one should select B and C alloys that accommodate a broad range of chemical composition for the major and minor alloying elements. However, group C alloys are mostly used for engine block and their compositional range is very wide therefore selecting this alloy as recycle-friendly will result in great variation in performance. The B group (319 type) alloys are important cast alloys in this aspect, silicon and copper are the main alloying elements, and magnesium is usually added for strengthening mechanism [106].

Alloy group A and E have higher alloy recycling index hence they can act as main source

material to target alloy B [98]. Therefore, target alloy B with minor modification could be adopted for component to component (cylinder head to cylinder head) recycling. The chemical composition range for the proposed target alloy is shown in Table 4.3.

Table 4.3: The proposed target alloy chemical composition

Alloy	Si	Cu	Mg	Fe	Mn	Ti	Zn	Ni	Others
B	4.0 - 7.0	2.0 - 4.0	0.50	1.0	0.60	0.25	1.0	0.35	0.55

4.3 Practical Alloy Developed

4.3.1 Results and Discussion

The actual recycled alloy (base alloy Table 3.2) obtained from scrap cylinder heads using equation 2.1 had its chemical composition which lies in the general alloy proposed in Table 4.3. Moreover, the predicted and the recycled alloy chemical compositions were similar with minor differences in some alloying elements as shown in Figure 4.1. Some of the deviation factors between the predicted and the recycled alloy elements composition were negative (i.e. below the predicted). This indicates the loss in the alloying elements in terms of dross or evaporation during the high temperature melting. Metal losses during scrap melting can reach up to 5% of the total charged material due to skimming and removal with the salt slag/dross formed [107].

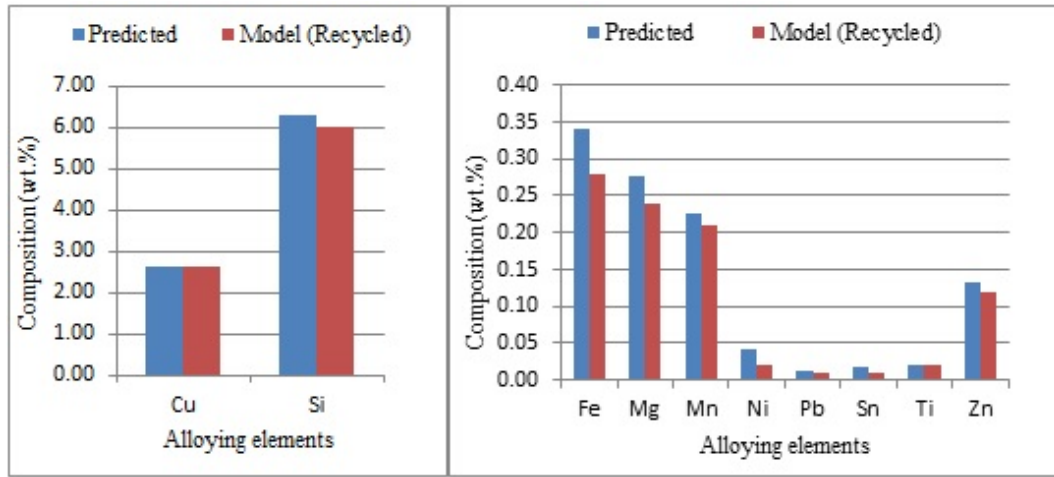


Figure 4.1: Difference in composition values between the predicted and recycled alloy.

Figure 4.2 shows the maximum and minimum composition of the proposed target alloy (Max TA and Min TA) and the composition of the actual recycle alloy (ARA).

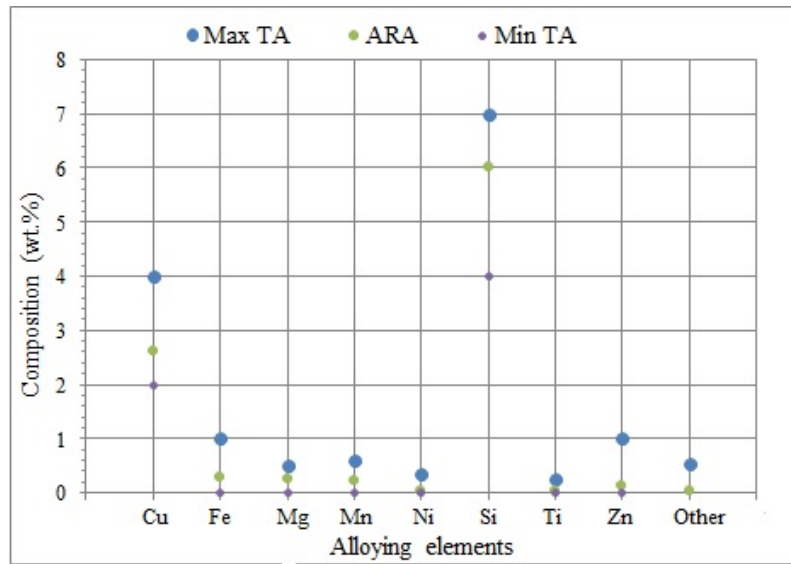


Figure 4.2: Difference in composition between the proposed target and recycled alloy.

The overall deviation factors of the alloying elements of the actual recycled alloy were zero since the percentage composition of each element was within the range of the proposed target alloy as presented in Figure 4.2. The chemical composition of the recycled alloy

has to relate to the pre-melt composition of the incoming mixture and the deviations of the recycled from the standard composition should be minimal [94]. Hence, the base alloy developed from the scrap cylinder heads has chemical composition of each alloying element within the specification of the proposed target alloy therefore it needs minor modification and proper heat treatment temper.

4.4 Microstructure

4.4.1 As-Cast Microstructure of the Model Alloy

4.4.2 Results and Discussion

Figure 4.3 (a) and (b) show the microstructure of the base alloy (SI) in the as-cast state without any element addition. Figure 4.3 (a) is at low magnification and (b) at higher magnification. Figure 4.3 (a) reveals phases such as primary Al-matrix, coarse acicular eutectic silicon particles and intermetallic phases of Fe and Cu. The eutectic silicon particles appear unmodified are fairly scattered throughout the micrographs. The amount of Fe - intermetallics observed in this microstructure are few and Cu - intermetallics are observed as small and circular phases. Figure 4.3 (b) reveals clearly the types of phases which are present in the microstructure. The eutectic silicon particles are seen as wide and irregular structures. Moreover, the Fe - intermetallic appears a skeleton-like phase and Cu-phases appear in the form of block-like structure.

Figure 4.4 shows the microstructure of an alloy obtained after addition of 0.02% Sr. In

this alloy (SI + 0.02% Sr), completely modified and partially modified eutectic silicon

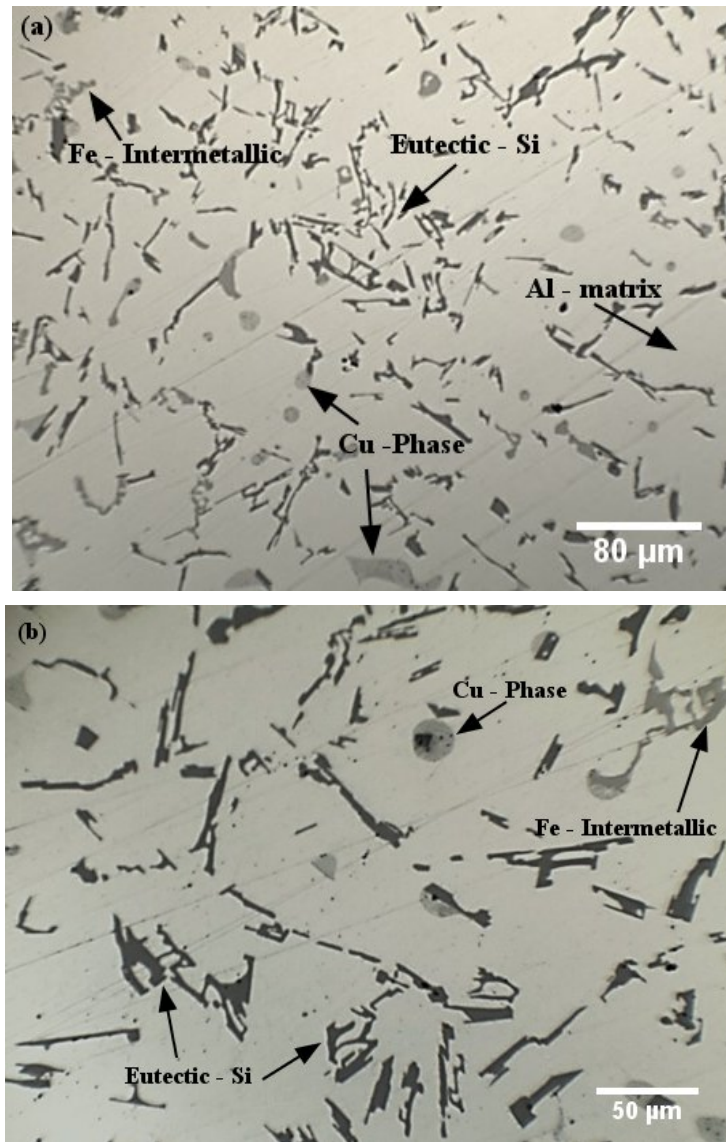


Figure 4.3: Microstructure of the base alloy as-cast with low magnification (400X) (a) and high magnification (1000X) (b)

particles and skeleton like Fe - intermetallics are observed. The irregular (acicular - Si) structures observed in the unmodified base alloy in Figure 4.3, are transformed into fine fibrous particles. Another important observation with this modifier is also the formation of fine and compact Fe - intermetallic. This could be due to the effect of strontium in low-

ering the precipitation temperature of the α - $\text{Al}_{15}(\text{Fe,Mn})_3 \text{Si}_2$ phase and fragmentation and dissolution of β - Al_5FeSi phase [54, 63, 106].

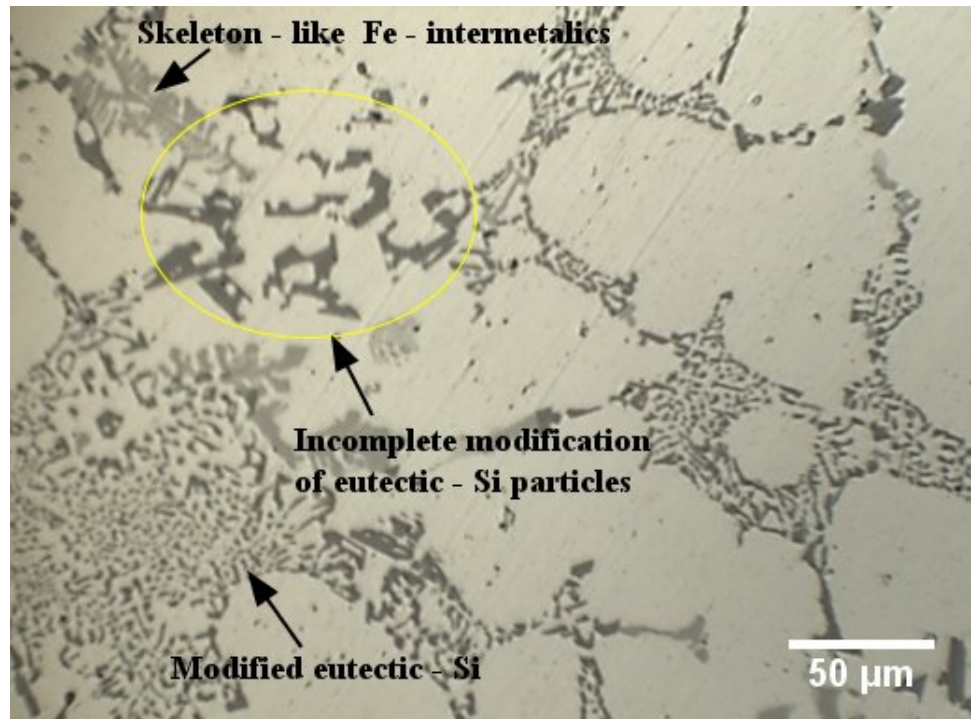


Figure 4.4: As-cast microstructure of the 0.02% Sr modified alloy (1000X).

Figure 4.5 (a) and (b) show Cu-phases in the base alloy and in the alloy modified by 0.02% Sr. The effect of strontium on the Cu-intermetallic phases is presented here. The Cu - phases in Figure 4.5 (a) are in the form of fine eutectic Al_2Cu phase while the Cu - phases in Figure 4.5 (b) appear in the form of blocky Al_2Cu phase. This transformation is due to the effect of strontium. Strontium segregates Cu in regions free of eutectic Al-Si and contributes to the free growth of blocky Al_2Cu [108].

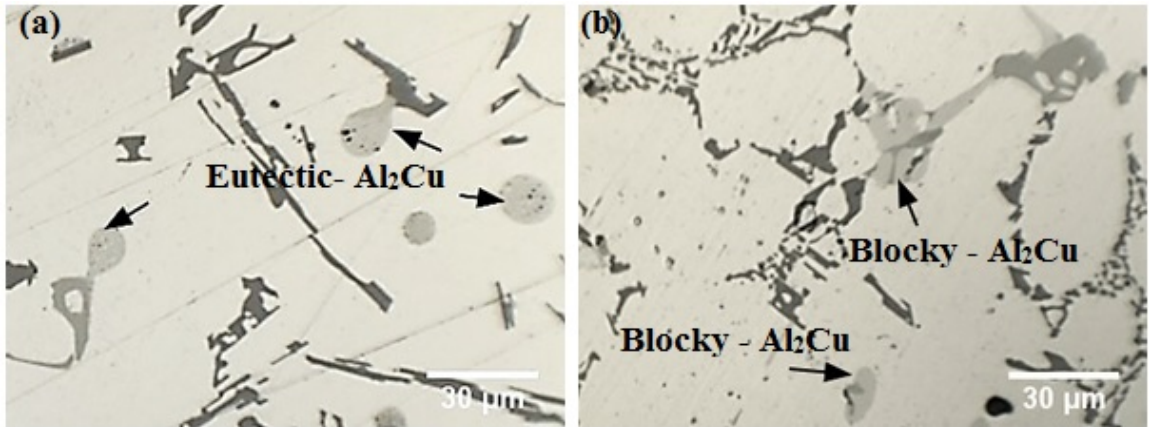


Figure 4.5: Effect of Sr on the Cu - intermetallics (a) Eutectic Al₂Cu in the base alloy (b) Blocky Al₂Cu in the alloy modified by 0.02% Sr (1000X).

Figure 4.6 shows the microstructure of the base alloy when its Fe content is increased to 0.38%. In this sample, eutectic silicon particles, Fe - rich intermetallics and Al₂Cu phases are observed.

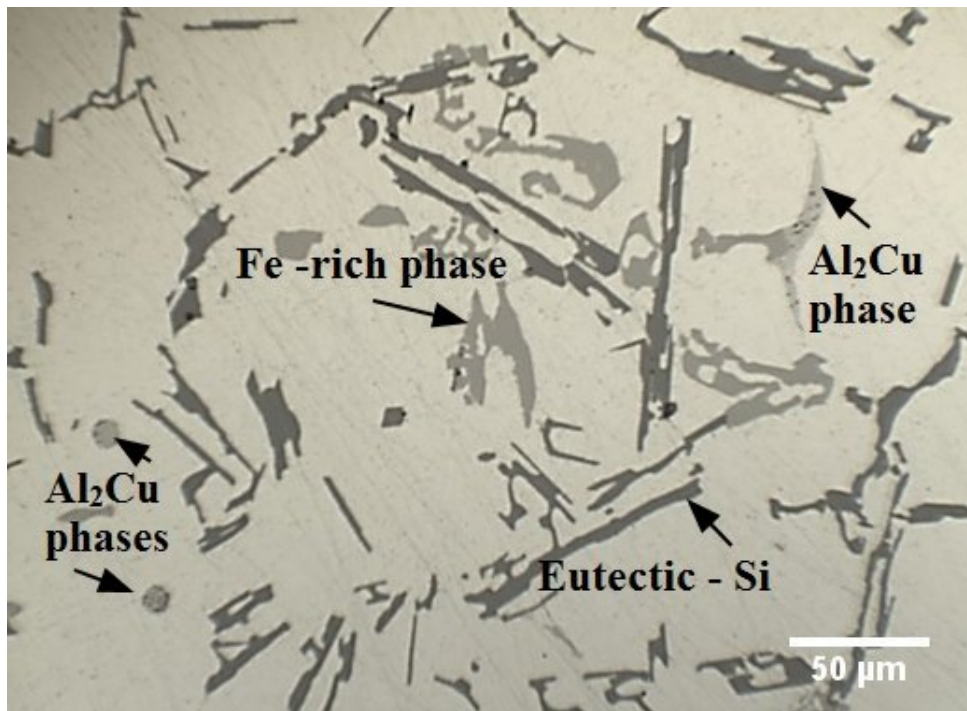


Figure 4.6: As-cast microstructure of an alloy with 0.38% Fe total content (1000X).

The eutectic silicon particles have acicular or needle - like morphology and they are also large in size as compared with the particles in the previous alloys. Large particles in an alloy are usually sources of failure. With the addition of 0.38% Fe, large Fe- phases are observed and a slight increase in the distribution of Fe- intermetallics is also noted.

Figure 4.7 shows the microstructure of the base alloy when Fe and Mn contents are increased to 0.9% and 0.45% respectively. With the addition of Fe and Mn in the ratio of Fe:Mn (2:1), long and interconnected Fe - intermetallics are observed.

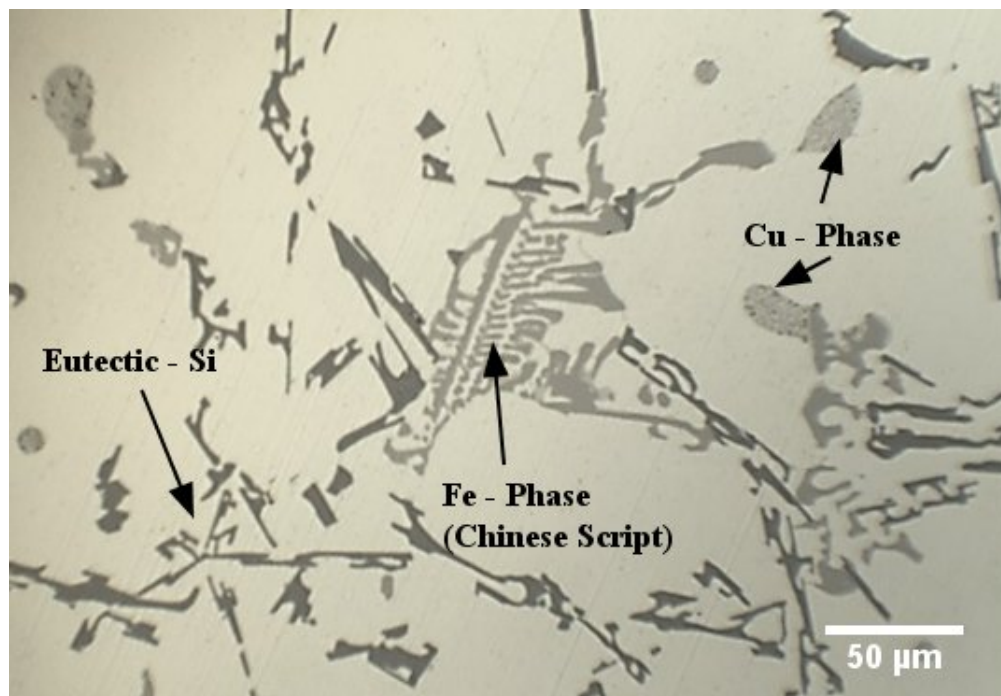


Figure 4.7: As-cast microstructure of an alloy with 0.9% Fe and 0.45% Mn total content (1000X).

Manganese increases the nucleation site of Fe - phase and suppress the formation of coarse β - phases. In a report by Mohamed *et al.* [23], at low level of manganese, increasing Fe up to 1%, plate - like α -Fe and Chinese script α - Fe intermetallics were observed. The

eutectic silicon particles in this sample appear as acicular structure. Cu - intermetallic phases are also observed in this alloy as small pockets of circular and block-like eutectic phases nucleating along the coarse Si particles and Fe - phases.

4.4.3 Heat Treated Microstructure

Cast Al-Si alloys are typically heat treated to various tempers depending on the application requirements. The most common heat treatment temper for automotive components is the T6 for ambient service temperatures and the T7 temper for higher temperature applications such as cylinder heads. Heat treatment is expected to impart significant microstructural changes as discussed in this section.

4.4.4 Results and Discussion

Figure 4.8 shows the microstructure of the base alloy (SI) after the sample was treated to the T6 temper. The sample was solution heat treated for 6 hours at a temperature of 495°C followed by natural aging for 24 hours and artificial aging for 8 hours at 170°C.

In this sample necking, fragmentation and spheroidization of eutectic Si particles are observed in Figure 4.8 at higher magnification. However, some of the eutectic silicon particles still possess coarse acicular shape. The rate of spheroidization is dependent on the size of the particles so fast spheroidization and coarsening is expected with smaller size particles [23]. Small size Fe - intermetallics are also observed in this microstructure but the Cu-phases observed in the as-cast condition seem to have disappeared after T6 heat treatment.

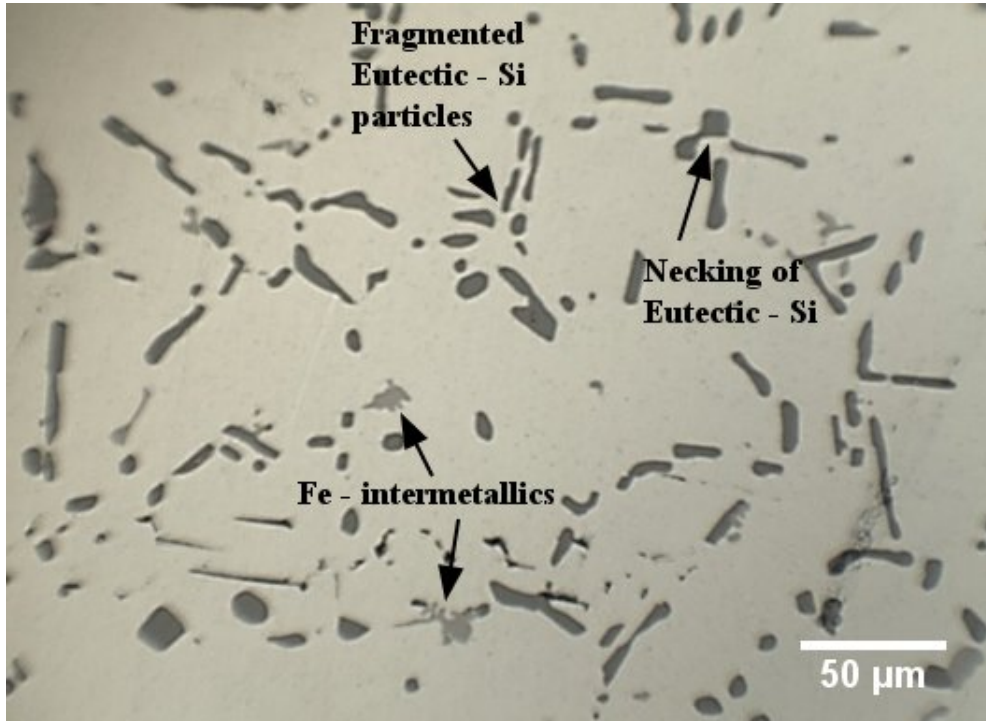


Figure 4.8: Microstructure of the base alloy after T6 heat treatment (1000X)

The microstructure of the alloy modified by 0.02% Sr after heat treatment is shown in Figure 4.9. The microstructure of this alloy reveals spheroidization of the eutectic Si particles and fragmentation of Fe - intermetallic phases.

The size of eutectic silicon particles are seen in this microstructure as small and fine when compared to the unmodified alloy. However, when this microstructure is compared to the as-cast and modified, it has large eutectic - Si particles. The modification and heat treatment results in the dissociation of iron intermetallics. This is consistent with Mohamed *et al.* [23] who reported that in the Sr modified alloy, partial dissolution of β - needles becomes more pronounced after solution heat treatment. Moreover, strontium addition leads to the transformation of the eutectic Al_2Cu -Phase into a hard and blocky structure that could not be dissolved during solution treatment.

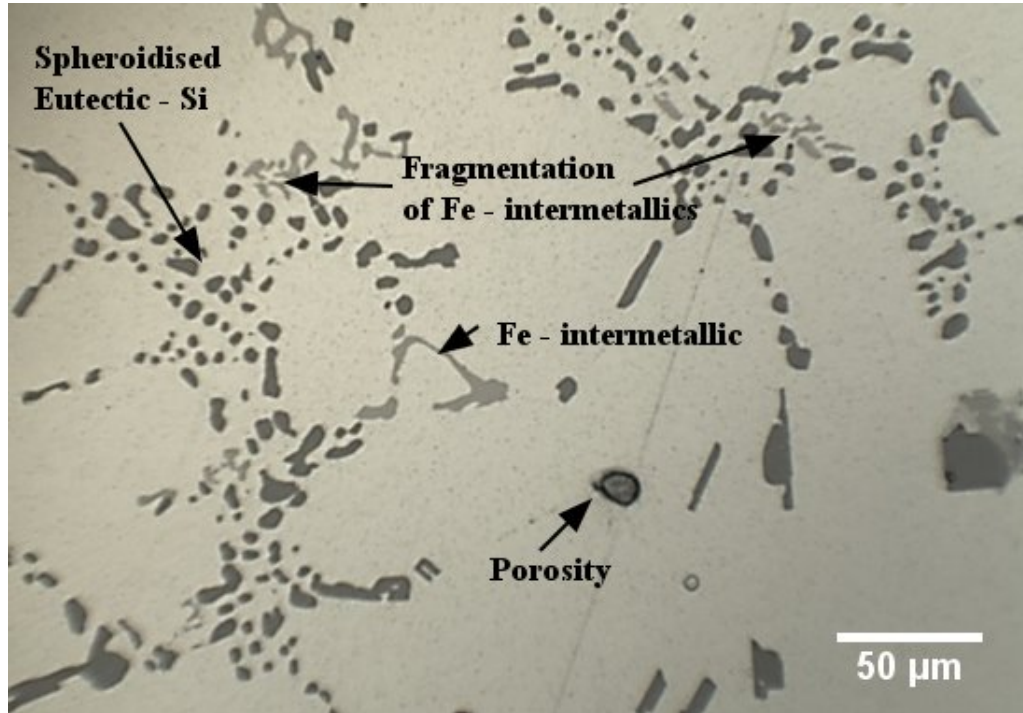


Figure 4.9: T6 heat treated microstructure of the alloy modified by 0.02% Sr (1000X).

In Figure 4.10 the microstructure of the 0.38% Fe containing alloy is shown after T6 heat treatment. From this microstructure it can be observed that the fairly distributed eutectic silicon particles elongate, neck, fragment and tend towards being spheroidised due to the effect of heat treatment.

The sharp edges of eutectic silicon particles observed in the as-cast state are seen to change into round boundary. However, complete transformation of the needle-like structure into fine fibrous morphology is not achieved in this alloy as the transformation rate is dependent on the size of the particles. Cu-phases are not seen in this microstructure but Fe-rich intermetallics are observed in this alloy.

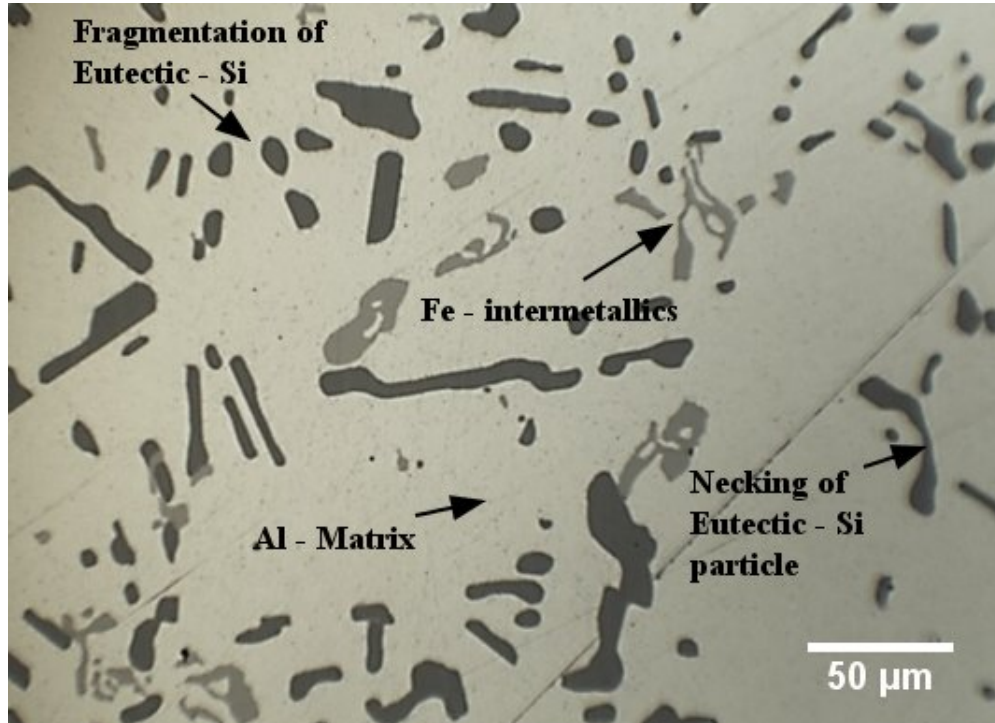


Figure 4.10: Microstructure of the alloy with 0.38% Fe after T6 heat treatment (1000X).

Figure 4.11 shows the microstructure of the alloy containing 0.9% Fe and 0.45% Mn after T6 heat treatment process. The figure displayed phases such as the Chinese-script ($\alpha\text{-Al}_{15}(\text{FeMn})_3\text{Si}_2$) and eutectic silicon particles.

The Chinese-script (Fe-phases) are highly dispersed in the eutectic region and can be seen to cover a large area. Spheroidization of the eutectic silicon particles is not observed in this alloy after heat treatment as it was observed in the previous alloys.

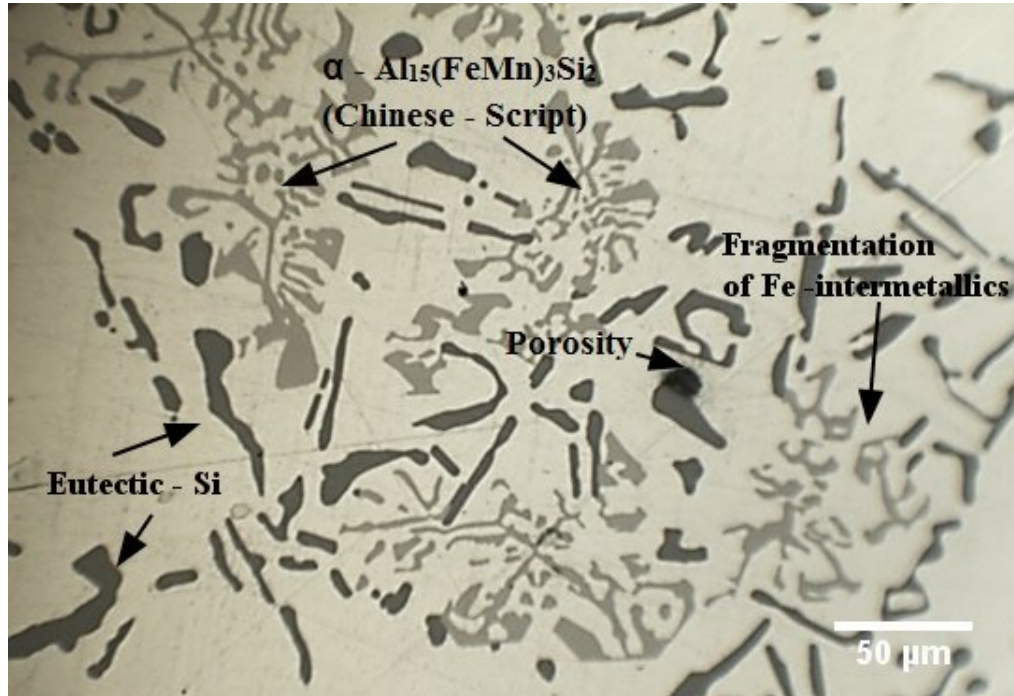


Figure 4.11: Microstructure of the alloy with 0.9% Fe and 0.45% Mn after T6 heat treatment (1000X).

4.5 Quantification of Si and Fe - Intermetallic particles

4.5.1 Results and Discussion

Table 4.4 shows the quantitative measurement of eutectic-Si and Fe-intermetallics in the four alloys in the as-cast state and heat treated conditions. The measurement is presented in terms of maximum equivalent circle diameter (D_{eq}) and maximum feret dimension (L_F) as measured by imageJ techniques. The equivalent circle diameter was obtained from the surface area of the particle using ($D_{eq} = \sqrt{4A/\pi}$) [105], where A is surface area of the particle. The feret dimension represents the largest length between two points within the boundary of the particle that measured on the longest particle.

The quantification of intermetallic particles can predict the effect of the size of the particles on the mechanical properties of an alloy. Large particles in a sample are always sources of failure since the coherence capacity with the Al-dendrite is low.

Table 4.4: Quantitative measurement of eutectic - Si and Fe - intermetallic (in μm)

Parameters	Base alloy (SI)	SI + 0.02%Sr	SI + 0.38%Fe	SI + 0.9%Fe + 0.45%Mn
As-cast				
D_{eq} , Max, Si	37	24	49.8	30
L_F , Max, Si	89.26	62	139.8	96.57
D_{eq} , Max, Fe	35	35.7	31.6	38
L_F , Max, Fe	87.74	109.9	57.2	118
Heat treated				
D_{eq} , Max, Si	29.7	24	38.5	33
L_F , Max, Si	73.4	56.4	87	95.7
D_{eq} , Max, Fe	17.2	20.3	23.5	35.1
L_F , Max, Fe	34	48.1	44.2	88.2

In as-cast, the Max L_F eutectic - Si phase is observed in the 0.38% Fe content alloy ($L_F=140 \mu\text{m}$) and the smallest Max L_F of eutectic - Si is observed in the Sr-modified alloy ($L_F = 62 \mu\text{m}$). The largest Max D_{eq} of eutectic - Si is also observed in the alloy containing 0.38% Fe ($D_{eq}= 49.8 \mu\text{m}$) and the smallest Max D_{eq} is observed in the Sr-modified alloy ($D_{eq}= 24 \mu\text{m}$). In the case of Fe - phases, the particles that covered wide surface area or Max D_{eq} were identified as Fe-intermetallic phases with Chinese

Script morphology as can be noted from the maximum equivalent circle diameter of Fe in as-cast in Table 4.4. The Max D_{eq} and Max L_F of the Fe - phases were in the alloy which added Fe and Mn.

After heat treatment the intermetallic phases are observed to decrease in both the Max D_{eq} and Max L_F as observed in Table 4.4. Heat treatment caused 17.8%, 9%, 37.8% and 0.9% decrease in the size (length) of eutectic - Si in the base alloy, Sr-modified, 0.38% Fe containing and 0.9% Fe + 0.45% Mn added alloys respectively. The change in size of the eutectic - Si in the 0.9% Fe + 0.45% Mn added alloy has not shown much difference by heat treatment.

The alloy (SI + 0.9% Fe + 0.45% Mn) had bulk networks of α - $Al_{15}(MnFe)_3Si_2$ intermetallics throughout the micrograph. However, the sizes of the α - Fe phases were smaller in the heat treated sample. The iron intermetallic phases were generally reduced both in their surface area and maximum feret dimension due to heat treatment.

It is clear that from this section the heat treatment has contributed in changing the size of the intermetallic second phase particles and is therefore expected to improve significantly the mechanical properties of the alloys as discussed in the next section.

4.6 Porosity

4.6.1 Results and Discussion

4.6.2 Microstructure Observation

Figure 4.12 shows porosity level distribution in the base alloy (Figure 4.12 (a)), Sr-modified alloy (Figure 4.12 (b)), 0.38% Fe alloy (Figure 4.12 (c)) and 0.9% Fe + 0.45% Mn alloy (Figure 4.12 (d)).

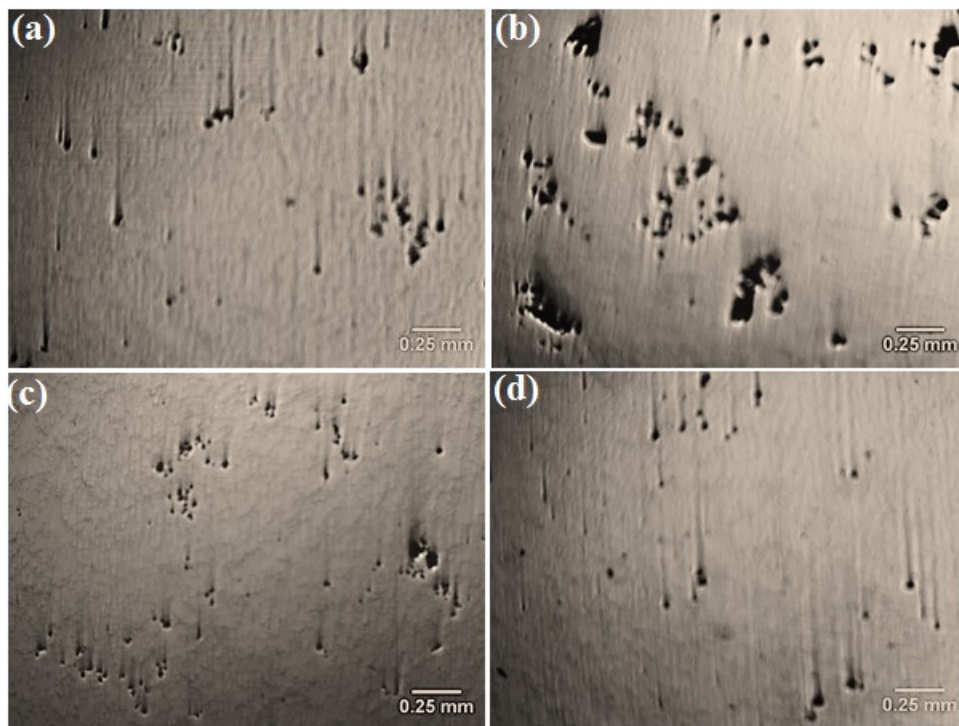


Figure 4.12: Porosity level distribution in (a) Base alloy, (b) SI + 0.02% Sr alloy, (c) SI + 0.38% Fe alloy and (d) SI + 0.9% Fe + 0.45% Mn alloy (80X)

Figure 4.12 (a), the pores are small and approximately circular with a random spatial distribution. Some pores are however seen to be interconnected. Figure 4.12 (b), the pores are observed as large, interconnected and clustered in some areas while in Figure 4.12

(c), the number of pores is higher in comparison with Figure 4.12 (a) and are observed to be of small and to medium size pores. Figure 4.12 (d) shows the lowest level of porosity.

Modification by strontium is seen to have significantly increased porosity. Strontium increases porosity on Al-Si alloys by increasing the inclusion content and by decreasing the solubility of hydrogen in the solid metal [22]. Strontium has high affinity for oxygen and hence increases the oxidation rate of an alloy.

The porosity level in the 0.38% and 0.9% Fe alloys shown in Figure 4.12 (c) and (d) indicates slight variation. The 0.38% Fe contains more pores than the 0.9% Fe alloy. The Fe - rich intermetallic phases observed in the microstructure of the 0.38% Fe alloy may have contributed significantly in blocking the molten metal that compensate solidification shrinkage [48]. Moreover, if the amount of Mn is greater than the recommended value to neutralize the β phase, it results in a brittle α phase that can generate porosity [33].

4.6.3 Porosity quantification

Figure 4.13 shows the binarized image of the four samples from which the porosity measurement was taken and Figure 4.14 depicts the range of pore sizes and count (number of pores) obtained from the analysis using imageJ.

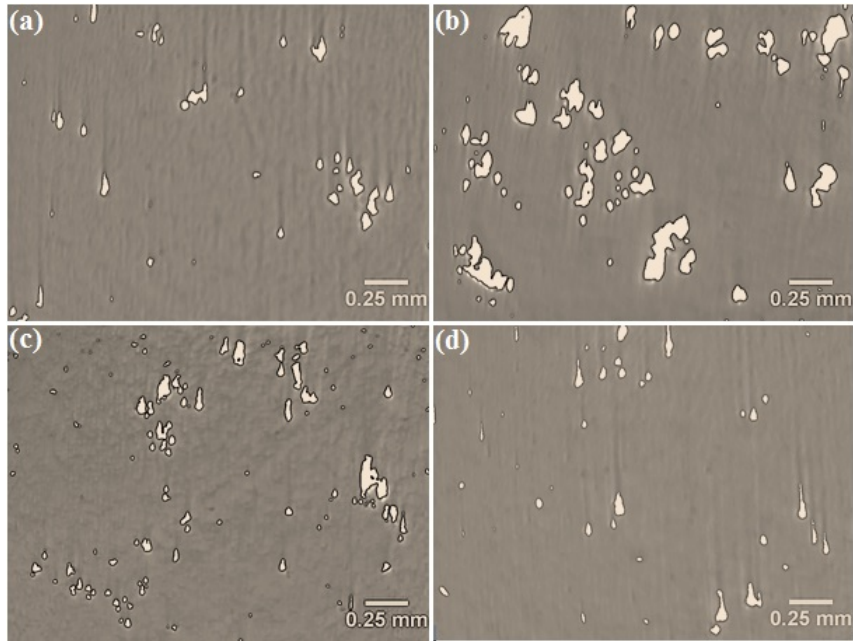


Figure 4.13: Binarized image using imageJ of the alloys (a) Base alloy, (b) SI + 0.02% Sr, (c) SI + 0.38% Fe and (d) SI + 0.9% Fe + 0.45% Mn (80X).

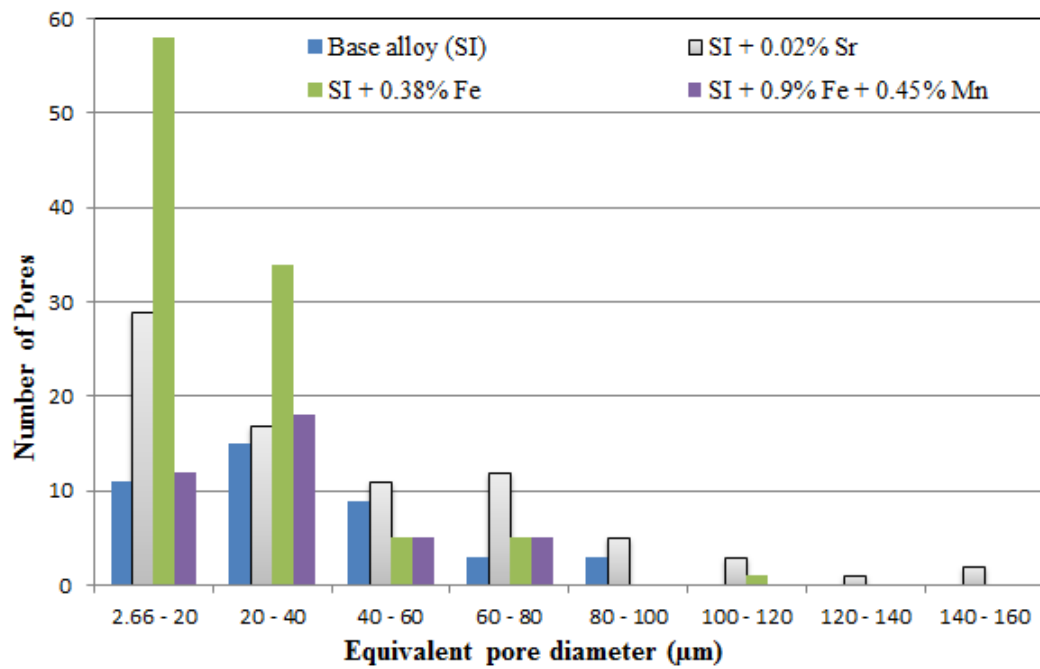


Figure 4.14: Pore size distribution for the alloys investigated.

The quantitative measurements of porosity were recorded in the range of 2.66 - 85 µm

in the base alloy, 2.66 - 160 μm in the Sr-modified alloy, 2.66 - 120 μm in the 0.38% Fe alloy and 2.66 - 70 μm in the 0.9% Fe + 0.45% Mn alloy. The number and size of the pores were high in the Sr- modified alloy and in the 0.38% Fe alloy. The pore sizes were large with these alloys, especially with the modified one. Pore sizes above 100 μm were not found in the base alloy and 0.9% Fe alloy whereas these were indeed observed in the modified and 0.38% Fe alloys. Hence there is a possibility of low mechanical properties for these latter alloys.

The pore size distribution in the base alloy is comparable to the alloy neutralized by Mn. The formation of α - Fe due to the addition of Mn results in fine pores since this phase facilitates feeding the interdendritic space with liquid metal better than β - Fe intermetallics [23].

4.7 Mechanical Properties

The mechanical properties of aluminium alloys are characterized largely by the shape, size and spatial distribution of microstructure features such as Si and intermetallic particles. Optimum tensile, impact and fatigue properties are obtained with small, spheroidized and evenly distributed particles and an appropriate heat treatment temper [23,109].

4.7.1 Tensile Strength

4.7.1.1 Results and Discussion

Figure 4.15 shows the average UTS values of each alloy, in as-cast state and after T6 heat treatment. Heat treated alloys are indicated as HT. (Table B.1) in Appendix B, on the other hand, shows the summary of results of the UTS of each the six specimens tested from the samples of base alloy, Sr-modified, 0.38% Fe and 0.9% Fe + 0.45% Mn content alloys.

Figure 4.15 shows that the UTS of the base alloy is 209.5 MPa in the as-cast state. After the addition of 0.02% Sr, increasing Fe to 0.38% and 0.9%, resulted in the UTS decrease by 2.8%, 6.9% and 3.8% (203.6, 195.4 and 201.5 MPa) respectively.

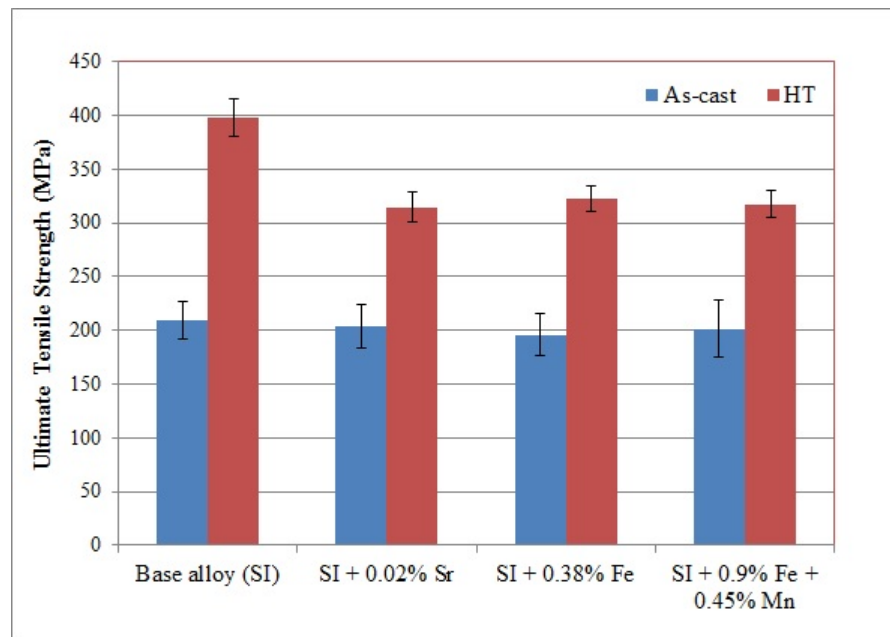


Figure 4.15: Average tensile strength in as-cast and T6 heat treated states

The modification has resulted in a slightly low value of UTS. This low value is associated

with the capacity of strontium in generating porosity in the casting.

The increase of Fe content in the base alloy to 0.38% is observed to decrease the UTS. Increasing iron content initiated the formation of Fe - rich intermetallics which could generate defects that deteriorate the properties. Moreover, the microstructure of this alloy in Figure 4.6 shows large and needle-like eutectic - Si phases. These phases fracture much more easily than the soft aluminium matrix under tensile loading [61]. Addition of Fe and Mn to the base alloy is also observed to decrease the UTS by 3.8% but this percentage decrease is lower than the decrease observed by increasing the Fe content to 0.38%. With the increase of Fe content in an alloy there is an increase of Fe - intermetallic and area fraction of porosity which leads to a reduction in UTS. In general, the UTS of the alloys have shown good results in as-cast state as compared with the equivalent standard alloys seen in this literature.

After T6 heat treatment, the UTS of the alloys is observed to increase by 89.6%, 54.3%, 64.8% and 57.5% in the base alloy, Sr, Fe and Fe + Mn added alloys respectively. The morphological change of the eutectic Si particles and precipitation of hardening phases during the T6 heat treatment greatly contributed to the improvement of mechanical properties. The increase of UTS in the base alloy is recorded as the highest after heat treatment as shown in Figure 4.15 with a value of 397.2 MPa. This could be attributed to the combined advantages of precipitate hardening, uniform distribution of intermetallics and less amount of porosity observed in this sample. The effect of heat treatment in the Sr - modified alloy is also observed to increase UTS remarkably. Further, heat treatment

is also noted to increase the UTS of 0.38% and 0.9% Fe containing alloys but those increases are also less than the base alloy's percentage increase in UTS. The strength of age hardened alloys is mainly determined by the effect of precipitates, the solid solution and the second phase distribution in the microstructure as well as porosity level [53]. The UTS of a material depends on the cross-sectional area of the specimen, hence, if the porosity level of an alloy increases the UTS decreases. The level of porosity due to modification was observed to increase consequently, the UTS of the alloy decreased. Moreover, the porosity and intermetallic phases associated with the increase of Fe also resulted in lower UTS value.

4.7.2 0.2% Proof Stress

Figure 4.16 illustrates measurement of the yield strength of some representative samples of the heat treated alloys after converting the load versus elongation graph into stress versus strain curve. The graphs indicate the test result for 0.2% strain of (a) base alloy, (b) Sr - modified alloy, (c) and (d) low and high Fe containing alloys respectively. The point of intersection between the stress-strain curve and the line parallel to the straight line on the stress-strain curve indicates the yield strength of the alloys based on 0.2% strain. The yield strength data obtained from these figures is given in (Table B.2) in Appendix B.

The heat treated base alloy is observed to possess the highest 0.2% proof stress as compared with the Sr - modified, 0.38% Fe and 0.9% Fe + 0.45% Mn containing alloys.

The effect of porosity and intermetallic particles was observed to decrease the YS of the alloy. As the porosity size and distribution of the alloy increases with the addition of modifier the proof stress decreases.

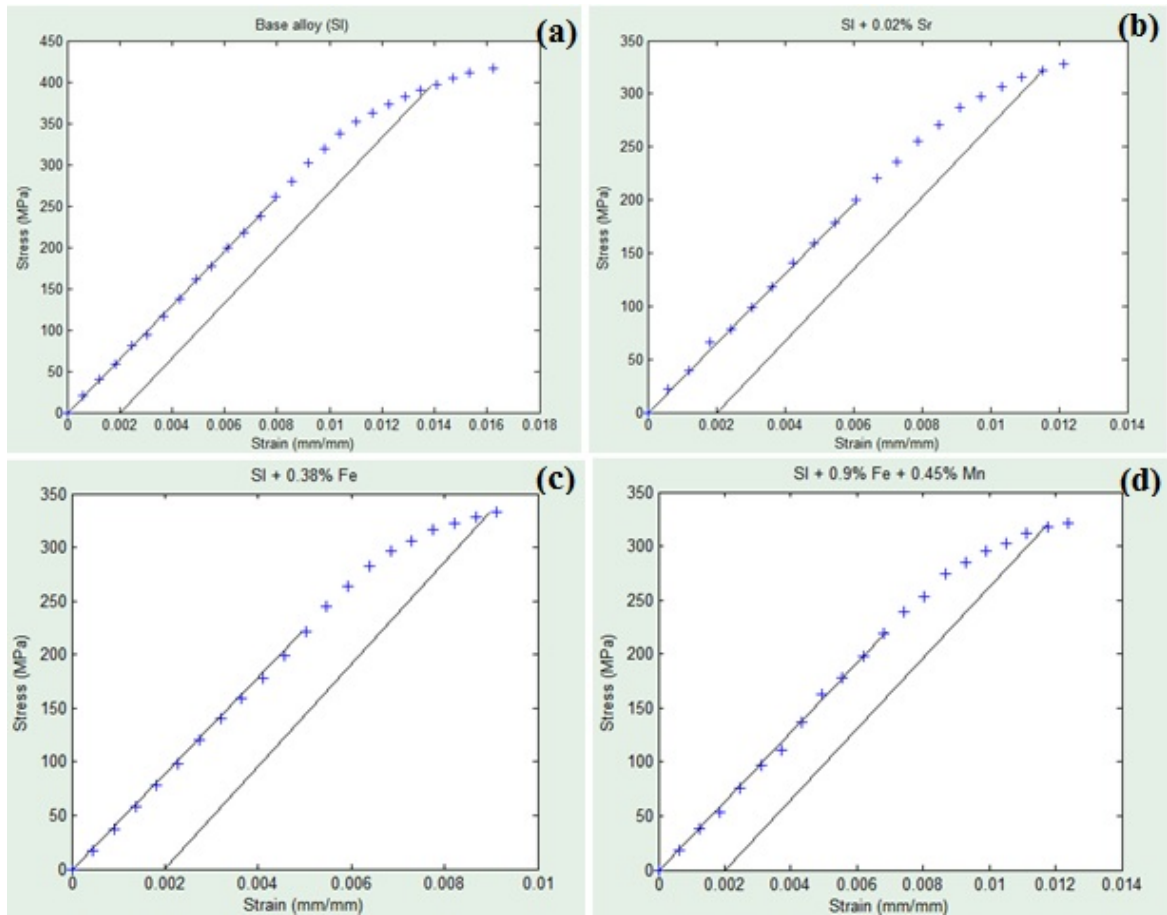


Figure 4.16: Representative stress-strain curves for obtaining 0.2% yield stress for the heat treated samples.

Alloys that have high yield strength prevent crack initiation by accommodating stress elastically. The representative 0.2% proof stresses of these model alloys are comparable with similar equivalent standard alloys used for cylinder head. For example, according to Kores [76] the YS and UTS of AlSi6Cu4 were 383 MPa and 408 MPa in the T6 heat treated temper whereas the representative 0.2% proof stress of the base alloy in this

research is 390 MPa and the corresponding UTS was also 417 MPa.

4.7.3 Percentage (%) Elongation

4.7.3.1 Results and Discussion

Figure 4.17 shows the average percentage elongation of the alloys in the as-cast state and T6 heat treated conditions. (Table B.3) in Appendix B on the other hand, shows the summary of recorded percentage elongation of the six specimens of each alloy in the as-cast state and after heat treatment.

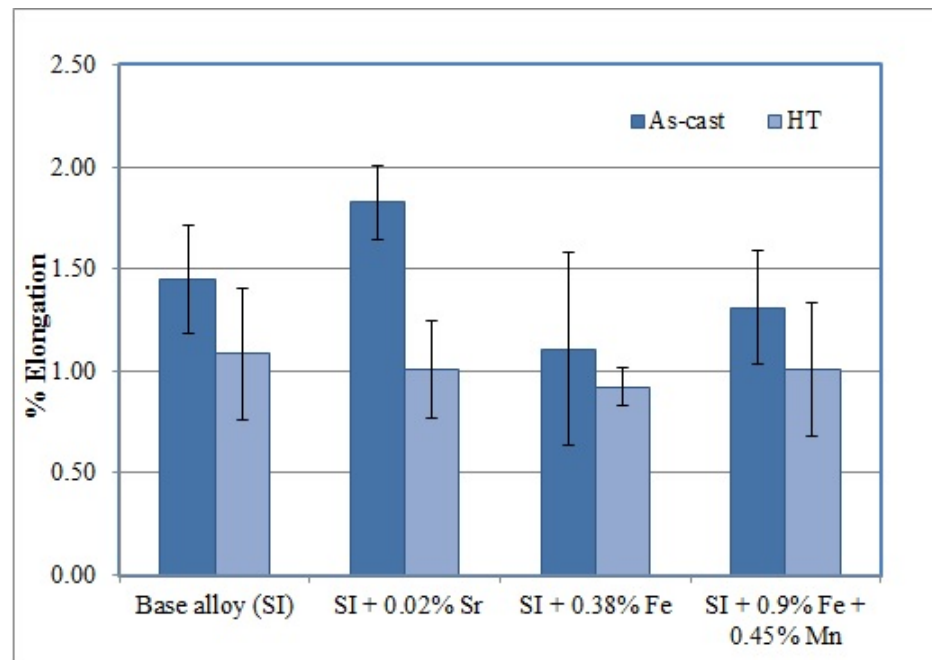


Figure 4.17: Average percentage elongation

The average percentage elongations in the as-cast state are 1.45%, 1.83%, 1.11% and 1.31% for the base, Sr-modified and for the low and high Fe alloys respectively. It is observed that modification through the addition of 0.02% Sr increased the percentage

elongation by 26.2% while the increase of Fe to 0.38% and 0.9% decreased the elongation by 23.5% and 9.7% respectively.

The ductility of aluminium alloys depend to a great extent on the size, morphology and, spatial distribution of brittle phases [17]. The brittle phases such as eutectic silicon and Fe- rich phases are responsible for the fracture in this type of material. Therefore, modifying the eutectic silicon phase improved the ductility of the alloy as observed in Figure 4.17.

After T6 heat treatment the % elongation of the alloys is observed to decrease by 25.5%, 45.5%, 17% and 31% in the base, Sr-modified and the low and high Fe alloys respectively. A maximum reduction in ductility of around 45% is observed in the Sr-modified alloy. The effect of heat treatment was more pronounced in the modified alloy. This effect could have emerged with the strengthening of the aluminium matrix with precipitate phases and the growth of micro-porosity upon solution heat treatment.

The reduction in % elongation is small in the alloy with 0.38% Fe. However, its % elongation is recorded as minimum after heat treatment, which is 0.92%. The morphology of eutectic silicon particles in this alloy were coarser and many of them were only on the verge of necking after heat treatment as seen in Figure 4.10. Coarser microstructure cause low elongation to fracture. However, porosity could have a great role in these experimental results, since some specimens were observed to fail before attaining of the 0.2% proof stress.

The reason for the low ductility of the alloys after heat treatment seems dependent on the porosity level especially with the modified and 0.38% Fe containing alloys. In these alloys the porosity distribution and size of the pores were relatively high.

4.7.4 Impact Toughness

4.7.4.1 Results and Discussion

Figure 4.18 shows the average results of impact energy values obtained for each of the alloys. (Table B.4) in Appendix B, on the other hand, shows the summary of results of impact energy of seven specimens for each alloy in the as-cast and heat treated conditions.

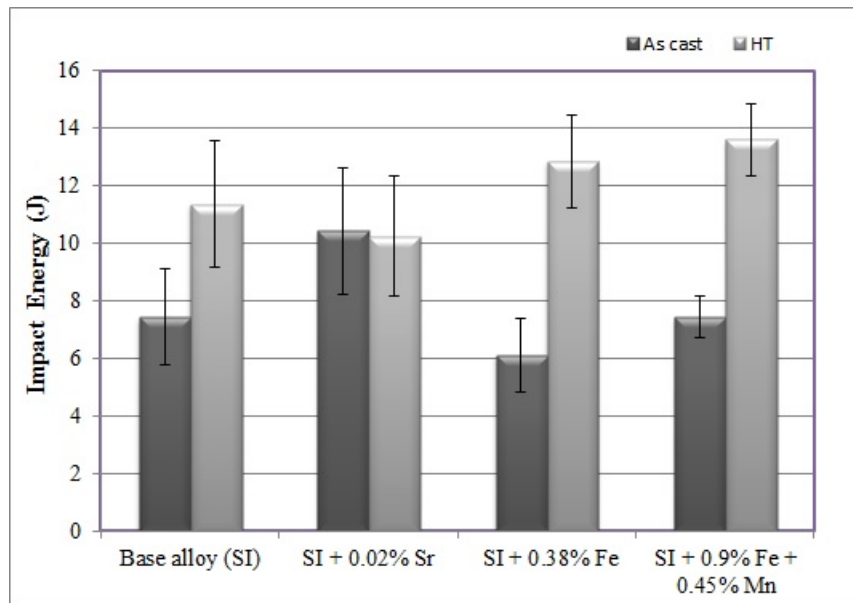


Figure 4.18: Average impact energy in the as-cast and heat treated conditions

From Figure 4.18, it can be observed that the values for the base alloy and the alloy with 0.9% Fe have the same impact energy (7.42J). The impact energy of the Sr-modified alloy is higher by 40.4% and that of the alloy with 0.38% Fe is lower by 17.7%. The

impact energy of Al-Si alloys is associated with microstructure, which strongly depends on the alloy composition and solidification conditions [59].

The maximum absorbed energy in the as-cast condition was in the alloy modified by 0.02% Sr. The improvement in this alloy may be explained by the modification of acicular eutectic silicon into fine Si particles. Modification with Sr and the consequent spheroidization of the Si particles would improve the alloys toughness due to the increase in the volume fraction of α -Al [50]. This, in turn, would compensate for the loss in energy caused by the presence of large brittle Fe-rich phases. However, Sr can also transform Al_2Cu phases from eutectic to block-like particles which may lead to brittle fracture. The two forms of the Cu - phase were shown in Figure 4.5.

The alloy with 0.38% Fe recorded a low impact energy value of 6.10 J. This was attributed to the presence of large acicular eutectic silicon particles and Fe - intermetallics as revealed in Figure 4.6. These structures serve as stress concentration sites, and facilitate crack formation and growth [50]. At a very high concentration of 0.9% Fe, the impact energy of the alloy does not show any change compared to the base alloy. There is also less scatter especially in the as-cast condition. This could be due to the neutralizing effect of manganese.

After heat treatment, the impact energy of the alloys is observed to increase by 53%, 110.5% and 83% in the base alloy, 0.38% Fe and 0.9% Fe alloys respectively. In the Sr-modified alloy, there is no change in its impact energy after T6 heat treatment. The solution heat treatment plays a great role in the first three alloys by distributing the

micro-constituents and partially dissolving some of the intermetallic phases into the aluminium matrix. Moreover, the fragmentation of Fe - intermetallics during solution treatment may have contributed to the elevation of the impact energy of the alloy with 0.9% Fe.

The average impact energy result for the Sr-modified alloy did not change after heat treatment. In this alloy, the porosity concentration and the pores size were significantly higher than the rest of the alloys. Hence, the impact toughness was not only depended on the Si morphology and distribution of the micro-constituents but was also sensitive to defects like porosity. Moreover, the size of eutectic-Si particles and Fe-intermetallics were small in this alloy. Therefore impact energy of an alloy decreases as the size and distribution of the porosity increase.

4.7.5 Artificial Ageing Study

4.7.5.1 Microhardness

4.7.5.2 Results and Discussion

Figure 4.19 shows the trend in hardness with increasing aging time at fixed aging temperature of 170°C. The zero aging time in all the graphs represents the value of T4 heat treatment temper. (Table B.5) in Appendix B, on the other hand, shows the summary of average values of 20 measurements for each sample in each of the heat treatment conditions.

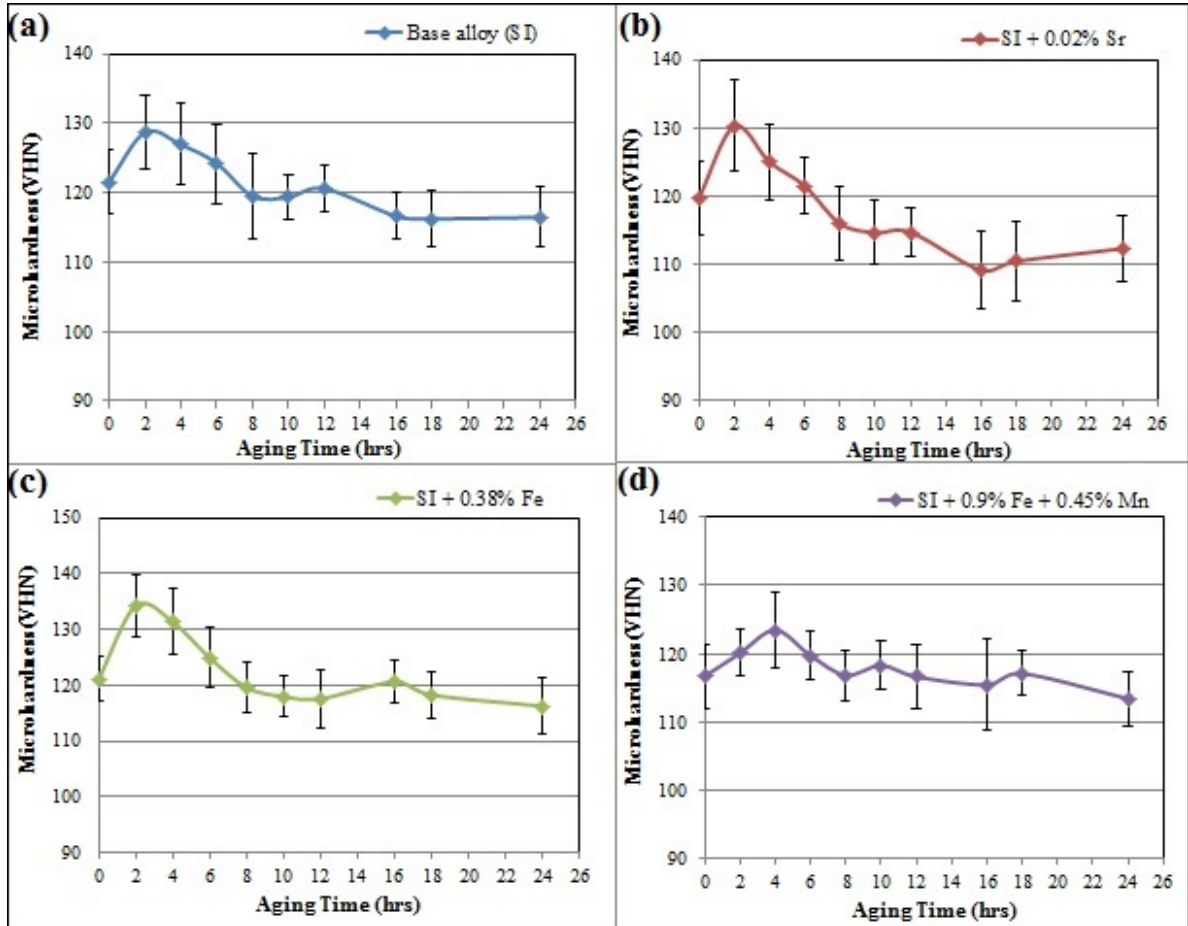


Figure 4.19: Average micro-hardness values of T4 and T6 heat treat samples

The hardness values in the as-cast state are recorded as 98.3, 94, 102.2 and 98.7 VHN for the base, Sr-modified, 0.38% Fe and 0.9% Fe alloys respectively. The as-cast hardness values are largely comparable except for the alloy with 0.38% Fe which is slightly higher value and this alloy has uniformly distributed hard eutectic silicon particles.

After T4 treatment, the hardness values are observed to increase by 23.6%, 27%, 18.5% and 18.3% in the base, Sr-modified, 0.38% Fe and 0.9% Fe alloys respectively. This increase is explained by the fact that when Al-Si-Cu alloys are solution heat treated,

the strengthening intermetallic phases dissolve and are retained in the Al-matrix up on quenching and some of the strengthening phases will also precipitate up on natural aging.

The hardness of the base alloy in Figure 4.19 (a) is observed to increase up to 2 h aging time and attaining a maximum value of 128.7 VHN then after followed by a gradual drop up to 8 h aging time. A plateau of hardness values is observed after 8 h. In a similar manner, the Sr-modified (Figure 4.19 (b)) and the 0.38% Fe alloy (Figure 4.19 (c)) attained their peak values (130.2 and 134.2 VHN respectively) after 2 h and then achieved a plateau values after 12 h aging time. However, the ageing response for the alloy with 0.9% Fe + 0.45% Mn is shown in Figure 4.19 (d) to be very slow and attained its peak hardness value (123.4 VHN) after 4 h and thereafter drops in a fluctuating manner throughout the aging process.

The samples treated in the T4 temper are observed to record higher hardness values than samples aged for longer hours in the T6 temper. However, the suitable aging hours for obtaining the highest hardness values at the given aging temperature (170°C) was in T6 temper between 2 and 6 hours. Most of the alloys are also observed to stabilized after 8 h aging time. This aging represents the T7 temper which is an overaged state.

The hardness of these alloys is clearly dependent on aging time at a given aging temperature as it is observed their hardness to change with aging hours. The age hardening responses for higher aging temperature are accelerated during the process with early peak-age hardness. At higher aging temperature the diffusion rate of solute atoms is very high [110], hence an early optimum hardness value could be expected as observed in

this study. The Cu - phases should be more responsive for the increase in the age hardening as those phases were fully dissolved during the solution treatment process. During aging, a very fine precipitates of Al_2Cu intermetallics are formed from the supersaturated solid solution and increases the hardness of the Matrix [111].

4.8 Comparison of Mechanical Properties of the Model Secondary Alloy with Similar Primary Alloys

Table 4.5 shows the mechanical properties of the model secondary alloy as compared with similar primary alloys. The mechanical properties of Al-Si casting alloys are highly dependent on the cooling rate and heat treatment conditions. Hence, it is difficult to compare experimental results based on the similarity of chemical composition. However, the obtained results of the model secondary alloy are similar to the primary alloys shown in the table. All the alloys are fabricated using permanent mould casting and the heat treatment condition used was also similar.

Table 4.5: Comparison of the model secondary alloy mechanical property results with some

primary alloys

Alloys	UTS (MPa)	YS (MPa)	% Elongation	E (J)	Hardness	Reference
Base alloy (SI)	397	390*	1.08	11.4	120 VHN	This research
319	376	258	4.77	9.82	110 VHN	[72]
A319	305	225	4.4	-	112.6 BH	[68]
AlSi7Cu3.3	335	195	8	-	-	[34]
AlSi6Cu4	408	383	1.09	-	-	[76]
319.0	275	185	3	-	95 BH	[2]

Note: * shows the representative YS not the average and its corresponding UTS is 417 MPa.

The UTS and YS of this research alloy were among the highest values in the table whereas the ductility was low but within the required range of ductility for cylinder heads. The hardness of this alloy was also high in comparison with those alloys produced from primary aluminium.

According to Medrano *et al.* [72], 319-type alloys are used in the fabrication of automotive engine cylinder heads with some desirable mechanical properties values in the range from 250 MPa to 300 MPa for YS and UTS, 1% for elongation, 10 J for impact toughness and 100 VHN for micro-hardness. In this research there is a satisfactory results of the mechanical properties in spite of the influences of the porosity and intermetallic phases generated by the addition of modifier and impurity levels.

4.9 Fluidity

4.9.1 Results and Discussion

Figure 4.20 shows the effect of the alloying elements on the average fluidity length of the base alloy when they are added in small percentage. (Table C.1) in Appendix C, on the other hand, shows the successive three test measured values, their mean and standard deviation of each of the alloy's fluidity length.

From Figure 4.20, it can be seen that there was a decrease in fluidity length of the alloy with the addition of modifier and impurity elements. With the addition of 0.02% Sr it

has been observed to decrease fluidity by 5.2% and an increase of iron content of the alloy to 0.38% Fe resulted a further decrease on the average fluidity length by 21.9%. Iron addition in combination with manganese in the ratio of 2:1 (Fe : Mn) was also observed to decrease the flow length by 12.1%.

The bar chart shows the variation of average recorded fluidity length in relation to the added alloying elements strontium, iron and manganese. The deviation of each successive

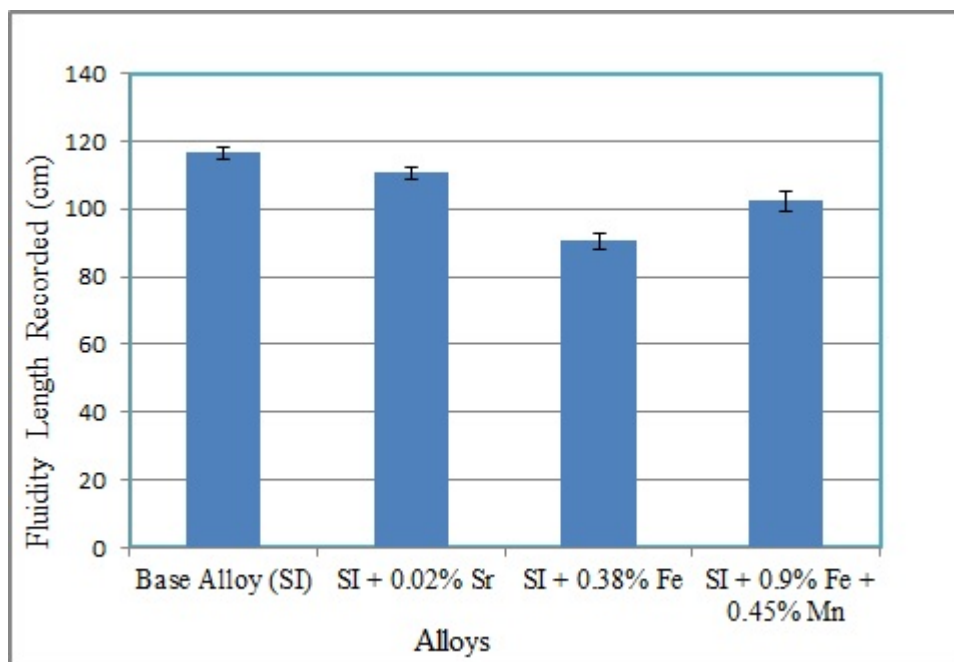


Figure 4.20: Variation of fluidity with alloying element

measured test results is indicated by standard deviation. These deviations are associated mostly with mould parameters, temperature and personnel errors. Such effects can be reduced through the proper control of mould parameters such as vent size and position, and controlling of pouring temperature of each successive test. For instance, if the vents (holes for escaping the gases from the mould) are on the cavity /channel, the flow of the

molten metal will be obstructed therefore reduces the flow length. These effects were observed during the experiment which resulted in discarding the casting that had such defects.

Figure 4.21 shows the test result when the recycled aluminium alloy was solidified in the cavity of the spiral fluidity mould. It shows the solidification of the alloy started by the flowing tip. The low surface temperature experienced by the leading tip must be facilitating the growth of the grains. Large size grains have a tendency in blocking the feeding channels. According to Fleming [83] the grains flow downstream with the liquid metal until a critical fraction solid is reached then the flow stops by choking at the tip of the freezing alloy.



Figure 4.21: The outcome of the alloy's fluidity when it is solidified

Figure 4.22 shows the microstructure of specimens taken 5 mm away from the tip of the casting spiral. It shows the primary aluminium dendrites, eutectic, Fe-intermetallics, Cu-intermetallics and oxides. Figure 4.22 (a) reveals the alloy containing some copper

phases nucleated along the thin iron phases, eutectic and oxides. Uniform distribution of phases of the eutectic silicon and Fe-intermetallics were observed in this alloy and no network of intermetallics were observed that could choke up the flowing molten metal.

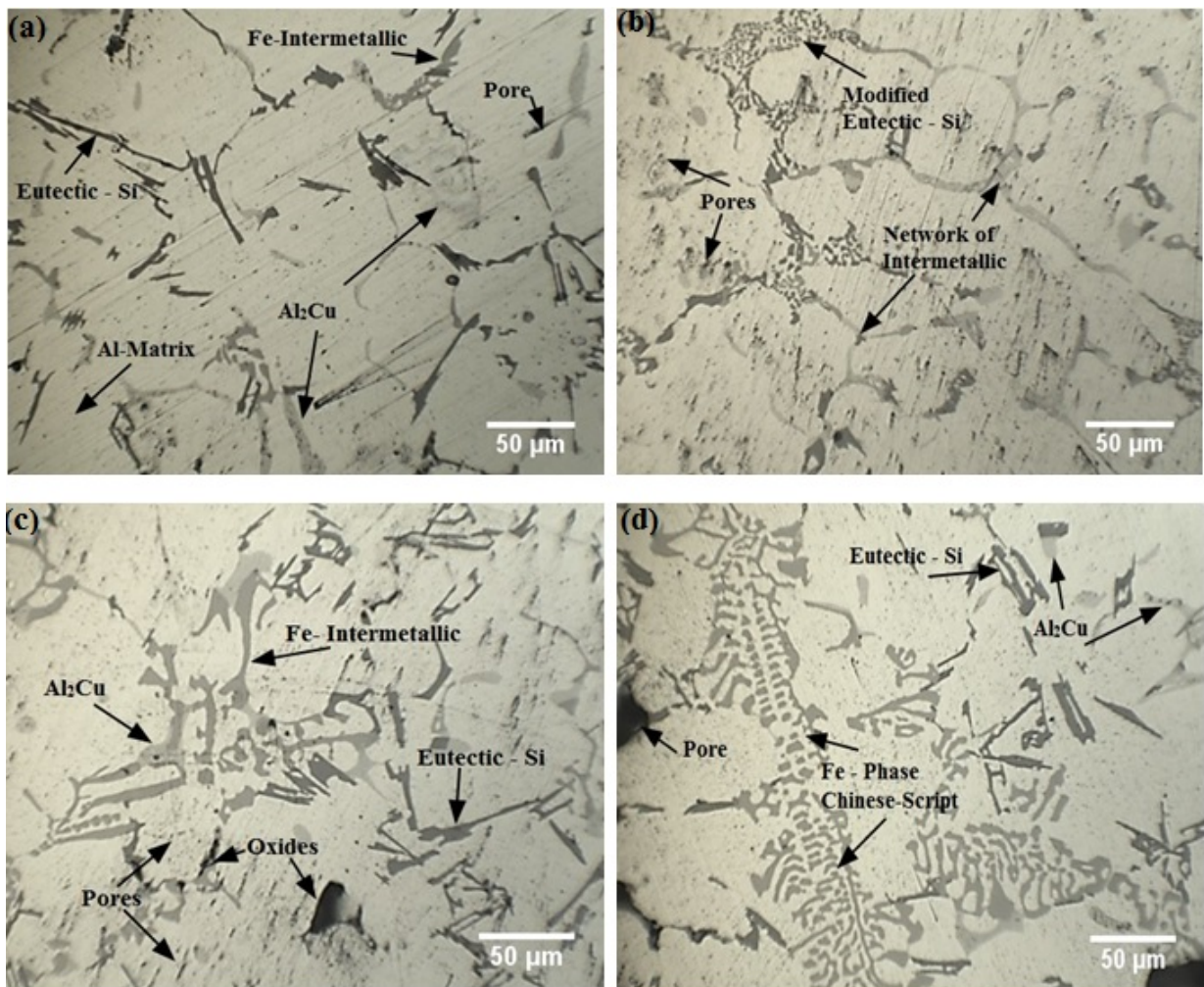


Figure 4.22: Micrograph of the alloys 5 mm from the tip of the fluidity casting, (a) Base alloy, (b) Sr - modified base alloy, (c) 0.38% Fe containing base alloy and (d) 0.9% Fe + 0.45% Mn containing base alloy

However, in Figure 4.22 (b) it was observed that strontium modification resulted in a network of intermetallic phases. These structures can block the flowing molten metal and then decrease the fluidity of the alloy if they solidify early before a coherent solid

network is formed.

Although Sr has a wide range of significant advantages in comparison with other chemical modifiers such as Na and Sb in foundry during casting [112], this study however, demonstrates that it reduces the fluidity of the alloy developed. Excess amount of Sr leads to porosity, which among others has been attributed to reduced surface tension of the melt and increased volumetric shrinkage [3]. Addition of Sr leads to segregation of the Cu-containing phases to regions away from the Al-Si eutectic. This can lead to blockage of the interdendritic channels if blocky Al_2Cu phases are formed during solidification [108]. If the modified alloy exposes to the atmosphere will react vigorously with ambient moisture to form hydrides and surface dross that can reduce the fluidity [112]. However, the use of rod type strontium modifier produces smaller Al_4Sr intermetallic particles that break and dissolve very rapidly which minimizes contact with the atmosphere.

Addition of Fe to this alloy has been observed to produce various intermetallic phases which have the potential to reduce the fluidity of the molten metal. Figure 4.22 (c) shows a number of Al_2Cu phases formed in addition to eutectic Si and oxides. The microstructure of Figure 4.22 (d) shows an increased number of Fe - intermetallics in comparison with Figure 4.22 (c). Moreover, the neutralizing effect of Mn is observed to result in fine Fe - intermetallics in the 0.9% Fe containing alloy. This may explain the higher fluidity reported in this alloy compared to the 0.38% Fe containing alloy.

Increase in the iron level in an alloy generally leads to an increase in the amount of insoluble iron-rich bearing phases which can reduce the alloy's fluidity. The β - phases

have largest surface to volume ratio, hence they have the largest interfacial region with the melt and are likely to be the most detrimental intermetallic in reducing fluidity [92]. Moreover, with an increase in size and amount of β and α phases, there is usually a concomitant increase in interconnected shrinkage porosity due to a reduction in the permeability/feeding in mushy zone [113].

CHAPTER 5

CONCLUSIONS AND RECOMMENDATIONS

5.1 CONCLUSIONS

Cylinder heads are identified as potential candidate for production of recycle-friendly cast aluminium alloys. Therefore component to component recycling of cylinder heads with or without modification are applicable for high quality products. Moreover, results of chemical composition analysis predicted that most of the cylinder heads in small vehicle engines in Kenya are manufactured from the JIS AC2B alloy which is equivalent to the 319 alloy.

Micrographs of the suggested model secondary alloy reveals coarse acicular eutectic silicon, Fe and Cu intermetallics in the as-cast state. Strontium modifies the eutectic silicon particle while Fe and Mn increases Fe-intermetallics. Heat treatment resulted in necking, fragmentation and spheroidisation of eutectic silicon particles and fragmentation of Fe - intermetallics.

Porosity level of the alloy increases with the addition of 0.02% Sr and 0.38% Fe and their maximum pores size are 120 μm and 160 μm respectively, in which they contributed in reducing the properties of the material.

The addition of strontium decreases the UTS and hardness and increases % elongation and impact toughness while addition of Fe and Fe + Mn decreases UTS, % elongation and impact toughness and increases hardness in the as cast state.

Heat treatment increases the mechanical properties by fragmenting and spheroidising the eutectic silicon particles. The suitable aging time of the alloy for obtaining peak hardness is between 2 and 6 hours at 170°C.

The fluidity of the recycled base alloy reduces with the addition of modifier and impurity levels.

5.2 RECOMMENDATIONS FOR FUTURE WORK

To pursue the need for a higher number and performance of recycle-friendly alloys, the following areas are recommended for further investigation.

- Automotive wheel alloys should be investigated by mixing with the alloys that possess high production recycling index.
- Fatigue and creep tests have to be conducted on the alloys developed in this research.
- Mechanical properties of these alloys should be investigated at different aging time at the same temperature of this research.
- Finally, detailed microstructural analysis such as SEM and TEM should be utilized to understand the effect of alloying elements on the microstructure and mechanical properties.

REFERENCES

- [1] Miller W.S., Zhuang L., Bottema J., Wittebrood A.J., De Smet P., Haszler A., Vieregge A. , “Recent Development in Aluminium Alloys for the Automotive Industry,” *Materials Science and Engineering*, vol. A280, pp. 37–49, 2000.
- [2] Kuafman J. G. and Rooy E. L., “Aluminium Alloys Casting: Properties, Processes and Application,” *ASM International*, www.asminternational.org, pp. 69–131, 2004.
- [3] Li Z, Samuel A.M., Samuel F.H., Ravindran C., Valtierra S., Doty H.W., “Parameters Controlling the Performance of AA319-type Alloys Part I Tensile Properties,” *Materials Science and Engineering* , vol. A 367, pp. 96–110, 2004.
- [4] European Aluminium Association, “Aluminium in Cars,” tech. rep., EAA, 2007.
- [5] Cui J. and Rove. H. J., “Recycling of Automotive Aluminium,” *Trans. Nonferrous Met. Soc. China*, vol. 20, pp. 2057–2063, 2010.
- [6] John Hartley, “The Increasing use of Aluminium Prospects and Implications,” tech. rep., European Commission Joint Research Centre, Institute for Prospective Technological Studies, 1996.
- [7] Das S.K., “Designing Aluminium Alloys for a Recycling Friendly World,” *Materials Science Forum*, vol. 519-521, pp. 1239–1244, 2006.

- [8] Sencakova L.E., Vircikova, “Lifecycle Assessment of Primary Aluminium Production,” *Acta, Metallurgical Slovaca*, vol. 13(3), pp. 412–419, 2007.
- [9] Musbah Mahfoud, Prasada Rao A.K., Daryoush Emadi, “The Role of Thermal Analysis in Detecting Impurity Levels During Aluminum Recycling,” *J. Therm Anal Calorim*, pp. 847–851, 2010.
- [10] Fabrizio Passarini, Luca Ciacci, Alessandro Santini, Ivano Vassura, Luciano Morselli, “Aluminium Flows in Vehicles: Enhancing the Recovery at End-of-Life,” *Springer Japan*, 2013.
- [11] Hatayama H, Daigo I, Matsuno Y, Adachi Y., “Evolution of Aluminum Recycling Initiated by the Introduction of Next-Generation Vehicles and Scrap Sorting Technology ,” *Resources, Conservation and Recycling* , vol. 66, pp. 8–14, 2012.
- [12] Moustafa M.A. , “Effect of Solution Heat Treatment and Additives on the Hardness, Tensile Properties and Fracture Behaviour of Al-Si (A413.1) Automotive Alloys,” *Journal of Material Science*, vol. 38, pp. 4523–4534, 2003.
- [13] M.Handbook, “Casting,” *ASM International, Metals Park, oH*, vol. 15(9th Edition), p. 286, 1988.
- [14] Mbuya T.O., Odera B.O. and Ng’ang’a S.P., “Influence of Iron on Castability and Properties of Aluminium Silicon Alloys, Literature Review,” *Int. J. cast. Met. Res.*, vol. 16(5), pp. 451–465, 2003.

- [15] Nissan Motor Corporation, “Recycling Efferts,” tech. rep., <http://www.nissan-global.com/EN/ENVIRONMENT/CAR/RECYCLE>, 2014.
- [16] Roja Modaresi, Amund N. Lvik and Daniel B. Mu ller, “Component and Alloy-Specific Modeling for Evaluating Aluminum Recycling Strategies for Vehicles,” *The Minerals, Metals & Materials Society*, 2014.
- [17] Sreeja kumari S.S., Pillai R.M., Rajan T.P.D, Paay B.C., “Effects of Individual and Combined Additions of Be, Mn, Ca, and Sr on the Solidification Behaviour, Structure and Mechanical Properties of Al-7Si-0.3Mg-0.8Fe alloy,” *Material Science and Engineering*, vol. A 460-461, pp. 561–573, 2007.
- [18] Kim C.Y., Umezawa O., Nagai K., “Materials,” vol. 4, pp. 1027–1031, 1998.
- [19] Lu S. Z. and Hellawell, “The Mechanism of Silicon Modification in Aluminium Alloys Impurity Induced Twinning,” *Metallurgy and Materials Transaction*, vol. 18A, pp. 1721–1733, 1987.
- [20] Heiberg G. , “Columnar to Equiaxed Transition of Eutectic in Hypoeutectic Aluminium-Silicon Alloys,” *Acta. Materials*, vol. 50, pp. 2537–2546, 2002.
- [21] Zolotorevsky V.S., Belov N. A., and Glazoff M.V., “Casting Aluminum Alloys (Oxford, UK, Elsevier,” *Oxford, UK, Elsevier*, p. 327, 2007.
- [22] Haizhi Y. , “An Overview of the Development of Al-Si Alloy Based Material for Engine Applications,” *ASM International*, vol. 12, pp. 288–297, 2003.

- [23] Mohamed A.M. A., Samuel A.M., Samuel F.H., Doty H.W. , “Influence of Additives on the Microstructure and Tensile Properties of Near Eutectic Al-10.8Si Cast Alloy,” *Materials and Design*, vol. 30, pp. 3943–3957, 2009.
- [24] Makhoulf M.M., Guthy H.V., “Al-Si Eutectic Reaction, Mechanisms and Crystallography,” *Journal of Light Metals*, vol. 1(4), pp. 199–218, 2001.
- [25] Samuel F.H., Samuel A.M., Liu H., “Effect of Mg Content on the Ageing Behaviour of Water Chilled Al-Si-Cu-Mg-Fe-Mn(380) Alloy Castings,” *Journal of Material Science*, vol. 30, pp. 2531–2540, 1995.
- [26] Liu D., Atkinson H.V., Kapranos P., Jirattiticharoean W., and Jones H., “Microstructure Evolution and Tensile Mechanical Properties of Thixoformed High Performance Aluminium Alloys,” *Mater. Sci. and Eng*, vol. A361, pp. 213–224, 2003.
- [27] Taylor J.A., StJohn D.H., Zheng L.H., Edwards G.A., Barresi J., Couper M.J., “Solution Treatment Effects in Al-Si-Mg Casting Alloys Part I Intermetallic Phase,” *Aluminium Transactions*, vol. 4-5, pp. 95–110, 2001.
- [28] Apelian D., “Aluminium Cast Alloys, Enabling Tools for Improved Performance,” *Worldwide Report*, vol. -, pp. 1–60, 2009.
- [29] Moller H., Gonasagren G., Waldo S. , “Factors Influencing Tensile Mechanical Properties of Al-7Si-Mg Casting Alloys A356/7,” *TMS (The Minerals, Materials Society)*, pp. 467–471, 2012.

- [30] NADCA, "Product Specification for Die Castings/sec.3," *Source ASTM B85-92a, Aluminium Association*, 1994.
- [31] Zhang B., Garro M., Tagliano C., "DAS in Aluminium Alloy Cylinder Heads Produced by Gravity Semi-Permanent Mold," *Metall. Sci. and Tech.*, vol. 21(1), 2003.
- [32] Mbuya T.O., Odera B.O., Ng'ang'a S.P. and Oduori F.M., "Effective Recycling of Cast Aluminium Alloys for Small Foundries," *JAGST*, vol. 12(2), 2010.
- [33] Hwang J.Y., Doty H.W., Kaufman M.J. , "The Effect of Mn Addition on the Microstructure and Mechanical Properties of Al-Si-Cu Casting Alloys," *Materials Science and Engineering*, vol. A 488, pp. 496–504, 2008.
- [34] Garat M.,Laslaz G., "Improved Aluminium Alloys for Common Rail Diesel Cylinder Heads," *AFS Transactions*, 2007.
- [35] Markus Bernd Grieb, Hans-Jrgen Christ, Burkhard Plege, "Thermo-Mechanical Fatigue of Cast Aluminium Alloys for Cylinder Head Applications Experimental Characterization and Life Prediction," *Procedia Engineering*, vol. 2, pp. 1767–1776, 2010.
- [36] Mousa Javidani and Daniel Larouche, "Application of Cast AlSi Alloys in Internal Combustion Engine Components," *International Materials Reviews*, vol. 59(3), pp. 132–158, 2014.
- [37] Feikus, F.J., "Optimization of Al-Si Cast Alloys for Cylinder Head Applications," *AFS Transactions*, vol. 105, pp. 225–231, 1997.

- [38] Garat M., “Casting Made from Aluminium Alloy, Having High Hot Creep and Fatigue Resistance,” *Patent Application Publication, US*, vol. US 2011/0126947 A1, 2011.
- [39] Mrwka-Nowotnik G., Sieniawski J., “Microstructure and Mechanical Properties of C355.0 Cast Aluminium Alloy,” *International Scientific Journal*, vol. 47(2), pp. 85–94, 2011.
- [40] Murray J.L. and McAlister A.J., “The Al-Si (Aluminium-Silicon) System.,” *Bulletin of Alloy Phase Diagram*, vol. 5(1), 1984.
- [41] The, “Aluminium Automotive, Casting Alloys and Products Manual,” *European Aluminium Association Version*, 2002.
- [42] Dwivedi D.K., Sharma R. and Kumar A., “Influence of Silicon Content and Heat Treatment Parameters on Mechanical Properties of Cast Al-Si-Mg Alloys,” *International Journal of Metals Research*, vol. 19(5), p. 275, 2006.
- [43] Caceres C.H., Svensson I.L., Taylor J.A., “Strength-Ductility Behaviour of Al-Si-Cu-Mg Casting Alloys in T6 Temper,” *International Journal of Casting Metals Research*, vol. 15, pp. 531–543, 2003.
- [44] Samuel A.M., Samuel F.H., Doty H.W., “Factors Controlling the type and Morphology of Copper Containing Phase in 319 Aluminium Alloy,” *AFS, Trans.*, vol. 104, pp. 893–901, 1996.

- [45] Rathod N.R., Manghani J.V., “Effect of Modifier and Grain Refiner on cast Al-Si Aluminium Alloy,” *A Review International Journal of Emerging Trends in Engineering and Development*, vol. 2, pp. 573–582, 2012.
- [46] Mallapur D.G., Mallapur U.K. & Kori S.A. , “Influence of Ti,B and Sr on Microstructure and Mechanical Properties of A356,” *International Journal of Mechanical Engineering and Technology*, vol. 1, pp. 49–59, 2010.
- [47] Mose B.R., Mbuya T.O., Maranga S.M., “Effect of Minor Elements on Castability, Microstructure and Mechanical Properties of Recycled Aluminium Casting Alloys,” Master’s thesis, JKUAT, 2009.
- [48] Dinnis C.M., Taylor J.A. and Dahle A.K., “Porosity Formation and Eutectic Growth in Al-Si-Cu-Mg Alloys Containing Iron and Manganese,” *Materials Forum*, vol. 28, pp. 1016–1021, 2004.
- [49] Wang Q.G., Caceres C.H., Griffiths J.R, “Cracking of Fe-Rich Intermetallics and Eutectics Si Particles in an Al-7Si-0.7Mg Casting Alloy,” *AFS Transactions*, pp. 131–136, 1998.
- [50] Li Z. , Samuel A.M., Samuel F.H., Ravindran C., Doty H.W. & Valtierra S., “Parameters Controlling the Performance of AA319-type Alloys Part II Impact Properties and Fractography,” *Material Science and Engineering*, vol. A367, pp. 111–122, 2004.

- [51] Sreeja Kumari S.S., Pillai R.M., Nogita K., Dahle A.K., Pai B.C., “Influence of Calcium on the Microstructure and Properties of Al-7Si-0.3Mg-XFe Alloy,” *Metall. and Mater. Trans.*, vol. A37, pp. 2581–2587, 2006.
- [52] Villeneuve C., Samuel A.M., Samuel F.H., Doty H.W., Valtierra S., “Role of Trace Elements in Enhancing the Performance of 319 Aluminium Foundry Alloys,” *AFS Transactions*, pp. 01–023, 2001.
- [53] Seifeddine S., “Influence of Iron on the Microstructure and Mechanical Properties of Al-Si Cast Alloy,” *Literature Review Vilmer Project-5.2 Casting*, 2007.
- [54] Khalifa W., Samuel A.M., Samuel F.H., Doty H.W. and Valtierra S., “Metallographic Observations of β -AlFeSi Phase and its Role in Porosity Formation in Al-7%Si Alloys,” *Int. J. Cast, Met. Res.*, vol. 9(3), 2006.
- [55] Djurdjevic M.B., Stockwell T.J. and Sokolwski J.H. *Int. J. Cast Metals Res*, vol. 12, pp. 67–73, 1999.
- [56] Alfonso I., Maldonado C., Gonzalez G., Bedola A., “Effect of Mg Content and Solution Treatment on the Microstructure of Al-Si-Cu-Mg Alloys,” *Journal of Materials Science*, vol. 41(7), pp. 1945–1952, 2006.
- [57] Edwards G.A., Sigworth G.K., Caceres C.H., St John D. and Barresi J., “Microporosity Formation in Al-Si-Cu-Mg Casting Alloys,” *AFS Trans.*, vol. 105, pp. 809–818, 1997.

- [58] Samuel A.M., Samuel F.H., “Effect of Alloying Elements and Dendrite Arm Spacing on the Microstructure and Hardness of an Al-Si-Cu-Mg-Fe-Mn (380),” *Journal of Material Science*, vol. 30, pp. 1698–1708, 1995.
- [59] Paray F., Kulunk B. and Gruzleski J.E., “Impact Properties of Al-Si Foundry Alloys,” *Int. J. Cast Metals Res*, vol. 13, pp. 17–37, 2000.
- [60] Rometsch P.A., Arnberg L. and Zhang D.L., “Modelling Dissolution of Mg₂Si and Homogenisation in Al-Si-Mg Casting A,” *Int. J. Cast Metals Res.*, vol. 12, pp. 1–8, 1999.
- [61] Taylor J.A., “Iron-Containing Intermetallic Phase in Al-Si Based Casting Alloys,” *Procedia Materials Science*, vol. 1, pp. 19–33, 2012.
- [62] Caceres C.H. , Davidson C.J., Griffiths J.R. and Wang Q.G., “Effect of Mg on the Microstructure and Mechanical Behaviour of Al-Si-Mg Casting Alloys,” *Metal. and Mater. Trans.*, vol. A 30, pp. 2611–2618, 1999.
- [63] Tash M., Samuel F.H., Mucciardi F., Doty H.W., “Effect of Metallurgical Parameters on the Hardness and Microstructural Characterization of As Cast and Heat treated 356 and 319 Aluminium Alloys,” *Materials Science and Engineering*, vol. A 443, pp. 185–201, 2007.
- [64] Garcia-Garcia G. Espinoza-Cuadra J. Mancha-Molinar., “Copper Content and Cooling Rate Effects Over Second Phase Particles Behavior in Industrial Aluminium-Silicon Alloy 319,” *Materials and Design*, vol. 28, pp. 428–433, 2007.

- [65] Metals Handbook *ASM International Handbook Committee*, vol. 9th Edition, p. 130, 1990.
- [66] Rana R.S., Purohit R., Das S., “Reviews on the Influences of Alloying Elements on the Microstructure and Mechanical Properties of Aluminium Alloys and Aluminum Alloy Composites,” *International Journal of Science and Research*, vol. 2(6), pp. 2250–3153, 2012.
- [67] Wang Q.G, and Caceres C.H., “Mg Effects on the Eutectic Structure and Tensile Properties of Al-Si-Mg Alloys,” *Materials Science Forum*, vol. 242, pp. 159–164, 1997.
- [68] Firouzdor V., Rajabi M., Nejati E., Khomamizadeh F., “Effect of Microstructural Constituents on the Thermal Fatigue life of A319 Aluminum Alloy,” *Materials Science and Engineering*, vol. A 454-455, pp. 528–535, 2007.
- [69] Bruner R.W. , “Metallurgy of Die Casting Alloys,” *SDCE, DETROIT, MI*, p. 25, 1976.
- [70] Paramo V., Rafael C., Eulogio V., and Salvador V., “Spheroidization of the Al-Si Eutectic in a Cast Aluminium Alloy,” *Journal of Materials Engineering and Performance*, vol. 9, pp. 616–622, 2000.
- [71] Francisco Javier Tavitias-Medrano, *Artificial Aging Treatments of 319-type Aluminum Alloys*. PhD thesis, McGill University, Montreal, 2007.

- [72] Tavitas-Medrano F.J., Gruzleski J.E., Samuel F.H., Valtierra S., Doty H.W., “Effect of Mg and Sr-Modification on the Mechanical Properties of 319-type Aluminium Cast Alloys Subjected to Artificial Aging,” *Materials Science and Engineering*, vol. A 480, pp. 356–364, 2008.
- [73] The Materials Information Company, “Heat Treating, Handbook,” *ASM, International*, vol. 4, 1991.
- [74] Toda H., Nishimura T., Uesugi K., Suzuki Y. and Kobayashi M., “Influence of High-Temperature Solution Treatments on Mechanical Properties of an AlSiCu Aluminium Alloy,” *Acta Materialia*, vol. 58, pp. 2014–2025, 2010.
- [75] Sjolander E. and Seifeddine S., “The Heat Treatment of Al-Si-Cu-Mg Casting Alloys,” *Journal of Material Processing Technology*, vol. 210, pp. 1249–1259, 2010.
- [76] Kores S., Zak H., Tonn B., “Aluminium Alloys for Cylinder Heads,” *RMZ-Materials and Geoenvironment*, vol. 55(3), pp. 307–317, 2008.
- [77] Jae-Gil Jung, June-Soo Park, Yang-Soo Ha, Young-Kook Lee, Joong-Hwan Jun, Hee-Sam Kang, and Jong-Dae Lim, “The Optimal Solution Treatment Condition in a Al-Si-Cu AC2B Alloy,” *J. Kor. Inst. Met. and Mater.*, vol. Vol. 47(4), pp. 223–227, 2009.
- [78] Di Sabatino M., Arnberg L., “Castability of Aluminium Alloys,” *Transactions of the Indian Institute of Metals*, vol. 62, pp. 321–325, 2009.

- [79] Timelli G. , Bonollo F., “Fluidity of Aluminium Alloy Die Casings,” *Int. Journal of Cast Metals Research*, 2007.
- [80] Arami H., Khalifehzadeh R., Akbari M., Khomamizadeh F., “Microporosity Control and Thermal-Fatigue Resistance of A319 Aluminium Foundry Alloy,” *Materials Science and Engineering*, vol. 472, pp. 107–114, 2008.
- [81] Ammar H.R., Samuel A.M., Samuel F.H., “Effect of Casting Imperfections on the Fatigue life of 319-F and A356-T6 Al-Si Casting Alloys,” *Materials Science and Engineering*, vol. 473, pp. 65–75, 2008.
- [82] Young-Dong K., Zin-Hyoung L., “The Effect of Grain Refining and Oxide Inclusion on the Fluidity of Al-5.5Cu-0.6Mn and A356 Alloys,” *Materials Science and Engineering*, vol. A360, pp. 372–376, 2003.
- [83] Flemings M. C., “Solidification Processing,” *Metallurgical Trans.*, vol. 5, pp. 2121–2134, 1974.
- [84] Di Sabatino M., Syvertsen F., Arnberg L., Nordmark A., “An Improved Method for Fluidity Measurement by Gravity Casting of Spirals in Sand Moulds,” *International Journal of Cast Metals Research*, vol. 18, pp. 59–62, 2005.
- [85] John Campbell, *The New Metallurgy of Casting Metals, Casting*. Elsevier Science Ltd, 2003.

- [86] Dahle A.K., Tondel P.A., Paradies C.J. and Arnberg L., “Effect of Grain Refinement on the Fluidity of two Commercial Al-Si Foundry Alloys,” *Metallurgical and Materials Transactions A*, vol. 27A, pp. 2305–2313, 1996.
- [87] Di Sabatino M., L. Arnberg, “A Review on the Fluidity of Al Based Alloys,” *Metallurgical Science and Technology*, Ed. by Teksid Aluminum, vol. 22, pp. 9–15, 2004.
- [88] Mose B. R., Maranga S. M., Mbuya T. O., “Effect of Minor Elements on the Fluidity of Secondary LM25 and LM27 type Cast Alloys,” *AFS Transactions*, pp. 93–101, 2009.
- [89] Lang G., “Aluminium,” vol. 48, pp. 664–672, 1972.
- [90] John Campbell and Richard A. Harding, “The Fluidity of Molten Metals,” Master’s thesis, IRC in Materials, Advanced lecture, The University of Birmingham, 1994.
- [91] Sanchez S., Velasco E., P.del C. Zambrano and Cavazos J. L., “Effect of Titanium and Strontium Addition on the Fluidity of A319 and A356 Aluminium Alloys,” *Materials Science Forum*, vol. 509, pp. 159–164, 2006.
- [92] Ahmad R., Sadeghi R., Asmael M. B. A, Mohamad H., Harun Z., Hasan S., “The Influence of Metallic Addition on Fluidity of Aluminium (LM6) Alloy,” *Applied Mechanics and Materials*, vol. 465-466, pp. 954–957, 2014.

- [93] Gowri S., Samuel F. H., “Effect of Alloying Element on the Solidification Characteristics and Microstructure of Al-Si-Cu Mg-Fe 380 alloy,” *Metall. and Mater. Trans.*, vol. 25 A, pp. 437–448, 1994.
- [94] Kevorkijan V., “Numerical Predicting of Recycling Friendly Wrought Aluminium Alloy Composition,” *Metall. Mater. Eng.*, vol. 19 (3), pp. 249–257, 2013.
- [95] Gaustad G., Olivetti E. and Kirchain R., “Design for Recycling, Evaluation and Efficient Alloy Modification,” *Journal of Industrial Ecology (Forum)*, vol. 14(2), pp. 286–308, 2010.
- [96] Varužan Kevorkijan, “Advances in Recycling of Wrought Aluminium Alloys for Added Value Maximisation,” *MJoM*, vol. 16(2), pp. 103–114, 2010.
- [97] Dimos Paraskevas, Karel Kellens, Renaldi, Wim Dewulf, Joost R. Duflou, “Closed and Open Loop Recycling of Aluminium: A Life Cycle Assessment Perspective,” in *Proceedings of the 11th Global Conference on Sustainable Manufacturing ,Berlin - Germany*, 2013.
- [98] Das K. S., “Aluminium Recycling Index,” in *11th International Conference on Aluminium Alloys, Aachen, Germany*, 2008.
- [99] Prasada Rao A. K., “An Approach for Predicting the Composition of a Recycled Al-Alloy,” *Trans Indian Inst Met* , vol. 64(6), pp. 615–617, 2011.
- [100] Das K.S., Green J.A.S., and Kaufman G.J., “The Development of Recycle-Friendly Automotive Aluminum Alloys,” *JOM*, pp. 47–51, 2007.

- [101] “Hadleigh Casting Limited, LM25 Aluminium Casting Alloy, England, www.hadleighcastings.com, Accessed, June 2013.”
- [102] The Aluminium Automotive Manual, “Applications Power train Cylinder Heads,” tech. rep., European Aluminium Association, 2011.
- [103] “Aluminium Casting Alloys, [www.milver.com /uploads/file/AAMAR.pdf](http://www.milver.com/uploads/file/AAMAR.pdf) .”
- [104] Hayashi S., Miyake J., Koyama M., Sakaguchi K., “Method for Manufacturing a Cylinder Head of Cast Aluminium Alloy for Internal Combustion Engines by Employing local Heat Treatment,” *United States Patent*, 1987.
- [105] Merkus G. H., *Particle Size Measurements, Fundamentals, Practice, Quality*. Springer, 2008.
- [106] Samuel F. H. Quillet P. Samuel A. M. and Doty H. W., “Effect of Mg and Sr Additions on the Formation of Intermetallics in Al₆Si_{3.5}Cu 0.45 to 0.8Fe 319 Type Alloys,” *Metallurgical and Materials Trans.A*, vol. 29A, pp. 2871–2884, 1998.
- [107] European Aluminium Association, “Aluminium Recycling in Europe the Road to High Quality Products,” tech. rep., EAA, 2006.
- [108] Li Z., Samuel A. M., Samuel F. H., “Effect of Alloying Elements on the Segregation and Dissolution of CuAl₂ Phase in Al-Si-Cu 319 Alloys,” *Journal of materials science*, vol. 38, pp. 1203 –1218, 2003.

- [109] Eva Tillov, Mria Chalupov and Lenka Hurtalov, “Evolution of Phases in a Recycled Al-Si Cast alloy During Solution Treatment,” *www.intechopen.com*, pp. 411–438, 2012.
- [110] Kuntongkum S., Wisutmethangoon S., Plookphol T. and Wannasin J., “Influence of Heat Treatment Processing Parameters on the Hardness and the Microstructure of Semi-Solid Aluminum Alloy A356,” *Journal of Metals, Materials and Minerals*, vol. 18(2), pp. 93–97, 2008.
- [111] Lenka Hurtalova , Juraj Belan, Eva Tillova, Mria Chalupova, “Changes in Structural Characteristics of Hypoeutectic Al-Si Cast Alloy After Age Hardening,” *ISSN 1392-1320 Materials Science*, vol. 18(3), pp. 228–233, 2012.
- [112] COMALCO, “Modification of Foundry Al-Si Alloys,” tech. rep., Comalco Aluminium Limited Technical Report no.4, Brisbane, Australia, 1997.
- [113] Wang Q.G, Jones P. E and Osborne M., “Effect of Iron on the Microstructure and Mechanical Properties of an Al7Si0.4Mg Casting,” *Advanced Materials Engineering*, 2003.
- [114] Clansey E. B., “Cylinder Heads Research Investigation,” *Clansey Metallurgical Auckland*, <http://www.aagaskets.com.au>, Accessed, June 2013.
- [115] Molina R., Amalberto P. and Rosso M., “Mechanical Characterization of Aluminium Alloys for High Temperature Applications Part1: Al-Si-Cu Alloys,” *Metallurgical Science and Technology*, vol. 29-1, pp. 5–15, 2011.

- [116] Caton M. J, Jones J. W. and Allison J. E., “The Influence of Heat Treatment and Solidification Time on the Behavior of Small-Fatigue-Cracks in a Cast Aluminum Alloy,” *Materials Science and Engineering*, vol. A314, pp. 81–85, 2001.
- [117] Mria Farkaov, Eva Tillov and Mria Chalupov, “Modification of Al-Si-Cu Cast Alloy,” *FME Transactions*, vol. 41, pp. 210–215, 2013.
- [118] Byczynski G. E., Kierus W. T., Northwood D. O., Penrod D., Sokolowski J. , “The Effect of Quench Rate on Mechanical Properties of 319 Aluminium Alloys Castings,” *Materials Science Forum*, vol. 217-222, pp. 783–788, 1996.
- [119] Engler-Pinto Jr , “Thermo-Mechanical Fatigue Behavior of Cast 319 Aluminium Alloys,” *Elsevier Science Ltd.*, pp. 3–9, 2002.
- [120] Cerri E., Evangelista E. and Bardi F., “Fracture Behaviour and Relationship with Mechanical Properties of a Thixocast Aluminium Alloy,” *Key Engineering Materials, Trans Technology Publications*, vol. 188, pp. 111 – 120, 2000.
- [121] Karthikeyan L., Senthilkumar V. S. and Padmanabhan K. A., “On the Role of Process Variables in the Friction Stir Processing of Cast Aluminum A319 Alloy,” *Materials and Design*, vol. 31, pp. 761–771, 2010.
- [122] Ji-Yong Yao, Geoffrey A. Edwards, and Daniel A. Graham , “Precipitation and Age-Hardening in Al-Si-Cu-Mg-Fe Casting Alloys,” *Materials Science Forum*, pp. 777–782, 1996.

APPENDIX A

Cylinder Head Alloys

Figure A.1 shows the percentage of availability of the alloys based on the literature survey collected data. The number of 319 alloys are very high (50%) followed by 356 alloys. The alloys 355 and 380 have equal amount while the 354 alloys are the least.

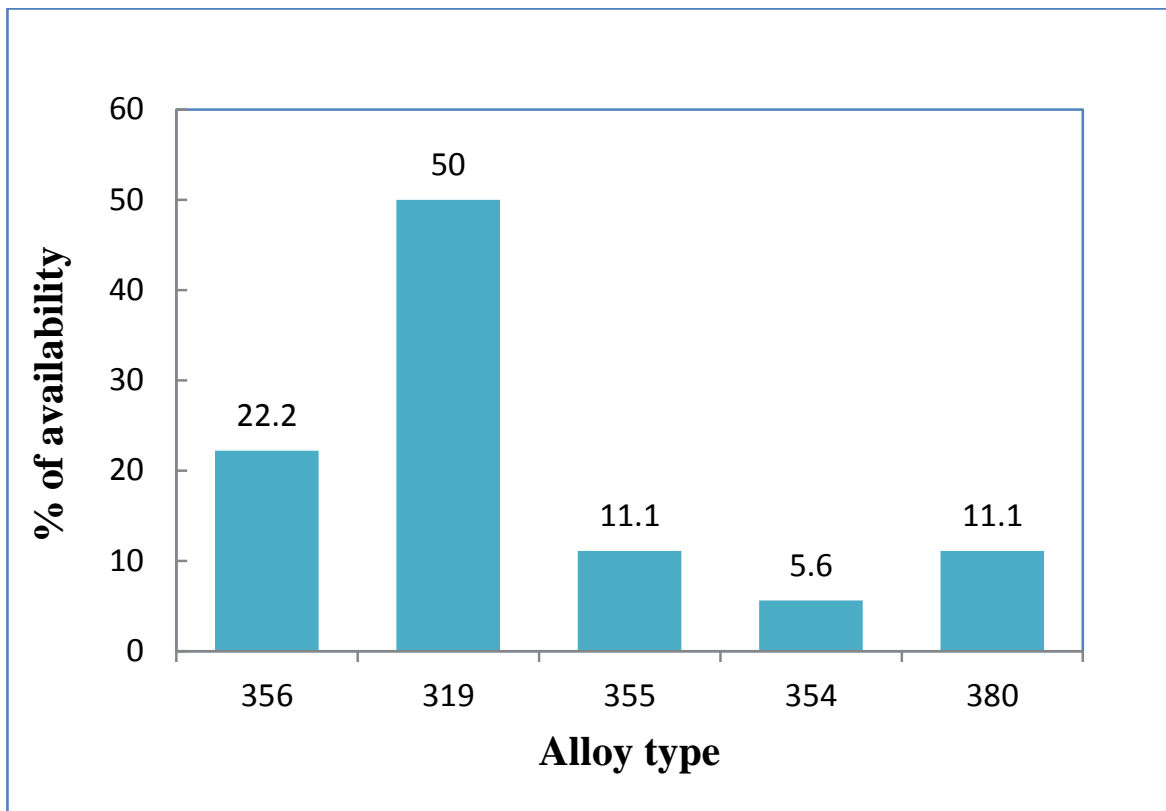


Figure A.1: Percentage of the alloys availability based on the literature survey

Table A.1: Cylinder head alloys produced by different manufacturers and researchers

Sr.No.	Alloy	Si	Cu	Mg	Fe	Mn	Ti	Zn	Cr	Sr	Ni	others	Ref.
1	BS1490LM25	6.5/7.5	0.2	0.2/0.6	0.5	0.3	0.2	0.1			0.1	Sn(0.05)	[101]
2	A356 (Hyundai)	6.5/7.5	0.2	0.25/0.45	0.2	0.1	0.1/0.2						[31]
3	A354 (fiat iveco)	9.0/10.0	0.8/1.3	0.25/0.5	0.3	0.1	0.1						[31]
4	319 (Fiat Ford)	6.5/8.0	2.8/3.5	0.25/0.5	0.8	0.5	0.25						[31]
5	380 (Mitsubishi)	8.3	3.64	0.3	0.6	0.33	0.11	0.7	0.03		0.07		[114]
6	A380 (Mazda)	8.49	2.76	0.15	0.69	0.36	0.07	0.69	0.05		0.08		[114]
7	AlSi9Cu1	9.4	1.05	0.4	0.25	0.1	0.05			0.05			[115]
8	319	5.5/6.5	3.0/4.0	0.1	1	0.5	0.25	1			0.35		[72]
9	Mn02	6.7	3.75	0.45	0.5	0.02							[33]
10	AlSi7MgCu	7	0.5	0.3	0.3	0.2	0.15	0.1					[76]
11	AlSi6Cu	7.21	3.84	0.33	0.36	0.45	0.16	0.88					[76]
12	A319	6.32	3.33	0.37	0.29	0.27	0.02			0.0002	0.001		[68]
13	W319	7.43	3.33	0.22	0.38	0.24	0.12	0.13	0.03	0.03	0.01		[116]
14	A380	9.4	2.4	0.28	0.9	0.24	0.05	1	0.04		0.05	Sn(0.03)	[111]
15	EN-AC-ALSi8Cu3 (A380.2)	7.5/9.5	2/3.5	0.05/0.55	0.8	0.15/0.65	0.25	1.2			0.35		[102]
16	EN-AC-ALSi6Cu4 (A319)	5.7	3/5	0.55	1	0.2/0.65	0.25	2			0.45		[102]
17	EN-AC-ALSi8Cu3 (LM25)	6.8/7.2	0.15	0.25/0.65	0.45	0.35	0.05/0.2	0.15			0.15		[102]
18	AlSi6Cu4 (Kia Ceed)	6.52	3.88	0.29	0.43	0.45	0.15	0.46	0.01		0.01		[117]

Table A.2: Cylinder head alloys produced by different manufacturers and researchers continued....

Sr.No.	Alloy	Si	Cu	Mg	Fe	Mn	Ti	Zn	Cr	Sr	Ni	others	Ref.
19	319	6.5	3.52	0.3	0.35	0.24	0.12			0.027			[118]
20	A356	7.13	<0.02	0.37	0.11	<0.02	0.14			170ppm			[34]
21	A356+Cu0.5	7.45	0.49	0.34	0.1	<0.02	0.13			199ppm			[34]
22	A356+Cu0.5+Mn0.15	6.84	0.48	0.3	0.11	0.15	0.12			159ppm		Zr0.14	[34]
23	AlSiCu3.3TiMn0.15	6.95	3.33	0.02	0.08	0.15	0.14			84PPm		Zr0.15V0.25	[34]
24	AlSiCu3.3TiMn0.15	7.01	3.76	<0.02	0.09	0.16	0.16			79ppm		Zr0.15V0.25	[34]
25	EA319	7.35	3.32	0.22	0.78	0.24	0.13			0.03			[119]
26	319 thixocast	5.8	2.9	0.3	0.13	0.02	0.02	0.02		215ppm	0.01		[120]
27	319	5.2	2.51	0.15	0.35	0.26	0.09	0.29			0.04	Sn0.01	[121]
28	355	4.5/5.5	1/1.5	0.4/0.5	0.06/0.6	0.03/0.5	0.04/0.25	0.03/0.35	0.25				[28]
29	C355.0	5.2	1.3	0.53	0.2	0.14	0.1						[39]
30	LM4	4.0/6.0	2.0/4.0	0.2	0.8	0.2/0.6	0.2	0.5			0.3	Sn0.1Pb0.1	[103]
31	LM16	4.5/5.5	1.0/1.5	0.4/0.6	0.6	0.5	0.2	0.11			0.25	Sn0.05Pb0.1	[103]
32	JIS AC2B	5/7	2/4	<0.5	<1.0	<0.5	<0.2	<1.0			<0.3		[104]
33	JIS AC4B	7/10	2/4	<0.5	<1.0	<0.5	<0.2	<1.0			<0.3		[104]
34	JIS AC4C	6.5/7.5	<0.2	0.2/0.4	<0.5	<0.3	<0.2	<0.3					[104]
35	HMG (320)	7.1	3.0	0.39	0.46	0.27	0.04	0.04	0.013	0.01	0.01	Bi0.004Pb0.01	[122]
36	LMg (320)	6.8	2.9	0.08	0.41	0.28	0.04	0.04	0.015	0.02	0.02	Bi0.005Pb0.02	[122]

APPENDIX B

Results of Mechanical Properties Tests

Table B.1: Summary of the UTS values from tensile tests for each alloy in the as-cast and heat treated conditions (MPa)

Alloys as-cast and HT	1 st	2 nd	3 rd	4 th	5 th	6 th	Mean	S.Deviation
Base alloy(SI)	212.31	231.54	223.42	182.27	215.41	192.21	209.53	17.14
HT (SI)	406.21	364.47	387.91	411.69	416.91	395.85	397.17	17.51
SI + 0.02% Sr	201.99	232.80	226.89	182.27	182.27	195.52	203.62	19.89
HT (Sr)	333.27	311.51	328.08	318.14	299.22	294.94	314.19	13.99
SI + 0.38% Fe	222.53	205.24	211.23	171.18	191.08	171.18	195.40	19.47
HT (Fe)	333.24	304.32	307.40	332.63	325.23	329.36	322.03	11.76
SI + 0.9% Fe + 0.45% Mn	244.16	201.70	229.37	178.95	172.33	182.27	201.46	26.85
HT (Fe + Mn)	337.16	304.69	314.54	321.81	324.97	300.60	317.29	12.38

Table B.2: Representative 0.2% yield stress of the heat treated sample (MPa)

Alloy	0.2% yield stress
Base alloy (SI)	390.1
SI + 0.02% Sr	321.4
SI + 0.38%Fe	332.5
SI+ 0.9%Fe + 0.45%Mn	321.7

Table B.3: Percentage elongation of the alloys in as-cast and heat treated conditions (%)

Alloys as-cast and HT	1 st	2 nd	3 rd	4 th	5 th	6 th	Mean	S.Deviation
Base alloy(SI)	1.19	1.40	1.20	1.58	1.95	1.37	1.45	0.26
HT (SI)	1.62	0.81	1.20	1.02	1.23	0.61	1.08	0.32
SI + 0.02% Sr	1.60	1.99	1.76	1.73	1.74	2.13	1.83	0.18
HT (Sr)	1.04	0.80	1.21	0.61	1.04	1.33	1.00	0.24
SI + 0.38% Fe	1.20	0.71	0.61	1.39	1.96	0.78	1.11	0.47
HT (Fe)	0.80	0.81	1.00	0.91	1.01	0.99	0.92	0.09
SI + 0.9% Fe + 0.45% Mn	1.72	1.01	1.20	1.59	0.98	1.36	1.31	0.28
HT (Fe + Mn)	1.59	1.01	0.60	1.24	0.80	0.79	1.00	0.33

Table B.4: Impact energy values of the alloys in the as-cast and heat treated conditions (J)

Alloys as-cast and HT	1 st	2 nd	3 rd	4 th	5 th	6 th	7 th	Mean	S.Deviation
SI(as-cast)	5.34	7.99	5.34	7.99	9.3	6.67	9.30	7.42	1.68
HT (SI)	10.61	6.67	13.22	10.61	13.22	11.92	13.22	11.35	2.20
SI + 0.02%Sr	10.61	11.92	11.92	6.67	7.99	11.92	11.92	10.42	2.20
HT (Sr)	7.99	9.3	13.22	7.99	11.92	11.92	9.30	10.23	2.10
SI + 0.38%	6.67	5.34	7.99	4.01	5.34	6.67	6.67	6.10	1.29
HT (Fe)	11.92	14.51	14.51	11.92	14.51	11.92	10.61	12.84	1.63
SI+ 0.9%Fe + 0.45%Mn	7.99	7.99	6.67	7.99	6.67	6.67	7.99	7.42	1.29
HT (Fe + Mn)	13.22	15.80	11.92	13.22	14.51	13.22	13.22	13.58	1.23

Table B.5: Average micro-hardness values in the as-cast and heat treat samples

Aging Time (h)	Base alloy (SI) (VHN)	SI + 0.02% Sr (VHN)	SI + 0.38%Fe (VHN)	SI0.9%Fe0.45%Mn (VHN)
As-cast	98.34	94.13	102.21	98.65
T4	121.58	119.66	121.13	116.69
2	128.70	130.24	134.22	120.07
4	126.94	125.00	131.37	123.42
6	124.22	121.50	124.93	119.71
8	119.49	115.95	119.61	116.84
10	119.37	114.61	118.00	118.29
12	120.62	114.68	117.63	116.62
16	116.62	109.11	120.63	115.44
18	116.26	110.42	118.28	117.10
24	116.48	112.28	116.25	113.42

APPENDIX C

Results of Fluidity Test

Table C.1: Experimental results of alloys fluidity test

Alloys	First test Length in (cm)	Second test Length in (cm)	Third test Length in (cm)	Average Length in (cm)	Standard deviation (cm)	Percentage Difference (%)
Base alloy (SI)	115.6	118.8	115.2	116.5	1.6	-
SI +0.02% Sr	108	112	111.5	110.5	1.8	5.2% decrease
SI + 0.38% Fe	93.5	90	88	90.5	2.3	21.9% decrease
SI + 0.9% Fe + 0.45% Mn	105	99.8	-	102.4	3	12.1% decrease